

EFFECTS OF TOPICAL APPLICATION OF COMBINED
PHYLLANTHUS EMBLICA LINN. AND SIMVASTATIN ON
DIABETIC WOUND IN MICE



A Dissertation Submitted in Partial Fulfillment of the Requirements
for the Degree of Doctor of Philosophy in Medical Sciences
Common Course
FACULTY OF MEDICINE
Chulalongkorn University
Academic Year 2020
Copyright of Chulalongkorn University

ผลของมะขามป้อมร่วมกับซิมีวาสแต่ดินแบบทากายนอกต่อแผลเบาหวานในหนูไมซ์



วิทยานิพนธ์นี้เป็นส่วนหนึ่งของการศึกษาตามหลักสูตรปริญญาวิทยาศาสตรดุษฎีบัณฑิต

สาขาวิชาวิทยาศาสตร์การแพทย์ ไม่สังกัดภาควิชา/เทียบเท่า

คณะแพทยศาสตร์ จุฬาลงกรณ์มหาวิทยาลัย

ปีการศึกษา 2563

ลิขสิทธิ์ของจุฬาลงกรณ์มหาวิทยาลัย

Thesis Title	EFFECTS OF TOPICAL APPLICATION OF COMBINED <i>PHYLLANTHUS EMBLICA</i> LINN. AND SIMVASTATIN ON DIABETIC WOUND IN MICE
By	Miss Tingting Liao
Field of Study	Medical Sciences
Thesis Advisor	Professor SUTHILUK PATUMRAJ, Ph.D.
Thesis Co Advisor	Assistant Professor CHAISAK CHANSRINIYOM, Ph.D.

Accepted by the FACULTY OF MEDICINE, Chulalongkorn University in
Partial Fulfillment of the Requirement for the Doctor of Philosophy

..... Dean of the FACULTY OF
MEDICINE
(Professor SUTTIPONG WACHARASINDHU, M.D.)

DISSERTATION COMMITTEE

..... Chairman
(Professor VILAI CHENTANEZ, M.D., Ph.D.)

..... Thesis Advisor
(Professor SUTHILUK PATUMRAJ, Ph.D.)

..... Thesis Co-Advisor
(Assistant Professor CHAISAK CHANSRINIYOM,
Ph.D.)

..... Examiner
(Assistant Professor WACHAREE
LIMPANASITHIKUL, Ph.D.)

..... Examiner
(Professor JURAIPORN SOMBOONWONG, M.D.,
M.Sc.)

..... External Examiner
(Associate Professor AMPORN JARIYAPONGSKUL,
Ph.D.)

ติงติง เหลี่ยว : ผลของมะขามป้อมร่วมกับซิมวาสแตตินแบบทาภายนอกต่อแผลเบาหวานในหนูไม่ซ้.
 (EFFECTS OF TOPICAL APPLICATION OF COMBINED
PHYLLANTHUS EMBLICA LINN. AND SIMVASTATIN ON
 DIABETIC WOUND IN MICE) อ.ที่ปรึกษาหลัก : ศ. ดร.สุทธิลักษณ์ ปทุมราช, อ.ที่ปรึกษา
 ร่วม : ผศ.ชัยศักดิ์ จันทร์นิม

การเกิดบาดแผลซึ่งรักษาไม่หายที่เท้าในผู้ป่วยโรคเบาหวานมักเป็นสาเหตุที่ทำให้เกิดการสูญเสียอวัยวะ ในปัจจุบัน การรักษาด้วยการให้ยาร่วมกันเป็นแนวทางการรักษาในการรักษาเฉพาะที่ในแผลเบาหวาน การศึกษานี้มีวัตถุประสงค์เพื่อศึกษา ผลและกลไกของสารสกัดหยาบจากมะขามป้อมร่วมกับซิมวาสแตตินต่อการหายของแผลในหนูไม่ซ้ที่ถูกทำให้เป็นเบาหวาน ใน การศึกษาครั้งนี้ใช้หนูไม่ซ้เพศผู้ แบ่งออกเป็น 5 กลุ่ม: กลุ่มหนูควบคุม กลุ่มหนูเบาหวาน โดยจะถูกเหนี่ยวนำให้เป็นเบาหวาน ด้วยสารสเตโรโตโซโดซิน 45 มิลลิกรัมต่อกิโลกรัมน้ำหนักตัวทางช่องท้อง วันละครั้งติดต่อกัน 5 วัน กลุ่มหนูเบาหวานซึ่ง ได้รับ สารสกัดหยาบจากมะขามป้อมในขนาด 100% (w/v), ซิมวาสแตตินในขนาด 5% (w/v) และสารสกัดหยาบ จากมะขามป้อมในขนาด 100% (w/v) ร่วมกับซิมวาสแตตินในขนาด 5% (w/v) 1 ครั้งต่อวัน ทั้งหมด 4, 7 และ 14 วัน ต่อเนื่อง ซึ่งทำให้เกิดบาดแผลชนิด **bilateral full-thickness wound excision** หลังถูกเหนี่ยวนำทำให้ เกิดเบาหวาน จะทำการตรวจวัดระดับมาโลนาลดีไฮด์ในแผล ระดับสารอินเตอร์ลิวคิน 6 การบูรณของนิวโทรฟิลล์ การหา ขนาดของแผล (% wound closure, WC) ปริมาณหลอดเลือดฝอย (% capillary vascularity, CV) และการออกซายของเยื่อผิวหนัง (%RE) การให้สารสกัดหยาบจากมะขามป้อมร่วมกับซิมวาสแตตินเพิ่มค่า % WC อย่างมี นัยสำคัญทางสถิติในวันที่ 14 การให้สารสกัดหยาบจากมะขามป้อมร่วมกับซิมวาสแตตินเพิ่มค่า % CV อย่างมีนัยสำคัญทาง สถิติทั้งวันที่ 7 และ 14 นอกจากนี้การให้สารสกัดหยาบจากมะขามป้อมร่วมกับซิมวาสแตตินมีการลดระดับมาโลนาลดีไฮด์ใน แผล อย่างมีนัยสำคัญทางสถิติในวันที่ 4 การให้สารสกัดหยาบจากมะขามป้อมร่วมกับซิมวาสแตตินมีการลดการอักเสบที่แผล เบาหวาน โดยลดระดับสารอินเตอร์ลิวคิน 6 ทั้งวันที่ 7 และ 14 แต่ไม่มีนัยสำคัญทางสถิติ ในทำนองเดียวกันการให้สารสกัด หยาบจากมะขามป้อมร่วมกับซิมวาสแตตินช่วยลดการบูรณของนิวโทรฟิลล์อย่างมีนัยสำคัญทางสถิติในวันที่ 4 นอกจากนี้พบ ความสัมพันธ์ในทางบวกระหว่างการเพิ่มขึ้นของปริมาณหลอดเลือดฝอย (%CV) กับการหายของแผล (%WC) ในวันที่ 7 ($r=0.7136, p=0.0019$) จากผลการทดลองแสดงให้เห็นว่าการให้สารสกัดหยาบจากมะขามป้อมร่วมกับซิมวาสแต ตินทางภายนอกสามารถช่วยการหายของแผลเบาหวานได้ โดยเพิ่มการเกิดหลอดเลือดใหม่ เพิ่มการหายของแผลโดยลดการเกิด ภาวะออกซิเดทีฟสเตรส และลดการเกิดการอักเสบในแผลเบาหวานในหนู

สาขาวิชา วิทยาศาสตร์การแพทย์
 ปีการศึกษา 2563

ลายมือชื่อนิสิต
 ลายมือชื่อ อ.ที่ปรึกษาหลัก
 ลายมือชื่อ อ.ที่ปรึกษาร่วม

5874858530 : MAJOR MEDICAL SCIENCES

KEYWORD: diabetic wound, *Phyllanthus emblica* Linn., simvastatin, wound closure, capillary vascularity, angiogenesis, re-epithelialization, oxidative stress, inflammation

Tingting Liao : EFFECTS OF TOPICAL APPLICATION OF COMBINED *PHYLLANTHUS EMBLICA* LINN. AND SIMVASTATIN ON DIABETIC WOUND IN MICE. Advisor: Prof. SUTHILUK PATUMRAJ, Ph.D. Co-advisor: Asst. Prof. CHAISAK CHANSRINIYOM, Ph.D.

Non-healing diabetic foot ulcers are the most common cause of lower extremity amputation. Drug combination treatment is the most recent emerging strategy in local treatment of diabetic wound. This study aimed to find out the combined effects and underlying mechanisms of combined *Phyllanthus emblica* Linn. (PE) and simvastatin (SIM) on diabetic wound in mice. Male BALB/C mice were divided into five groups: control group (CON+Vehicle), diabetic wounded group (DM+Vehicle, streptozotocin 45 mg/kg. i.p. daily for 5 days), diabetic wounded groups with daily treatment of 100%PE cream, 5%SIM cream, and 100%PE+5%SIM combined cream, w/v, for 4 days, 7 days and 14 days. Mice bilateral full thickness wound excision was made after diabetic mice model establishment. Wound tissue malondialdehyde (MDA) level, IL-6 protein level, number of infiltrated neutrophils, percentages of wound closure (%WC), percentage of capillary vascularity (%CV) and percentage of re-epithelialization (%RE) were analyzed. The results showed that PE and simvastatin combination treatment increased %WC significantly on day 14. PE and simvastatin combination treatment increased %CV significantly both on day 7 and day 14. PE and simvastatin combination treatment downregulated number of infiltrated neutrophils significantly on both day 4 and day 7. PE and simvastatin combination treatment has tendency to reduce IL-6 protein level in diabetic wound both on day 4 and day 7. Further, PE and simvastatin combination treatment reduced MDA content significantly on day 4. Moreover, increasement of %CV had a strong positive correlation ($r=0.7136$, $p=0.0019$) with %WC on day 7. These findings showed that topical application of PE and simvastatin combination treatment could enhance wound healing by upregulating VEGF protein level, angiogenesis, and wound closure based on the combined effects on inhibiting oxidative stress and inflammation in diabetic mice.

จุฬาลงกรณ์มหาวิทยาลัย
CHULALONGKORN UNIVERSITY

Field of Study: Medical Sciences
Academic Year: 2020

Student's Signature
Advisor's Signature
Co-advisor's Signature

ACKNOWLEDGEMENTS

First of all, I would like to give thanks to International Ph.D. program of Medical Sciences and the Center of Excellence in Microcirculation, Department of Physiology, Faculty of Medicine, Chulalongkorn University, for providing the precious study opportunity.

Especially, I want to give my most sincere gratitude and appreciation to my thesis advisor Professor Suthiluk Patumraj, Department of Physiology, Faculty of Medicine, Chulalongkorn University, for the persuasive enlightenment, continuous encouragement, and great patience during the study. Also, I would like to give my sincere thanks to my co-advisor Assistant Professor Chaisak Chansriniyom for the kind guidance and help for the extraction work in the lab.

Additionally, I would like to give gratitude and appreciation to my thesis committee Professor Vilai Chentanez, Professor Juraiporn Somboonwong, Professor Wacharee Limpanasithikul, Faculty of Medicine, Chulalongkorn University, and external examiner Associate Professor Amporn Jariyapongskul, Department of Physiology, Faculty of Medicine, Srinakharinvirot University, for the insightful comments and critical questions that incited me to the deeper and wider perspectives on the research.

I also would like to give the sincere thanks to Ms. Natchaya Wongeakin and Ms. Supakanda Sukpat for the lab skill guidance and help in our lab, and Ms. Janjira Koonam, Department of Pathology, Faculty of Medicine, Chulalongkorn University for help. Additionally, my thanks also go to Ms. Apinya Butlee for the documentation help during the study.

Further, I would like to give my thanks to Ms. Wei Li, Mr. Dhammika Leshan Wannigama, Ms. Titiporn Mekrungruangwong, Mr. Wasin Manuprasert, Mr. Fatis Okrit, and Ms. Jiayu Li, for the kind encouragement and friendship during my study life.

Last but not least, I would like to give special thanks to my parents, my sister and other family members for their love and great support for my study in Thailand.

Tingting Liao

TABLE OF CONTENTS

	Page
ABSTRACT (THAI)	iii
ABSTRACT (ENGLISH).....	iv
ACKNOWLEDGEMENTS.....	v
TABLE OF CONTENTS.....	vi
LIST OF TABLES	x
LIST OF FIGURES	xii
ABBREVIATIONS	1
CHAPTER I INTRODUCTION.....	3
1.1. Background and Rationale.....	3
1.2. Research Questions.....	6
1.3. Research Objectives.....	6
1.4. Hypothesis	6
1.5. Key Words	6
1.6. Conceptual Framework.....	7
CHAPTER II LITERATURE REVIEW.....	9
2.1. Physiology of Normal Wound Healing	9
2.1.1. Inflammation Stage	9
2.1.2. Proliferation Stage.....	11
2.1.3. Remodeling Stage.....	12
2.2. Diabetic Wound Healing	13
2.2.1. Oxidative Stress.....	15
2.2.2. Interleukin 6	17
2.2.3. Vascular Endothelial Growth Factor (VEGF).....	19
2.3. Simvastatin and <i>Phyllanthus emblica</i> Linn.	21
2.3.1. Simvastatin	21

2.3.1.1. Pleiotropic Effects of Simvastatin	22
2.3.1.1.1. Pleiotropic Effects of Simvastatin in Various Diseases	22
2.3.1.1.2. Pleiotropic Effects of Simvastatin on Wound Healing.	24
2.3.2. <i>Phyllanthus emblica</i> Linn.....	26
2.3.2.1. Hypoglycemic Activity of <i>Phyllanthus emblica</i> Linn.	31
2.3.2.2. Antioxidant Activity of <i>Phyllanthus emblica</i> Linn.	31
2.3.2.3. Anti-inflammatory Activity of <i>Phyllanthus emblica</i> Linn.	33
2.3.2.4. Effects of <i>Phyllanthus emblica</i> Linn. on Wound Healing.....	33
CHAPTER III MATERIALS AND METHODOLOGY.....	36
3.1. Chemicals	36
3.1.1. PE Fruit Extraction.....	36
3.1.2. Simvastatin	36
3.1.3. Other Chemicals Used.....	36
3.2. Drug Cream Preparation	37
3.3. Animals.....	38
3.4. Induction of Diabetic Wound Model.....	38
3.5. Wound Creation.....	38
3.6. Experimental Design	40
3.6.1. To Study the Dose-Response of Simvastatin	40
3.6.2. To Study the Dose-Response of PE	41
3.6.3. To Study the Effects of Combination of PE and Simvastatin on Diabetic Wound Healing in Mice	42
3.7. Measurement of Parameters	43
3.7.1. Percentage of Wound Closure (%WC)	43
3.7.2. Percentage of Capillary Vascularity (%CV)	46
3.7.3. Percentage of Re-Epithelialization (%RE).....	50
3.7.4. Measurement of Neutrophil Infiltration	51
3.7.5. Immunoassays and TBARS Assay.....	53
3.7.5.1. Wound Skin Sample Supernatant Preparation	53

3.7.5.2. Total Protein Content Measurement.....	53
3.7.5.3. Measurement of Tissue MDA	55
3.7.5.4. Measurement of Tissue VEGF	57
3.7.5.5. Measurement of Tissue IL-6	59
3.8. Statistics.....	59
CHAPTER IV RESULTS.....	60
4.1. Results of the Dose-Response of Simvastatin and PE on Wound Closure (%WC) and Capillary Vascularity (%CV)	61
4.1. Correlation of Doses and Percentage of Wound Closure (%WC) and Capillary Vascularity (%CV) in Protocol 1	67
4.2. Protocol 2.....	70
4.2.1. Results of Physiological Parameters in Protocol 2.....	70
4.2.1.1. Result of Percentage of Body Weight Change (%BW) in Protocol 2	70
4.2.1.2. Results of Fasting Blood Glucose in Protocol 2.....	72
4.2.2. Effects of combined treatment of PE and Simvastatin on Percentage of Wound Closure (%WC) and capillary vascularity (%CV)	74
4.2.3. Effects of Combined Treatment of PE and Simvastatin on VEGF Protein Level.....	80
4.2.4. Effects of Combined Treatment of PE and Simvastatin on Percentage of Re-Epithelialization (%RE).....	83
4.2.5. Effects of Combined Treatment of PE and Simvastatin on Neutrophil Infiltration.....	87
4.2.6. Effects of Combined Treatment of PE and Simvastatin on IL-6 Protein Level.....	90
4.2.7. Effects of Combined Treatment of PE and Simvastatin on Tissue MDA	92
4.2.8. Correlation Analysis between Parameters.....	97
4.2.8.1. Correlation Analysis of %WC and VEGF on Day 7.....	97
4.2.8.2. Correlation Analysis of %CV and VEGF on Day 7.....	98
4.2.8.3. Correlation Analysis of %WC and %CV on Day 7	99

4.2.8.4. Correlation Analysis of %WC and %CV on Day 14	100
4.2.8.5. Correlation Analysis of %WC and IL-6 Protein Level on Day 7	101
4.2.8.6. Correlation Analysis of %RE and VEGF Protein Level on Day 7	102
CHAPTER V DISCUSSION	103
5.1. Results of Physiological Parameters	104
5.2. Protocol 1	107
5.2.1. Results of the Dose-Responses of Simvastatin and PE on Wound Closure (%WC) and Capillary Vascularity (%CV)	107
5.3. Protocol 2	112
5.3.1. Effects of Combined Treatment of PE and Simvastatin on Percentage of Wound Closure (%WC) and Capillary Cascularity (%CV)	112
5.3.2. Effects of Combined Treatment of PE and Simvastatin on VEGF Protein Level	113
5.3.3. Effects of Combined Treatment of PE and Simvastatin on Percentage of Re-Epithelialization (%RE)	117
5.3.4. Effects of Combined Treatment of PE and Simvastatin on Neutrophil Infiltration	118
5.3.5. Effects of Combined Treatment of PE and Simvastatin on IL-6 Protein Level	120
5.3.6. Effects of Combined Treatment of PE and Simvastatin on Tissue MDA	122
5.4. Proposed Potential Mechanisms	129
CHAPTER VI CONCLUSIONS	130
REFERENCES	132
APPENDIX	133
VITA	150

LIST OF TABLES

	Page
Table 1. Simvastatin Dose in Wound	25
Table 2. Phytochemicals in <i>Phyllanthus emblica</i> Linn. Fruit.....	27
Table 3. Bioactive Components from <i>Phyllanthus emblica</i> Linn.....	28
Table 4. PE Doses in Wound Healing and Skin Care.....	34
Table 5. Percentage of Wound Closure (%WC) of Every Group in Various Doses of PE (DM+10%PE, DM+100%PE, and DM+200%PE groups) on Day 14 in Protocol 1	62
Table 6. Percentage of Capillary Vascularity (%CV) of Every Group in Various Doses of PE (DM+10%PE, DM+100%PE, and DM+200%PE groups) on Day 14 in Protocol 1	62
Table 7. Percentage of Wound Closure (%WC) of Every Group in Various Doses of SIM (DM+0.5%SIM, DM+5%SIM, and DM+10%SIM groups) on Day 14 in Protocol 1.....	65
Table 8. Percentage of Capillary Vascularity (%CV) of Every Group in Various Doses of SIM (DM+0.5%SIM, DM+5%SIM, and DM+10%SIM groups) on Day 14 in Protocol 1	65
Table 9. Percentage of Body Weight Change (%BW) of Experimental Mice on Day 4, 7, and 14 in Protocol 2	70
Table 10. Fasting Blood Glucose (FBG) Levels of Experimental Mice on Day 4, 7, and 14 in Protocol 2	72
Table 11. Results of Percentage of Wound Closure (%WC) of Groups on Day 7 in Protocol 2.....	76
Table 12. Results of Percentage of Capillary Vascularity (%CV) of Groups on Day 7 in Protocol 2.....	76
Table 13. Results of Percentage of Wound Closure (%WC) of Groups on Day14	77
Table 14. Results of Percentage of Capillary Vascularity (%CV) of Groups on Day 14.....	77
Table 15. VEGF Protein Level (pg/mg total protein) of Wound Site on Day 7 and Day 14 in Protocol 2	81

Table 16. Percentage of Wound Re-epithelialization (%RE) at Wound Site (H&E staining, 400x magnificence) on Day 7 and Day 14 in Protocol 2	85
Table 17. Number of Infiltrated Neutrophils of Wound Site (H&E staining, 400x magnificence) on Day 4 and Day 7 in Protocol 2.....	88
Table 18. IL-6 protein level (pg/mg total protein) of Wound Site on Day 4 and Day 7 in Protocol 2.....	90
Table 19. MDA Content (nmol/mg total protein) of Wound Site on Day 4, Day 7, and Day14 in Protocol 2	92
Table 20. Summarization of Parameters on Day 4 in Protocol 2.....	94
Table 21. Summarization of Parameters on Day 7 in Protocol 2.....	95
Table 22. Summarization of Parameters on Day 14 in Protocol 2.....	96



LIST OF FIGURES

	Page
Figure 1. Conceptual Framework.	7
Figure 2. Physiological Process of Wound Healing.	13
Figure 3. Pathophysiological Features of Diabetic Wound Healing.....	20
Figure 4. Chemical Structure of Simvastatin.....	21
Figure 5. <i>Phyllanthus emblica</i> Linn.....	26
Figure 6. Wound Positions on Dorsal Skin of BALB/C Mouse.	40
Figure 7. Experimental Design Used for the Study of Dose-Response of Simvastatin.	41
Figure 8. Experimental Design Used for The Study of Dose-Response of PE.....	42
Figure 9. Experimental Design Used for The Study of The Effects of Combination of PE and SIM on Diabetic Wound Healing in Mice.....	43
Figure 10. Equation of Calculation of Percentage of Wound Closure (%WC).....	44
Figure 11. Wound Area Analysis by Using Image-Pro Plus Program (A-E).	46
Figure 12. Microscopic Photography of Vascular Network of Wound Site.....	47
Figure 13. Equation of Calculation of Percentage of Capillary Vascularity (%CV)..	48
Figure 14. AOI Windows for Percentage of Capillary Vascularity (%CV) Analysis.	48
Figure 15. Demonstrating How the %CV Was Obtained from Each AOI.	49
Figure 16. Measurement of Re-epithelialization of Wound Tissue.....	51
Figure 17. Equation of Calculation of Percentage of Re-epithelialization.	51
Figure 18. Neutrophil Infiltration Micrograph.....	52
Figure 19. The Reaction of MDA and TBA to Form MDA-TBA Adduct.	56
Figure 20. Principle of Sandwich ELISA.	58
Figure 21. Wound Area Images and Confocal Microscopic Images of Areas Around Full-thickness Dorsal Skin Wound in STZ-induced Diabetic BALB/C Mouse Model in Protocol 1 from PE Treatment Groups.	61
Figure 22. Percentage of Wound Closure (%WC) and Capillary Vascularity (%CV) of Every Group in Various Doses of PE (DM+10%PE, DM+100%PE, and	

DM+200%PE groups) on Day 14 in Protocol 1. (All data were expressed as mean \pm SEM).....	63
Figure 23. Wound Area Images and Confocal Microscopic Images of Areas Around Full-thickness Dorsal Skin Wound in STZ-induced Diabetic BALB/C Mouse Model in Protocol 1 from SIM Treatment Groups.....	64
Figure 24. Percentage of Wound Closure (%WC) and Capillary Vascularity (%CV) of Every Group in Various Doses of SIM (DM+0.5%SIM, DM+5%SIM, and DM+10%SIM groups) on Day 14 in Protocol 1. (All data were expressed as mean \pm SEM).....	66
Figure 25. Pearson's Correlation Analysis between Data Sets of %CV and PE Doses on Day 14 in Protocol 1. (Details of each data set were shown in Appendix 8)	67
Figure 26. Pearson's Correlation Analysis between Data Sets of %WC and SIM Doses on Day 14 in Protocol 1. (Details of each data set were shown in Appendix 9)	68
Figure 27. Pearson's Correlation Analysis between Data Sets of %CV and SIM Doses on Day 14 in Protocol 1. (Details of each data set were shown in Appendix 10)	69
Figure 28. Percentage of Body Weight Change (%BW) of Experimental Mice Measured on Day 4, 7, and 14 in Protocol 2. (All data were expressed as mean \pm SEM)	71
Figure 29. Fasting Blood Glucose (FBG) Levels of Experimental Mice on Day 14 in Protocol 1. (All data were expressed as mean \pm SEM).....	73
Figure 30. Wound Area Images and Confocal Microscopic Images of Areas Around Full-thickness Dorsal Skin Wound in STZ-induced Diabetic BALB/C Mouse Model on Day 7 in Protocol 2.	74
Figure 31. Wound Area Images and Confocal Microscopic Images of Areas Around Full-thickness Dorsal Skin Wound in STZ-induced Diabetic BALB/C Mouse Model on Day 14 in Protocol 2.	75
Figure 32. Percentage of Wound Closure (%WC) and Capillary Vascularity (%CV) of Groups on Day 7 in Protocol 2. (All data were expressed as mean \pm SEM).....	78
Figure 33. Percentage of Wound Closure (%WC) and Capillary Vascularity (%CV) of Groups on Day 14 in Protocol 2. (All data were expressed as mean \pm SEM).....	79
Figure 34. VEGF protein level (pg/mg total protein) of Wound Site on Day 7 and Day 14 in Protocol 2. (All data were expressed as mean \pm SEM).....	82
Figure 35. Images of Re-Epithelialization of Groups on Day 7 and Day 14.....	84

Figure 36. Percentage of Re-Epithelialization at Wound Site (H&E staining, 400x magnificence) on Day 7 and Day 14 in Protocol 2.....	86
Figure 37. Images of Infiltrated Neutrophils of Each Group on Day 4 and Day 7 in Protocol 2.....	87
Figure 38. Number of Infiltrated Neutrophils of Wound Site (H&E staining, 400x magnificence) on Day 4 and Day 7 in Protocol 2.....	89
Figure 39. IL-6 Protein Expression (pg/mg total protein) of Wound Site on Day 4 and Day 7 in Protocol 2. (All data were expressed as mean \pm SEM).....	91
Figure 40. MDA Content (nmol/mg total protein) of Wound Site on Day 4, Day 7 and Day 14 in Protocol 2. (All data were expressed as mean \pm SEM).....	93
Figure 41. Pearson's Correlation Analysis between Data Sets of Percentage of Wound Closure (%WC) and VEGF Protein Level (pg/mg total protein) of Groups on Day 7. (Details of each data set were shown in Appendix 19).....	97
Figure 42. Pearson's Correlation Analysis between Data Sets of Percentage of Capillary Vascularity (%CV) and VEGF Protein Level (pg/mg total protein) of Groups on Day 7 in Protocol 2. (Details of each data set were shown in Appendix 20).....	98
Figure 43. Pearson's Correlation Analysis between Data Sets of the Percentage of Wound Closure (%WC) and Percentage of Capillary Vascularity (%CV) of Groups on Day 7 in Protocol 2. (Details of each data set were shown in Appendix 13).....	99
Figure 44. Pearson's Correlation Analysis between Data Sets of the Percentage of Wound Closure (%WC) and Percentage of Capillary Vascularity (%CV) of Groups on Day 14 in Protocol 2. (Details of each data set were shown in Appendix 16).....	100
Figure 45. Pearson's Correlation Analysis between Data Sets of the Percentage of Wound Closure (%WC) and IL-6 Protein Level (pg/mg total protein) of Groups on Day 7 in Protocol 2. (Details of each data set were shown in Appendix 27).....	101
Figure 46. Pearson's Correlation Analysis between Data Sets of the Percentage of Re-Epithelialization (%RE) and VEGF Protein Level (pg/mg total protein) of Groups on Day 7 in Protocol 2. (Details of each data set were shown in Appendix 31).....	102
Figure 47. Isoble Additivity Graph.....	111
Figure 48. Equation of Additive Isoble.....	111
Figure 49. Proposed Mechanisms of Topical Application of PE and SIM Combined Cream in Diabetic Wound.	129

ABBREVIATIONS

SIM = simvastatin

PE = *Phyllanthus emblica* Linn.

HMG-CoA = 3-hydroxy-3-methylglutaryl coenzyme A

ROS = reactive oxygen species

SOD = superoxide dismutase

CAT = catalase

GPx = glutathione peroxidase

GSH = glutathione

MPO = myeloperoxidase

MDA = malondialdehyde

AGEs = advanced glycation end products

TBARS = thiobarbituric acid reacting substance

H₂O₂ = hydrogen peroxide

O₂^{••} = superoxide radical

•OH = hydroxyl radical

HO₂• = hydroperoxyl radical

ONOO⁻ = peroxynitrite

HOCl = hypochlorous acid

NO = nitric oxide

NO₂ = nitrogen dioxide

DPPH• = 2,2-diphenyl-1-picrylhydrazyl

ABTS•+ = 2,2'-azino-bis (3-ethylbenzothiazoline-6-sulphonic acid)

OxLDL = oxidized low-density lipoprotein

TNF- α = tissue necrosis factor alpha

IL-6 = interleukin 6

VEGF = vascular endothelial growth factor

PAF = platelet activation factor

FGF-2 = fibroblast growth factor 2

KGF = keratinocyte growth factor

TGF- β = transforming growth factor beta

EGF = endothelial growth factor

MMPs = matrix metalloproteinases

MCP-1 = monocyte chemoattractant protein 1

LFA-1 = leukocyte function-associated antigen 1

NF- κ B = nuclear factor-kappa B

PDGF = platelet-derived growth factor

COX-2 = cyclooxygenase 2

INF- β 2 = interferon beta 2

CVD = cardiovascular disease

IsoP = isoprostane

CHAPTER I

INTRODUCTION

1.1. Background and Rationale

Diabetes mellitus (DM) is a group of metabolic disorders with hyperglycemia as its hallmark. DM is a prevalent medical problem throughout the world and continues to increase in number and significance due to lifestyle changes. It ranks the 7th cause of leading death in the US in 2015, with a total of 252,806 death taking diabetes as a contributing cause of death. It is estimated that the number of DM patients will triple by 2050, which will cause a major health and economic burden. Up to 15% of diabetic patients may suffer chronic non-healing diabetic foot ulcers (DFUs), with approximately 85% of persons with diabetes will end up with lower extremity amputations [1, 2]. It has been reported that one leg is lost due to diabetes every 30 seconds in the world [3].

The predominant risk factors leading to diabetic foot ulcers are diabetic neuropathy and peripheral arterial diseases [4, 5]. Diabetic neuropathy is the common factor in almost 90% of diabetic foot ulcers. Peripheral arterial diseases are up to 8 times more common in diabetic patients. An inadequate blood supply at the foot injury may result in foot ulceration, potentially leading to limb amputation [1]. The causative factor of these leading risk factors is hyperglycemia-induced oxidative stress.

In diabetic wound, hyperglycemia can induce an imbalance of free radicals and an endogenous enzyme system composed of antioxidant enzymes. Oxygen-free radicals like hydrogen peroxide (H_2O_2), superoxide radical ($O_2^{\bullet-}$), hydroxyl radical ($\bullet OH$) and nitric free radicals are overproduced, oxidant enzymes such as superoxide dismutase (SOD), catalase (CAT), glutathione peroxidase (GPx), glutathione (GSH) are downregulated, thus leading to oxidative stress in the peripheral vessels. At the wound

site, there exists both pro-oxidative free radicals and excessive inflammatory cells. The oxidative stress and the pro-inflammatory cytokines at the wound site can disturb the orchestrated wound healing process by making it stuck at the inflammation phase, leading foot ulcer slow to heal [6].

Control of risk factors such as hyperglycemia, and hyperglycemia-induced endothelial function, oxidative stress, diabetic neuropathy, and peripheral arterial diseases could be the management approaches for diabetic foot ulcers [1, 7]. The gold standards for diabetic foot ulcer treatment include diabetic control, management of infection, and revascularization [1]. So this provides the rationale that reducing reactive oxygen species (ROS) induced oxidative stress and correcting peripheral vessel dysregulation could improve diabetic wound healing. Clinical trials proved that antioxidants application to the wound site could enhance wound healing [8].

Diabetic patients are commonly associated with dyslipidemia, so statins are widely used in diabetic patients. Simvastatin is a mostly used medication to lower lipid by decreasing cholesterol synthesized in the liver through inhibiting 3-hydroxy-3-methylglutaryl (HMG) coenzyme A reductase. It is the first line chemical drug that has been used in metabolic disorders for a long time. The cardiovascular protective effects of simvastatin that are independent of LDL-cholesterol lowering are called pleiotropic effects [9-13]. Recently, a number of researches showed that simvastatin exerting its lipid-lowering-independent effect on wound healing by decreasing pro-inflammatory mediators such as interleukin-1 β (IL-1 β), tumor necrosis factor (TNF- α), improving angiogenesis regulating protein level like vascular endothelial growth factor (VEGF), and other wound healing enhancement effect like accelerating wound closure, improving granulation tissue formation, promoting re-epithelialization, increasing collagen deposition and tensile strength, etc. [9-17].

Phyllanthus emblica Linn. (PE) is a plant widely used in ayurvedic, traditional Thai, and Chinese medication systems with long histories. The fruit, leaf, seed, flower, and tree bark of PE could all be used as medicine to treat various diseases [18]. The main bioactive components of PE include ascorbic acid, polyphenols, tannins, and alkaloids[19]. PE extract showed antioxidant property against α , α -diphenyl- β -picrylhydrazyl (DPPH'), 2,2'-azino-bis (3-ethylbenzothiazoline-6-sulphonic acid)

(ABTS^{•+}), superoxide radical ($O_2^{\bullet-}$) *in vitro*, reducing oxidative stress *in vivo*, endothelial dysfunction regulation effect in diabetic patients, and also showed the anti-inflammatory property in the diabetic wound and other models [20-27]. Furthermore, PE has been reported to exert wound healing improvement via upregulating angiogenesis and collagen deposition through reducing antioxidant stress [28]. So that, PE could be used in the topical treatment of diabetic wound healing based on its strong free radical scavenging, antioxidative and anti-inflammation properties.

Topical drug administration for skin disorders minimizes systemic exposure. Systemic absorption does occur and varies with the area, site, drug, and state of the skin. Topical drug administration for skin disorders reduces systematic side effects, reduces the development of drug resistance, and could also improve the patient compliance and provides a combined effect to enhance therapy benefits [29, 30]. Furthermore, the chronic wound usually has insufficient arterial perfusion, local treatment with an effective drug delivery system can compensate for the poor concentration of poor drug delivery system when the drug is administered systematically. Fixed-dose combination therapy is also used in antidiabetic therapy such as bilayer tablets, which may reduce side effects, provide more beneficial effects than monotherapy and reduce economic investment [29]. Recent new research on drug combination showed faster healing and better outcomes of the wound [31, 32]. The existing drug combination research shows the evidence and potential of new therapy trends of the drug combination treatment in wound healing. The use of PE in the treatment of diabetic foot ulcers could also reduce the growing economic burden for its fluent resources and low prices.

Both simvastatin and PE showed antioxidant and anti-inflammation effects, which have potential benefits to diabetic wound healing. This is the first topical combination of simvastatin and a natural plant medicine on diabetic wound healing. Thus, we measured the combined effect of topical application of simvastatin and PE on diabetic wound healing in mice.

1.2. Research Questions

Whether the topical application of PE and simvastatin will have a combined effect on diabetic wound healing or not? And what are the possible pathway(s) that may involve their effects?

1.3. Research Objectives

1. To find out the combined effect of topical application of PE and simvastatin on diabetic wound healing in mice.
2. To find out the possible pathway(s) of the combination of topical application PE and simvastatin whether they involve in anti-inflammation, anti-oxidative stress, and pro-angiogenesis or not.

1.4. Hypothesis

The topical application of PE and simvastatin combination has a combined effect on diabetic wound healing by the possible pathway(s) of anti-inflammation, anti-oxidative stress, and its enhanced angiogenesis.

1.5. Key Words

diabetic wound healing, simvastatin, *Phyllanthus emblica* Linn., inflammation, neutrophil, oxidative stress, MDA, VEGF, IL-6, angiogenesis.

CHULALONGKORN UNIVERSITY

1.6. Conceptual Framework

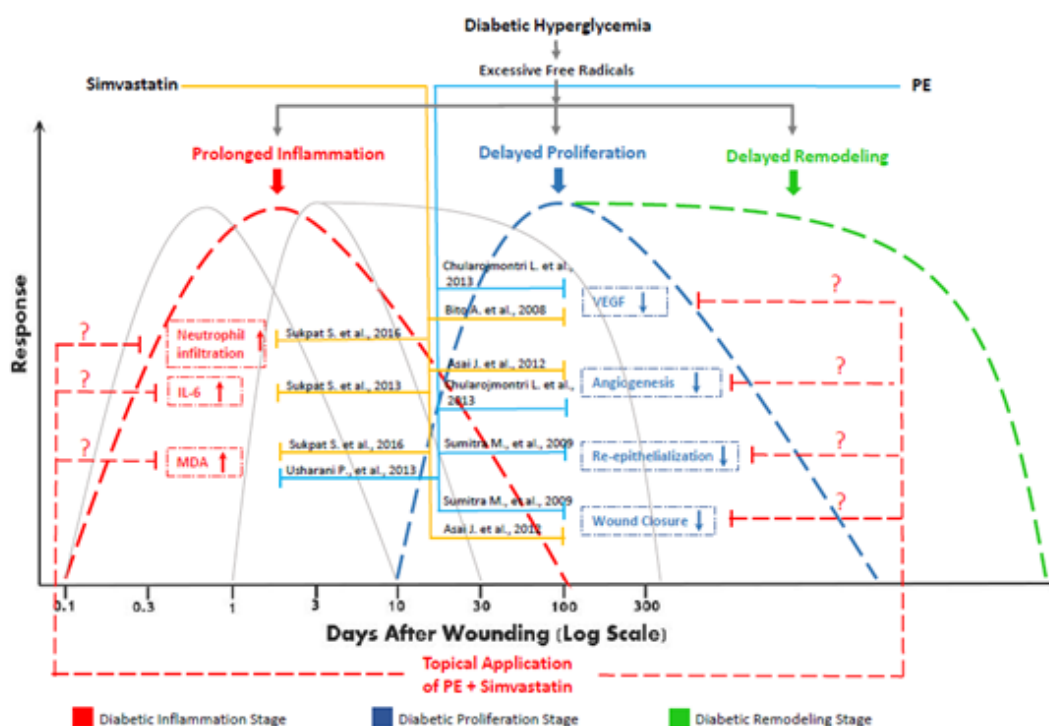


Figure 1. Conceptual Framework.

In diabetic ulcers, the normal pathophysiology of wound has been changed. Oxidative stress and inflammation status are worsened by diabetic hyperglycemia. MDA content, neutrophil infiltration, and IL-6 protein level were all increased dramatically in diabetic wound [33-36]. In the proliferation stage, VEGF protein level, angiogenesis, re-epithelialization, granulation tissue formation, and wound closure were also all downregulated in diabetic wounds [9, 12, 13, 28]. Previous studies have proved that both Simvastatin and PE could enhance diabetic wound healing [12, 28]. This diabetic wound healing may exert wound closure improvement through antioxidant and anti-inflammatory effects. In previous work from our lab, simvastatin reduced MDA content, neutrophil infiltration, and IL-6 protein level in diabetic wound [9, 37]. In 2008, Bitto A. and colleagues have proved that intraperitoneal injection of simvastatin could upregulate VEGF protein level in diabetic wound [10]. Further, in 2012, Asai J. and colleagues used topical application of simvastatin to improve angiogenesis in diabetic wound [12]. In 2013, Usharani P. and colleagues showed that PE has strong

antioxidant and downregulated MDA content in type 2 diabetic patients [25]. Further, Chularojmontri L. and colleagues proved that PE fruit powder enhanced VEGF protein expression and angiogenesis in human umbilical vein endothelial cells [38]. Sumitra M. and the colleagues increased re-epithelialization in rat wound by using topical application of PE [28].

The conceptual framework shown in **Figure 1** could describe in brief that in diabetic ulcers, the normal pathophysiology of wound has been changed. Oxidative stress and inflammation status are worsened by diabetic hyperglycemia. In prolonged inflammation stage, increased oxidative stress in diabetic wound was downregulated by both simvastatin and PE. The increased IL-6 protein level and infiltrated neutrophils were also decreased by simvastatin. In delayed proliferation stage, both decreased VEGF, angiogenesis and wound closure were upregulated by both simvastatin and PE. Also in delayed proliferation stage, the reduced re-epithelialization was increased by PE. Thus, the hypothesis is proposed that the topical application of PE and simvastatin combination has a combined effect on diabetic wound healing by the possible pathway(s) of anti-inflammation, anti-oxidative stress, and its enhanced angiogenesis.



CHAPTER II

LITERATURE REVIEW

Skin is the largest organ system of the body. Its integrity plays a pivotal role in keeping the normal physiological homeostasis of a human body. However, any situation could break the cutaneous integrity which needs necessary medical interventions. Chronic conditions such as diabetes mellitus or peripheral vascular disease can probably lead to impaired wound healing. Wound healing mechanisms and underlying pathophysiological courses are still unknown [39]. This literature review delineates normal physiological processes of wound healing and pathophysiology processes in diabetic wound healing impairment, providing us the potential targets of treatment of diabetic ulcers.

2.1. Physiology of Normal Wound Healing

In normal physiology, wound healing is a complex process with over-lapping stages of inflammation, proliferation, and tissue remodeling.

2.1.1. Inflammation Stage

When an open injury is made on the skin, the dermis induces bleeding. The damaged macro- or micro arterial vessels will constrict to minimize blood loss which causes reflex vasodilatation and relaxation of the arterial vessels. Simultaneously, vascular permeability also increases, leading to the increased influx of inflammatory cells into the extracellular area around the wound. This explains the clinical symptoms such as the warm, red, swollen phenomenon of early wounds. Immediately after the injury, platelet and polymorphonuclear leukocytes (PMNs) aggregation induce the clotting process. Formation of the platelet plug and blood clot induce a temporary seal of the wound by the polymerized fibrin and platelets forms a clot over a wound site, wound gradually closes, and scar forms [40]. At the same time, the inflammation phase begins with various immune cells infiltration into the wound site. Among these immune cells, neutrophils arrive at the wound site firstly, followed by monocyte,

which later differentiates into mature macrophage in the wound tissue [41]. Pro-inflammatory cytokines, such as IL-6 and TNF- α are secreted by these innate immune cells, and large amounts of reactive oxygen species (ROS), which are essential in protecting the organism against invading bacteria and other microorganisms in normal physiological condition [41]. During the process, abounding of blood and serous fluid are also produced to clear the wound surface contamination [42]. Besides, in response to the injured cell membranes, signaling molecules such as prostaglandins (PG), leukotrienes (LT), and thromboxanes (TXA) also play roles in activating the inflammatory response [43].

In the early phase of inflammation, the complement pathway is activated and leads to the infiltration of granulocyte neutrophils, while in the later phase of inflammation, blood monocytes changing into tissue macrophages is typical [34]. This inflammatory phase of wound healing lasts till the excessive bacteria and debris cleared. Within one hour of the insult of the skin barrier, **neutrophils** firstly respond and migrate to the wound site and keep a certain concentration level within the first 48 hours. They provide the initial protection against infection by destroying debris and bacteria, scavenging excessive oxygen free radicals, causing the creamy yellow fluid in the inflammation tissues. After their job is finished, neutrophils undergo apoptosis or phagocytosed by macrophages [42, 43]. Accordingly, the pro-inflammatory cytokines produced by the immune cells decrease. **Macrophages** are attracted to the wound site at 48-72 hr post-injury by chemical messengers from platelets and damaged cells. They can produce a large number of growth factors to increase angiogenesis and the formation of granulation tissue. However, patients with suppressed immunology are unable to produce a typical inflammatory response so that the normal wound healing procedure cannot be orderly and timely activated [42, 43]. **Lymphocytes** appear at the wound site after 72 hr to join the wound healing procedure by producing extracellular scaffold and collagen remodeling. Besides neutrophils and macrophages, many other cell types also react to the initial inflammatory signals and begin to migrate to the wound site and then start to proliferate, among which including keratinocytes and endothelial cells [44]. Once the inflammatory response is balanced and the wound is cleared of debris, the proliferative stage of the healing process begins to restore the

wound [42, 43]. The responsibility of the inflammation stage is to activate the wound repair. New tissue formation will not occur until the wound bed has been cleansed by the inflammatory process and enough stimuli from macrophages. After the cell migration to the wound area, they will undergo proliferation, migration, and differentiation to produce substances needed for the new tissue formation. As the immune cells undergoing apoptosis and pro-inflammatory cytokine level decreasing, the stage of inflammation is in the transition to the proliferative stage.

2.1.2. Proliferation Stage

The main aim of the proliferative stage is to reduce the lesion area to build an epithelial barrier, which includes angiogenesis, re-epithelialization, and granulation tissue formation [45]. This stage starts from within 2 days after injury to 14 days [46]. During the proliferation phase, endothelial cells, keratinocytes, and fibroblasts all migrate to help heal the wound [34, 41]. **Re-epithelialization** is one of the main healing processes happening in the proliferative stage. It starts after about 1 to 2 days post-injury, by keratinocytes migration from the wound edge to the injury wound center. The repair of the dermis occurs when re-epithelialization begins [41]. The wound closure procedure is achieved by a combination of the process of granulation formation, contraction, and epithelialization [40]. Keratinocytes, fibroblasts, and endothelial cells migrate to the wound site and proliferate to contract the new tissue formation, forming a muscular red color and fluent vascular area of the healing tissue [44]. In this stage, angiogenesis, the formation of granulation tissue formation, epithelialization, and wound retraction happens at the same time [43]. **Angiogenesis** is also called neovascularization. It is imperative for wound healing, involving endothelial cellular proliferation, rupture, rearrangement of the basal membrane, migration, and association in tubular structures, and the recruitment of perivascular cells [45]. The formation of a new vascular network keeps replenishing the newly formed granulation tissue, supporting the new tissue with oxygen and necessary nutrients [41]. In the wound healing process, new capillary vascularity can reach 2 or 3 times than in normal tissue, sometimes even 10 times more [47]. Angiogenesis is mainly induced by VEGF-A [48]. Fibroblasts contributed **collagen deposition** in the granulation tissue formation, and myofibroblasts contributed contraction also happens

in the proliferative stage. At the later period of the proliferative stage, the long remodeling stage overlaps. The pink, vascular and fibrous tissue that replaces the clot is called granulation tissue. The **Granulation tissue formation** is mainly regulated by fibroblasts which lay down extra-cellular matrix proteins, including hyaluronan, fibronectin and proteoglycans. Subsequently, collagen and fibronectin are also produced by fibroblasts to be compositions of the granulation tissue. Fibroblast changes to myofibroblast phenotype to help exert wound contraction function [43]. **Wound contraction** begins about 7 days after injury, mainly regulated by myofibroblasts. Action and myosin interaction pull the cell bodies close to each other to reduce the wound area. Wound shape is one the factors that influence contracting speed [43].

2.1.3. Remodeling Stage

The remodeling stage is the last stage which starts after the formation of the granulation tissue, which begins 2 or 3 weeks after injury and could take more than 1 year to recover the normal tissue structure. It is marked by the maturing of the elements with deep changes in the extracellular matrix and the resolution of the initial inflammation. The collagens comprise the main structural component and comprise the highest protein concentration in the ECM, with 85% of the dermis being collagen. When collagen production and degradation reach an equilibrium, the remodeling phase of tissue repair begins [49]. Reorganization, degradation, resynthesis of the extracellular matrix of this stage makes the wound **tensile strength restoring**, but wounds can only reach tissue strength as much as 80% of the original skin [45, 50]. Collagens synthesized by fibroblasts are the key component in providing strength to tissues. Type III collagen, which is prevalent during proliferation, is replaced by type I collagen gradually in the remodeling stage [45]. Meanwhile, **collagen fibers reorganizing** process, in which originally disorganized collagen fibers are rearranged, cross-linked, and aligned along tension lines, also adds up to the tensile strength restoring. Besides, there are also composition changes in in **extracellular matrix remodeling**. Hyaluronic and fibronectic acid are degraded by cells and plasmatic metalloproteinase. Also the collagen phenotype proportion also changes like mentioned above [45]. Based on the above events, a denser extracellular matrix forms

slowly, along with scar loses, red color fades and capillary regresses as the long-lasting remodeling stage proceeds.

These major stages of normal wound healing stages are summarized in **Figure 2**.

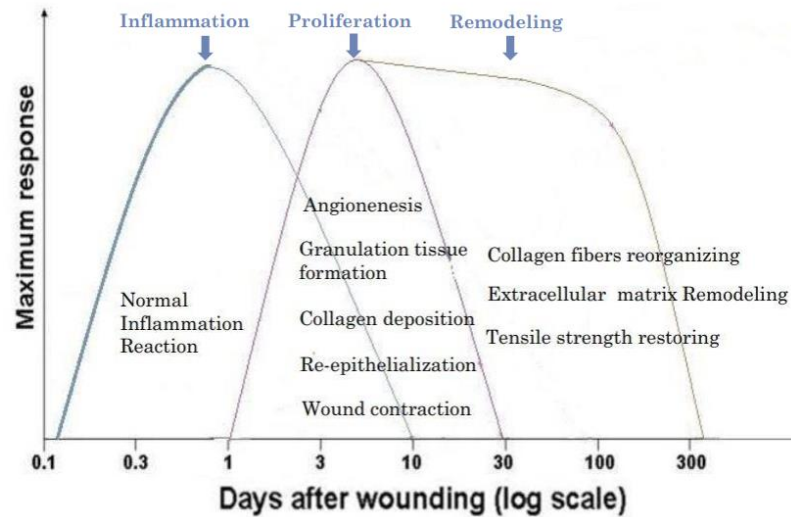


Figure 2. Physiological Process of Wound Healing.

2.2. Diabetic Wound Healing

Diabetic wound healing is impaired due to hyperglycemia-induced oxidative stress and prolonged inflammation, which finally leads to delayed diabetic wound healing. In diabetic ulcers, impairment of wound healing is caused by intrinsic factors like peripheral neuropathy, peripheral vascular damage, and systematic consequence of diabetes and extrinsic factors [4]. Among these peripheral vascular diseases (PVD) and peripheral neuropathy (PN) are the leading causes of Diabetic Foot Ulcers (DFUs). Hyperglycemia situation in diabetic patients causes mitochondrial superoxide overproduction in endothelial cells in peripheral blood vessels. The imbalance between the free radicals and the endogenous antioxidant capacity is detrimental to wound healing [51]. The activated oxidative stress in endothelial cells is caused by a high-glucose environment through pathways such as the advanced glycation end products (AGEs) pathway, the classical polyol pathway, PKC pathway, the sorbitol pathway, the acetylglucosamine pathway, etc. [52]. Further, the increased higher permeability of vascular vessels lets more inflammatory cells infiltrate to prolong the inflammation stage of wound healing. So that the following proliferation stage and

subsequent remodeling process are also delayed and chronic diabetic wound forms, leading to amputation and even life-threatening situations in diabetic patients. All the information emphasizes that the prolonged inflammatory phase under diabetic situation is the very critical stage leading to the chronic diabetic wound.

The inflammation stage of the diabetic wound is characterized by PMNs and monocytes over infiltration from blood vessels after tissue injury [37, 53, 54]. Activated neutrophils can produce protease, which can downregulate growth factors needed in the wound healing process while degrade the extracellular matrix to enlarge the wound area, thus leading to persistent inflammation and tissue damage [54]. For the prolonged inflammation stage, the proliferation stage in the diabetic wound is also delayed. The cellular functions and related wound processes are impaired in the diabetic wound, which includes fibroblasts, keratinocytes, endothelial cells, ECM, blood circulation, and granulation formation. Besides low levels of VEGF in the diabetic wound as mentioned before, transforming growth factor beta (TGF- β) and fibroblast growth factor 2 (FGF-2) are downregulated in diabetic angiogenesis [9, 55]. ECM proteins are over degraded by overexpressed matrix metalloproteinases (MMPs) in the diabetic wound [55]. Keratinocytes migrate to repair injured dermis by re-epithelialization undergrowth factors such as endothelial growth factor (EGF), keratinocyte growth factor (KGF) and fibroblast growth factor-2 (FGF-2) is also slowed downregulated [55, 56]. Studies showed that angiogenesis, re-epithelialization, granulation tissue formation, and wound closure are all downregulated in diabetic wound animal models [9, 12, 13, 28]. The delayed proliferation stage then also postpones the sequencing remodeling stage, thus finally leading to unhealed diabetic ulcers. The remodeling stage in diabetic wound healing, new collagen synthesis, collagen fiber phenotype change is impaired by overexpressed MMPs. In diabetic wounds, the cross-linking of collagen fibers is disturbed to decrease the wound tensile strength in the remodeling stage [55, 56]. Evidence showed that in diabetic remodeling stage, total collagen content and tensile strength are significantly lower than in the normal animal models, with collagen pattern also impaired [28].

2.2.1. Oxidative Stress

Oxidative stress is an imbalance shift between normal status and intracellular antioxidant system interruption. Both ROS and RNS can cause oxidative stress, with ROS the main component of oxidative stress. ROS means all oxygen-associated species that have higher oxidative potential (higher reactivity) than molecular oxygen: singlet oxygen, superoxide anion, hydrogen peroxide, and hydroxyl radical (OH•) [57]. The main components of oxidative stress include singlet oxygen 1O_2 , superoxide anion $O_2^{\bullet-}$, hydroperoxyl radical $HO_2\bullet$, hydrogen peroxide H_2O_2 , hydroxyl radical $\bullet OH$, hypochlorous acid HOCl and trioxocarbonate radical CO_3 . They are thought to be the key mediator in initiating, mediating, and regulating the cellular and biochemical complexity of oxidative stress both in physiological and pathophysiological processes [58]. Normally, each day human body uses about 250g of oxygen, 2-5% of which is turned into reactive oxygen species (ROS). Molecular oxygen is in a relatively inert triplet state 3O_2 for the ground state, the change of electron spin pairing makes oxygen shift from molecular status to free radical anions, which is reactive to cause damage to the host cell. In mammals, ROS are produced in cells through the respiratory chain. Superoxide is the main component of ROS.

The superoxide radical anion can be dismutated by SOD to H_2O and hydrogen peroxide (H_2O_2), which can cause serious damage to the cell at the presence of iron or copper ions in reaction of Fenton reaction. Hydroxyl radicals ($\bullet OH$) are highly oxidative, it can cause cellular macromolecules oxidation.

To keep normal redox homeostasis, the antioxidant defense system, which can reduce (scavenge) and/or dismutation of $O_2^{\bullet-}$ and/or $HO_2\bullet$ and their protonated forms, take the responsibility to detoxification to keep the low levels of free radicals and reactive nonradical species in physiology process. On the other hand, ROS as a signaling molecular can induce the genetic response of expression of enzyme antioxidants, such as catalase (CAT), various peroxidases and peroxiredoxins, heme oxygenase (HO), to reduce the oxidated DNA, lips, and protein products. For example, peroxiredoxins can detoxify lipid peroxides. Besides the enzymatic antioxidants, low molecular weight

antioxidants also contribute to the redox regulation in skin wounds. Both exogenous and endogenous molecules are included, such as glutathione, ubiquinone, uric acid, lipoic acid, vitamins E, vitamin C, carotenoids, and phenolic compounds [41, 59, 60].

However, when the antioxidant defense system fails to eliminate the oxidants, or the oxidants level too low, the process of redox homeostasis and oxidant detoxification process goes into an imbalanced way, oxidative stress occurs, resulting in severe cell damage [41, 58].

In wounded and inflamed tissue, large amounts of ROS, especially highly reactive superoxide radical anion, are produced by the NADPH oxidase enzyme complex, especially in highly inflamed cells by respiratory burst [61, 62]. In the wound healing process, neutrophils, macrophages, endothelial cells, and fibroblasts all produce superoxide and a lot of derivatives via the phagocytic isoforms of NADPH oxidases. In the wound healing process, superoxide can be released from endothelial cells by stimulation of thrombin, PDGF, and TNF- α . While in fibroblast, superoxide can be released under influence of IL-1, TNF- α , and PAF [63]. Under ischemic conditions in wounds, high concentrations of $O_2^{\bullet-}$, H_2O_2 , and $\bullet OH$ are produced by endothelial cells [58]. Most hydrogen peroxide anions are contributed by neutrophils and macrophages.

The beneficial effect of physiological level ROS is vital to downregulate local blood flow via vasoconstriction and thrombus formation. The onset of ROS short time high level can stimulate platelet aggregation, thus contribute to chemotaxis and adhesion molecule expression for the sequencing platelet and inflammatory cell recruitment [64]. What's more, the release of ROS can also provoke diapedesis of adherent leukocytes infiltration for cleaning against the microorganism at the injury wound site. In wound healing stages, ROS can promote fibroblast proliferation and migration, FGF expression collagen deposition and fibronectin production, VEGF expression and angiogenesis, ECM formation, and re-epithelialization processes [64, 65].

Diabetic patients suffer from abnormal healing of diabetic ulcers with primary index change of oxidative stress and wound healing parameters [59]. Hyperglycemia can

induce excessive and prolonged production of $O_2^{\bullet-}$ in wounds, the detoxification process is much slower than the ROS generation rate, thus the balance of oxidative is impaired, leading to oxidative stress [57]. Excessive ROS caused oxidative stress induces endothelial dysfunction, which is a hallmark of impaired healing, So the rationale that reducing reactive oxygen species (ROS) induced oxidative stress and correcting peripheral vessel dysregulation could improve diabetic wound healing. AGEs are a set of heterogeneous molecules that produced from nonenzymatic reaction of reducing sugars with amino groups of lipids, DNA and proteins. During abnormal metabolism process, such as hyperglycemic, hyperlipidemic and excessive oxidative stress conditions, the AGEs accumulate gradually [66]. Oxidative stress is difficult to characterize in various diseases and conditions, with various measure methods [66]. MDA in serum sample a marker for oxidative stress in diabetes patients [66, 67]. It is reported that serum MDA content was significantly higher in patients with peripheral vascular disease-related foot ulcers, while antioxidants were significantly lower [68]. For the lasting oxidative stress, the wound becomes stagnant at the inflammatory state, the transition from inflammation stage to proliferation stage is delayed [57, 58]. However, overproduction of ROS or insufficient ROS detoxification leads to oxidative stress, the major cause of non-healing chronic wounds. Growing evidence showed that antioxidant targeting therapy can improve the healing process in chronic wounds [69-75]. All this evidence suggests that targeting oxidative stress therapy is a promising perspective on diabetic wound healing treatment. Among the various pathways, the Nrf2 pathway plays a role in the chronic wound healing process [69]. It is also involved in the antioxidative pathway which affects re-epithelialization and angiogenesis in diabetic wound healing [76, 77].

2.2.2. Interleukin 6

Interleukin 6 (IL-6) is also known as Cytotoxic Differentiation Factor (CDF), Hepatocyte Growth Factor (HGF), Hepatocyte-Stimulating Factor (HSF), B-cell Stimulatory Factor 2 (BSF-2), and Interferon beta 2 (INF- β 2) [78]. Interleukin-6 is the main member of the IL-6 superfamily (PfamPF00489), which also includes Granulocyte/Colony-Stimulating Factor (G-CSF), IL23A, and Cardiotrophin-Like

Cytokine Factor 1 (CLCF1) [78]. IL-6 gene is located at chromosome 7 and 5 in the human and mouse genomes, respectively [79, 80]. The gene for human, mouse, and rat IL-6 all contain four introns and five exons [81]. In the protein-coding region of the IL-6 gene, exon lengths, cysteine location, and the positions of exon/intron boundaries are conserved among different species [81]. IL-6 was firstly identified as a B-cell differentiation factor. It can be secreted by various types of cells mainly fibroblasts, leukocytes, and endothelial cells, to exert multiple functions in hemopoiesis, immune response, and inflammation [82]. It has interaction with the interleukin-6 receptor, glycoprotein 130, and galectin-3 [83].

IL-6 is produced at the site of inflammation and plays a key role in the acute phase response as defined by a variety of clinical and biological features such as the production of acute-phase proteins [84, 85]. It plays roles in various diseases such as diabetes, depression, Alzheimer's Disease, systemic lupus erythematosus, prostate cancer, rheumatoid arthritis and et al. [86-93]. IL-6 is also essential in normal wound healing by promoting angiogenesis, re-epithelialization, wound closure, collagen accumulation, in normal wound healing [94, 95]. However, IL-6 has a bilateral effect, at some level it plays a beneficial effect, but in chronic inflammation, it plays a pro-inflammatory role, such as in chronic wound healing. One study found that there was a positive correlation between high serum IL-6 levels in diabetic patients with foot ulcers comparing with patients without foot ulcers. This indicates that high IL-6 protein level has a detrimental effect on diabetic wound healing [95]. This is probably IL-6 has inclination to transient acute inflammation into chronic one for its stimulatory property on both T and B cells [96]. Upregulation of IL-6 protein expression is accompanied by hyperglycemia in macrophage cells both isolated from normal mice and diabetic mice [97]. The evidence showed that IL-6 plays an important role in the wound healing process. Expression of IL-6 has been significantly elevated in a diabetic rabbit and mice cutaneous wound model comparing with control [35, 98]. It is a critically important cytokine in host defense in inflammation in the diabetic wound healing process. Hyperglycemia could produce excessive ROS, which could increase the overexpression of IL-6 [34]. A diabetic animal model also showed a higher level of IL-6 and delayed wound healing [35]. In

diabetic patients, IL-6 protein levels and the circulating acute-phase protein levels were significantly higher than those without foot ulcers [99]. Much other evidence also showed the high IL-6 in diabetic wounds. So, it is important to control the excessive amount of IL-6 in diabetic wounds.

2.2.3. Vascular Endothelial Growth Factor (VEGF)

Vascular endothelial growth factor (VEGF) is a significant signaling protein produced by various cells. VEGF is also known as VEGF-A, is a protein with vascular permeability activity that was originally purified from a fluid secreted by a tumor and later been shown to exert angiogenic property [100-102]. The VEGF family includes VEGF-A, VEGF-B, VEGF-C, VEGF-D, PGF (placental growth factor), VEGF-E (Orf-VEGF), and trimeresurus flavoviridis VEGF, in which the former 5 members exist in mammals, including human. The vascular endothelial growth factor (VEGF) and its receptor (VEGFR) have been proved to play major roles both in physiological and pathological angiogenesis. VEGF family genes share 8 conservative residues at definite zone, which are very similar to PDGF family genes such as M-CDF, SCF and Flt3-L. 6 residues of the 8 are from 3 S-S intramolecular bonds and generate 3 loop structures. The other two cysteines are form 2 S-S intermolecular bonds, making contributions to the stable homodimer structure of VEGF [103]. By activating 2 receptors of VEGFR-1 (Flt-1) and VEGFR-2 (KDR/Flk1 in mice), in which VEGFR-2 is mainly a signal transducer for angiogenesis, with a preference to activate the PLC γ -PKC-MAPK pathway for signaling, VEGF-A regulates angiogenesis and vascular permeability. While on the other hand, VEGF-C, VEGF-D, and their receptor VEGFR-3 (Flt-4) regulate lymphangiogenesis mainly [100]. **VEGF** plays a key role in the wound healing proliferation stage by increasing angiogenesis, for neovascularization, the hallmark of an established healing response, is the indispensable process to providing oxygen and needed nutrients during the formation of granulation tissue [104]. VEGF is a major angiogenesis promoting factor that could increase wound healing in diabetic incisional wounds [105]. It is secreted at a suitable time to promote a vigorous and mature vasculature. Studies showed that in the hypoxia context, VEGF is the most dominant proangiogenic factor in wound healing [47, 48, 106]. While the evidence

showed that both **VEGF** mRNA and protein levels are severely decreased in the diabetic animal models and clinical diabetic patient foot ulcer [12, 105, 107-109]. Upregulation of expression of VEGF protein in animal cutaneous wound model increased angiogenesis thus promoting wound healing in both nondiabetic and diabetic mice model [12, 110]. Furthermore, there is also evidence which has proved that upregulated VEGF level can enhance wound healing in the clinical patient [108]. Topical application of VEGF enhanced angiogenesis in diabetic mice wounds [111]. From the information above, VEGF is pivotal in wound healing angiogenesis.

This summarization of pathophysiological features of wound healing in the diabetic situation is shown in **Figure 3**.

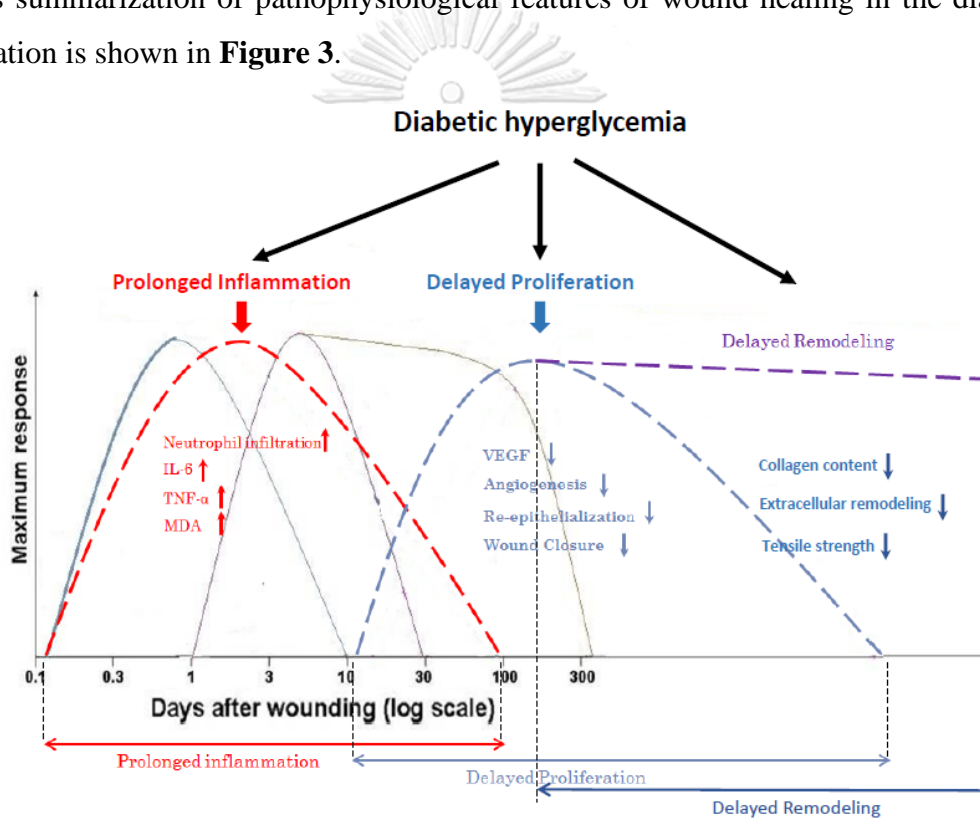


Figure 3. Pathophysiological Features of Diabetic Wound Healing.

In all, optimal healing of a cutaneous wound requires a well-orchestrated integration of the complex biological process including inflammation, proliferation, and remodeling. Responses to inflammatory mediators, growth factors, and cytokines, and mechanical forces, should be in a normal and timely order. However, this orderly progression of the healing process is impaired in diabetic wounds. Abnormalities

including insufficient blood supply, weakened angiogenesis, low degree of granulation tissue regeneration, and prolonged remodeling in the wound healing process. Luckily, the emerging occurrence of treatment targeting different stages of wound healing has been increasing in recent years in diabetic wound healing preclinical and clinical research. A deeper understanding of the cellular and molecular pathologies in diabetic wound, together with technological breakthroughs and strict adherence to diabetic wound care, is giving enlightenment and hope for the diabetic wound healing [112].

2.3. Simvastatin and *Phyllanthus emblica* Linn.

2.3.1. Simvastatin

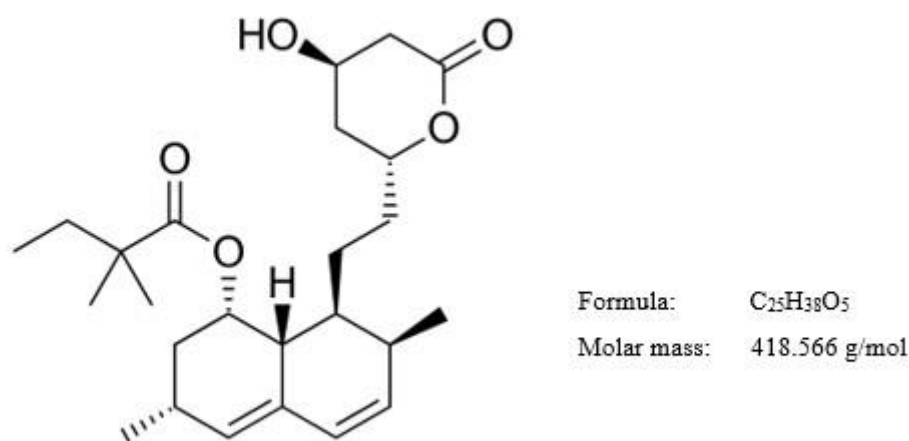


Figure 4. Chemical Structure of Simvastatin.

(<https://en.wikipedia.org/wiki/Simvastatin>)

Simvastatin (SIM) is a mostly used medication to lower lipid by decreasing cholesterol synthesized by the liver through inhibiting 3-hydroxy-3-methylglutaryl (HMG) coenzyme A reductase, obtained by synthesis from lovastatin, first introduced in 1988. **Figure 4** shows the chemical structure of simvastatin. The bioavailability of simvastatin is about 5% with the protein binding 95%, with a half-life of 2 hours for simvastatin and 1.9 hours for simvastatin acid. The side effects of simvastatin taken

orally may include indigestion, eczema, constipation, headaches, and nausea, liver problems, muscle breakdown, and a chance of increased blood glucose levels. It has interaction with some cardiovascular disease treatment drugs, such as verapamil, diltiazem, amiodarone, amlodipine, and ranolazine, and also interaction with grapefruit juice [113]. Vascular redox signaling imbalance can induce oxidative stress in vascular vessels. It is suggested as a rational therapeutic target in vascular disease pathogenesis. 3-hydroxy-3-methyl-glutaryl-CoA reductase inhibitors or statins are potent lipid-lowering drugs that have beneficial effects on vascular redox signaling to improve cardiovascular outcomes [114].

2.3.1.1. Pleiotropic Effects of Simvastatin

2.3.1.1.1. Pleiotropic Effects of Simvastatin in Various Diseases

The canonical effect of simvastatin treatment lies in hyperlipidemias, including hypercholesterolaemias, combined mixed hyperlipidemia hyperlipoproteinemias, hypertriglyceridemia, and primary dysbetalipoproteinemia. The fundamental mechanism of this effect is to inhibit hepatic cholesterol biosynthesis, upregulate the hepatic low-density lipoprotein (LDL) receptors, and decrease serum LDL-cholesterol and triglyceride levels. The cardiovascular protective effects of simvastatin that are independent of LDL-cholesterol lowering are called pleiotropic effects [9-17]. Clinical observation studies in the UK, US, Canada, and Denmark showed that simvastatin and other statins use in clinical patients is associated with lower mortality in pneumonia patients [115-119]. Due to the immunomodulatory and neuroprotective properties, high-dose simvastatin (80mg) showed the ability to reduce the annualized rate of whole-brain atrophy in patients with secondary progressive multiple sclerosis [120]. Furthermore, statin (including simvastatin) treatment can reduce mortality by 30% in patients with coronary artery disease and congestive heart failure [121]. Another a pooled analysis of randomized trial data showed that the use of statin therapy was associated with a lower risk of pancreatitis in patients with normal or mildly elevated triglyceride levels [122].

Besides the pleiotropic effects of simvastatin on cardiovascular diseases, it also has pleiotropic effects on non-cardiovascular-related diseases. 20 mg/day dose of simvastatin showed a low anti-inflammatory effect in rheumatoid arthritis patients

with good safety, and statin treatment is also associated with lower mortality risk in patients with rheumatoid arthritis [121, 123-125]. Simvastatin can increase bone formation, bone strength in rodents and reduce hip and vertebral fractures in aged women [126-128]. A population-based case-control study showed that long-term lipid-lowering treatment by using simvastatin included statin medication could decrease the risk of gallstone disease in clinical patients [129]. Furthermore, simvastatin has been widely used in the treatment of asthma, for but not limited to its anti-inflammation effect [130, 131]. Simvastatin has been proved to improve ischemic stroke in animal models and clinical stroke patients by neuron-protection property [132, 133]. Simvastatin can reduce cardiac allograft rejection and increase survival after a heart transplant [134]. Simvastatin also exerts anti-inflammatory function by decrease CRP to enhance endothelial dysfunction in rheumatoid arthritis patients [135]. At the cell level, simvastatin has been proved to enhance eNOS expression and activity downregulate Plasminogen activator inhibitor-1 expression and enhance tissue-type plasminogen activator expression in endothelial cells and human vascular smooth muscle cell [136, 137]. It can also increase peroxisome proliferator-activated receptor- α and γ expression in the endothelial cell line [138, 139], decrease proinflammatory cytokines (IL-1 β , IL-6, and COX-2) expression [140, 141], and downregulate CD40 expression [142]. In vascular smooth muscle cells, simvastatin has been proved to downregulate NADPH oxidase activity, downregulate PDGF, and downregulate cell migration and proliferation [143-145]. In myocardium cell, simvastatin showed the property in increasing nitric oxide production [146]. In platelet, simvastatin can inhibit platelet activation while activating PPAR α and PPAR γ *in vitro* and *in vivo* [147]. In monocyte and/or macrophage cells, simvastatin decreased MMP expression and secretion [148]. Besides, simvastatin can also prevent endothelial tissue factor expression and activity through downregulation of Rho/Rho-kinase and activation of Akt [149]. Downregulate proinflammatory cytokines (IL-1 β , IL-6, IL-8, and TNF- α) expression by simvastatin was also observed both in an animal model and clinical patients [138, 150]. Moreover, downregulation of MCP-1 secretion in human macrophage and in clinical hypercholesterolemic patients were observed [142, 150]. Simvastatin can also reduce vascular inflammation by reduce of

leukocyte-endothelial cell adhesion [151, 152], T-cell activation [152-155], and inhibition of transcription factor nuclear factor- κ B activation [156].

In summarization, simvastatin has a prevalent pleiotropic effect on diseases besides its classical lipid-lowering function, based on its antioxidant and anti-inflammatory properties. This provides great potential for simvastatin use in the treatment of wound healing.

2.3.1.1.2. Pleiotropic Effects of Simvastatin on Wound Healing

In recent years, simvastatin has been reported for its lipid-lowering-independent effect on wound healing. Several topical application studies of simvastatin in the animal models showed that simvastatin has wound healing potential [157]. Asai J. et al have proved that topical application of simvastatin accelerates wound closure and other wound healing characters in STZ-induced diabetic mice [12]. Bitto A. et al have shown evidence that simvastatin increased both VEGF mRNA and protein level of the wound while increasing the breaking strength in diabetic mice, leading to improved diabetic wound healing [10]. Rego A. et al applied simvastatin micro-emulsion to increase wound healing in infected rat wounds by exerting its anti-inflammatory and anti-bacterial effect through downregulation of the expression of IL-1 β and TNF- α in the wound [11]. **Table 1** shows the research doses of simvastatin in the wound healing effect.

Table 1. Simvastatin Dose in Wound

Route of Administration	Animal Model	Wound Size	Drug Amount	Dose (mg/kg BW) (based on mice=25g, rat=300g)	% W/V (mg/ml)	Reference
Topical	Infected mice wound (excisional wound)	6-mm biopsy punches (28 mm ²)	1.25µg	0.1	6.25%	[13]
Topical	Infected rat wound (excisional wound)	Squared skin wound (1cm ²)	2mg	6.7	1000%	[11]
Topical	Diabetic wound mice (excisional wound)	8-mm biopsy punch (50mm ²)	50µg	2	0.5%	[10]
Oral	Diabetic wound mice (excisional wound)	0.6mm × 0.6mm square full-thickness	–	0.25	–	[9]

2.3.2. *Phyllanthus emblica* Linn.



Figure 5. *Phyllanthus emblica* Linn.

(Picture from the website: www.google.com)

Phyllanthus emblica Linn. (Syn. *Embllica Officinalis* Gaertn.) (PE or EO) has profuse sources in tropical and subtropical countries as Thailand, India, China, and other Southeast Asia countries. Common names of *Phyllanthus emblica* Linn. are Indian gooseberry, Amla or Amlaki in India, Makhham Pom in Thailand, and Yu'ganzi in China. Medical use parts include dried fruit, fresh fruits (as shown in **Figure 5**, seed, flower, and bark. They have been used as a potent medicine in Ayurveda medication for a long history for fever, cough, jaundice, anemia, worms, diabetes, diabetic therapy, antibilious therapy, and help to relieve thirst, dyspesia, burning throat, and other digestive systems, and also as a tonic to restore vigor [18, 19]. Nowadays scientific research has proved that *Phyllanthus emblica* Linn. has antioxidant, anti-inflammatory, antidiabetic, antihyperlipidemic, immunomodulatory, hepato-protective, cardio-protective, cerebro-protective, anti-brain aging, anti-cancer, anti-microbial, wound healing property, and dermato-protective effects, etc. [19].

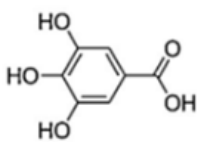
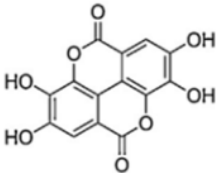
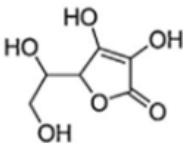
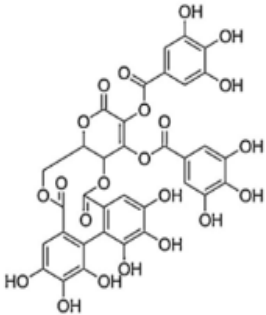
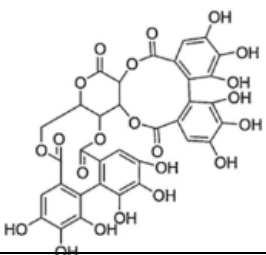
Phyllanthus emblica Linn. contains fluent protein, carbohydrates, and high vitamin C (200-900 mg per 100 g of edible portion) [158], which are important factors aiding wound healing. Additionally, *Phyllanthus emblica* Linn. also contains numbers of tannins and phenolic compounds such as phyllembelin, rutin, curcuminoids, phyllembelic acid, and emblicol, gallic acid, emblicanin A and emblicanin B,

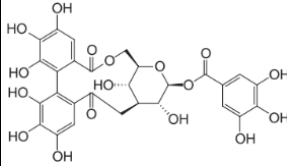
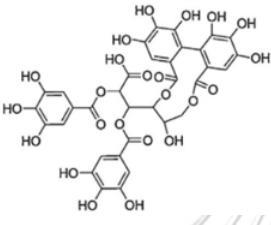
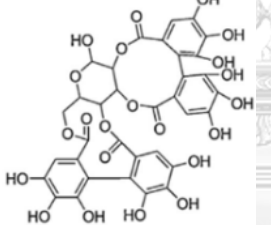
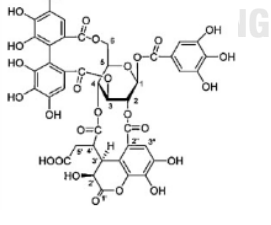
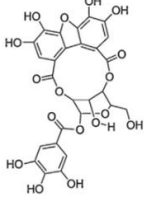
punigluconin, pedunculagin, and others phytoconstituents, as shown in **Table 2** [19]. The free radical scavenging, antioxidant, anti-inflammatory, and other effects of bioactive compounds from *Phyllanthus emblica* Linn. are shown in **Table 3**. The HPLC graph by Middha S.K. et al. has shown that major components of PE include ascorbic acid, quercetin, rutin, gallic acid, mucic acid, and β -glucogallin in methanolic extract of PE fruit [159].

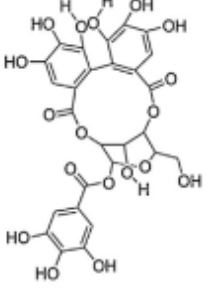
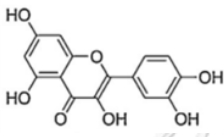
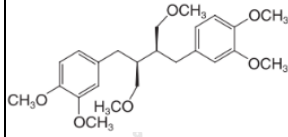
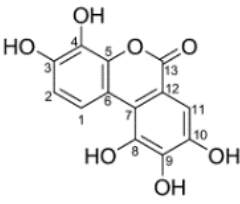
Table 2. Phytochemicals in *Phyllanthus emblica* Linn. Fruit

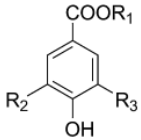
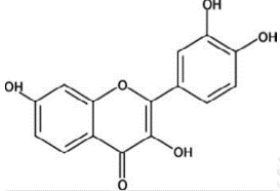
Chemical Category	Chemical Constituents
Hydrolysable Tannins	Emblicanin A and B, Punigluconin, Pedunculagin, Chebulinic acid (Ellagitannin), Chebulagic acid (Benzopyran tannin), Corilagin (Ellagitannin), Geraniin (Dehydroellagitannin), Ellagotannin
Alkaloids	Phyllantine, Phyllantidine
Phenolic Compounds	Gallic acid, Methyl gallate, Ellagic acid, Trigallayl glucose, Phyllembein.
Amino Acids	Glutamic acid, Proline, Aspartic acid, Alanine, Cystine, Lysine
Carbohydrates	Pectin
Vitamins	Ascorbic acid
Flavonoids	Quercetin, Kaempferol
Organic Acids	Citric acid

Table 3. Bioactive Components from *Phyllanthus emblica* Linn.

Active Chemical component	Chemical Structure	Model	Route of Drug Administration	Dosage	Effect	Reference
Gallic acid		–	–	–	Antioxidant effect (DPPH [•] scavenging)	[160, 161]
Ellagic acid		–	–	–	Antioxidant effect (DPPH [•] scavenging)	[160, 161]
Ascorbic acid		–	–	–	Antioxidant effect (ABTS ^{•+} DPPH [•] scavenging)	[162]
Emblicanin A		T2DM patients	Oral	250mg, 500mg, twice daily (Capros [®])	Antioxidant, Anti-platelet	[25, 161, 163]
Emblicanin B		T2DM patients	Oral	250mg, 500mg, twice daily (Capros [®])	Antioxidant, Anti-platelet	[25, 161, 163]

Corilagin		–	–	–	Antioxidant effect (hydroxyl radical scavenging, DPPH [•] , Superoxide anion,)	[160]
Punigluconin		T2DM patients	oral	250mg, 500mg, twice daily (Capros®)	Antioxidant (MDA), Anti-platelet	[25, 163]
Pedunculagin		T2DM patients	Oral	250mg, 500mg, twice daily (Capros®)	Antioxidant (MDA), Anti-platelet, Anti-tumor,	[25, 163]
Chebulagic acid		–	–	–	Antioxidant (DPPH [•] scavenging), Anti-inflammation (cyclooxygenase assay)	[164]
Phyllanemblin in A		Isoproterenol-induced cardioto	Oral	100mg/kg, 250mg/kg, 500mg/kg. (with	Antioxidant, free radical scavenging effect	[165]

		xicity rat model		Phyllanem blinin B)		
Phyllanemblin in B		Isoprote renol- induced cardioto xicity rat model	Oral	100mg/kg, 250mg/kg, 500mg/kg. (with Phyllanem blinin A)	Antioxidant, free radical scavenging effect	[165]
Quercetin		Diabetic neuroph athy rat	Oral	15 mg/100 g, 10mg/kg	Antioxidant	[166]
Phyllanthin		—	—	—	Antioxidant effect (Hydroxyl radical, DPPH [•] , superoxide anion scavenging)	[160]
3,4,8,9,10- pentahydroxy- dibenzo[b,d] pyran-6-one		H ₂ O ₂ - induced PC12 <i>in</i> <i>vitro</i> cell	—	—	DPPH [•] scavenging (stronger than Vitamin E) ROS scavenging effect	[167]

Ethyl gallate and Methyl gallate	 <p>14 R₁=CH₂CH₃ R₂=R₃=OH 15 R₁=CH₃ R₂=R₃=OH</p>	H ₂ O ₂ - induced PC12 <i>in</i> <i>vitro</i> cell	-	-	DPPH [•] scavenging (stronger than Vitamin E)	[167]
Fisetin		LPS- stimulat ed RAW26 4.7 cells	-	-	Antiinflam- mation effect	[168]

2.3.2.1. Hypoglycemic Activity of *Phyllanthus emblica* Linn.

In Ayurvedic medicine, *Phyllanthus emblica* Linn. seeds or dried amla powder are daily taken with bitter gourd juice to stabilize the blood sugar level as a household remedy. Tribal practitioners in Bangladesh use the leaves or fruit of *Phyllanthus emblica* Linn. to treat diabetes. Besides the traditional use of PE and in modern research, both have showed that *Phyllanthus emblica* Linn. has a significant hypoglycemic effect in both animal models and clinical diabetic patients [164, 166, 167, 169-171].

2.3.2.2. Antioxidant Activity of *Phyllanthus emblica* Linn.

Both in animal models and clinical diabetic patients, *Phyllanthus emblica* Linn. has been proved to increase the antioxidant defense system enzymes, such as GPx, SOD, CAT, and GSH [25, 163, 169, 172]. In the human HepG2 *in vitro* model, GSH, SOD, CAT, and GSH have been proved to be upregulated after treatment of *Phyllanthus emblica* Linn. fruit aqueous extract [173]. Zhang et al. also proved that some compounds isolated from *Phyllanthus emblica* Linn. fruits showed significant DPPH[•] scavenging and cytoprotective effects in H₂O₂-induced PC12 cell injuries [167]. Several studies showed that *Phyllanthus emblica* Linn. has DPPH[•] and ABTS^{•+} radical scavenging activities, and also hydroxyl, superoxide, H₂O₂, peroxy nitrite, single oxygen, hypochlorous acid scavenging activities *in vitro* [174].

The polyphenols and hydrolyzable tannins, which have ascorbic acid-like action from *Phyllanthus emblica* Linn. fruits, such as gallic acid, ellagic acid, emblicanin B, and emblicanin even have stronger superoxide anion radical scavenging ability than vitamin C [10, 12]. *In vitro* cell model, GSH, SOD, and CAT have been proved to upregulated after treatment of *Phyllanthus emblica* Linn. Extract [174, 175]. Besides, in various animal models *Phyllanthus emblica* Linn. have been proved to increase the antioxidant defense system enzymes and lipid peroxidation markers, such GPx, SOD, CAT, and GSH [25, 28, 174-176]. Usharani P. et al. also proved that *Phyllanthus emblica* Linn. extract could decrease MDA content and increase GSH level to prove that *Phyllanthus emblica* Linn. can reduce the systemic oxidative stress and inflammation in T2DM patients [25]. Yokozawa T. et al showed that *Phyllanthus emblica* Linn. extract exerts aortic anti-oxidative stress by inhibiting NF-KB in the rat aging model [172].

Low molecular weight hydrolyzable tannins of *Phyllanthus emblica* Linn., mainly Emblicanin A and Emblicanin B, Pedunculagin and Punigluconin are the main ingredients for the antioxidant effect of *Phyllanthus emblica* Linn. [177-179]. This low molecular tannin PE antioxidant has been found to have broad-spectrum antioxidant activity in quenching singlet oxygen, quencher for superoxide anion and hydroxyl radicals, with equivalent or even better performance than vitamin C, vitamin E, grape antioxidant, and Trolox C [178, 180-182].

Furthermore, PE low molecular tannin antioxidants also show good iron- and copper-chelating activity and MMP-1 and MMP-3 inhibitory activity. PE antioxidant utilizes a multilevel cascade of antioxidant compounds resulting in a long-lasting and stable antioxidant activity, while other antioxidants react from active form to inactive one [178]. PE extract together with Epigallocatechin-3-Gallate (EGCG) showed a strong antioxidant effect in diabetic patients. PE leaves extract can restore reduced glutathione, glutathione peroxidase, superoxide dismutase, catalase, and decrease LPO level in the liver and kidney of diabetic rats [169].

2.3.2.3. Anti-inflammatory Activity of *Phyllanthus emblica* Linn.

The active ingredients containing alkaloids, phenolates, tannoids, amino acids, and carbohydrates, have been proved to have an anti-inflammatory effect in different model studies by relieving pain or inhibiting inflammatory mediators [21, 23, 24]. *Phyllanthus emblica* Linn. powder has been proved to show anti-inflammatory effect in both acute and chronic wound of inflammation by comparing to diclofenac [176]. Water fraction of methanol extract of the plant leaves has shown an anti-inflammatory effect on carrageenan- and dextran-induced rat hind paw edema. The same fraction part showed an inhibition effect on human polymorphonuclear leukocytes (human-PMNs) migration *in vitro* [20]. In clinical T2DM patients, 500 mg/day extract of *E. officinalis*, which contains emblicanin-A, emblicanin-B, pedunculagin, and punigluconin, showed a significant downregulation effect on the aggregation of platelet in both single and multiple doses [183]. 150–600 mg/kg dosage range of *Phyllanthus emblica* Linn. aqueous extraction in rat showed dose-dependent anti-inflammatory and analgesic effect [22]. Muthuraman A. et al. reported anti-inflammation activity of 20 and 40 mg/kg dosage phenolic compounds from *Phyllanthus emblica* Linn. showed anti-inflammatory effect against both acute and chronic inflammation [24]. A component containing gallic acid and fisetin has been proved to have an anti-inflammatory effect *in vitro* cell model [168].

2.3.2.4. Effects of *Phyllanthus emblica* Linn. on Wound Healing

Additionally, *Phyllanthus emblica* Linn. has also been proved to show wound healing benefits in diabetic mice models. It has been proved that alcoholic extract of *Phyllanthus emblica* Linn. fruits could upregulate antioxidant enzymes like SOD, CAT, GPx and decrease MDA content at the wound site [28]. It also increases wound contraction speed, tensile strength, total collagen in granulation tissue in the rat wound model [28]. There is an oxidative and inflammatory environment in diabetic foot ulcers, antioxidants and anti-inflammation drug application to the wound site could enhance wound healing has been proved [8]. Therefore, there is a reason to infer the great potential that PE could enhance diabetic wound healing through its antioxidant and anti-inflammatory effects. **Table 4** shows the doses of PE used in wound healing and skincare.

Table 4. PE Doses in Wound Healing and Skin Care

PE extract	Route of Drug Administration	Model	Dosage (mg/kg BW) (calculation based on Human BW=60kg, rat=300g mice=25g)	The Equivalent Dose in Mice	Reference
PE extract for acne patients	Topical	Acne patients	10% (w/w) PE fruit extract	–	[184]
Skin Care: Moisturizing Lotion by Merck.	Topical	–	0.5% PE fruit extract	6.15% (w/w)	[185]
PE fruit extract (80% methanol)	Oral	Diabetic neuropathic pain rat model	10mg/kg	140mg/kg/d	[166]
Aqueous extract of PE fruit pulp	Oral	Diabetic rat	1250mg/kg	1.75g/kg/d	[26]
Capros® (commercial PE extract)	Oral	Diabetic patients	500, 1000mg/d	130mg/kg/d	[25]
PE fruit pulp crude powder	Oral	Diabetic patients	1,2,3g/d	–	[170]
Alcoholic extract of PE fruit	Topical	Diabetic wound mice	PE extract 2g in 200ml 90% ethanol (no volume shown)	–	[28]

PE also has been topically used in the treatment of skincare and diseases. In ayurvedic polyherbal formulations, Indian gooseberry is a common constituent, such as Triphala. Nowadays, natural products in the diabetic ulcer treatment area are attracting more and more attention. This suggests that antioxidant targeted therapy from natural medicinal products has great potential in wound healing treatment. More and more natural medicinal products are under exploration. Most medical plants exert their treatment effect in various diseases through antioxidant and anti-inflammation effects. Some still own potential anti-bacterial effects, especially essential oils extracted from medicinal plants. Some of the most commonly used essential oils against multidrug-resistant microorganisms, such as tea tree, St. John's Wort, lavender, and oregano, together with their incorporation into wound dressings are presented [186]. PE and its extract are mostly externally used in skincare research. It is also used externally in shampoos and hair oils. The topical application of PE extract in diabetic wound healing is very rare. However, the evidence presented before indicates that PE has great potential in the treatment of diabetic wound healing for its strong free radical scavenging, antioxidant and anti-inflammatory properties. For these beneficial properties in wound healing processes. This information supports that exploration of PE in the treatment of wound healing is very promising.

CHAPTER III

MATERIALS AND METHODOLOGY

3.1. Chemicals

3.1.1. PE Fruit Extraction

10.0 kg of fresh *Phyllanthus emblica* Linn. Fruits (PE) from Kanchanaburi, Thailand, were squeezed to get 3.4 kg minced pulp. After that, the squeezed *Phyllanthus emblica* Linn. pulp was extracted with distilled ethanol (1:2, w/v) for 72 hours, three times, as described previously [27]. The alcoholic extraction solution then was filtered through filter paper and dried by using vacuum rotary evaporation (BÜCHI Rotavapor R-114, Switzerland) below 45°C to yield 219.81 g of ethanol extract. The dried PE ethanol extract was kept under an airtight and light-protection condition at 4°C in refrigerator.

3.1.2. Simvastatin

Simvastatin was purchased from Sigma Aldrich (St. Louis, MO), with analytical purity > 97% (HPLC), Lot number 116M4716V, kept at 2-8°C with light protection.

3.1.3. Other Chemicals Used

PMA2 cream base (Paragon Cosmetics Co., Ltd., Thailand) component: aqua, propylene, caprylic/capric triglyceride, glycerin, glyceryl laurate, C13-14, iso-paraffin, C9-11 pareth-6, phenoxyethanol, dimethicone, xanthan gum, allantoin, polyacrylamide.

Other chemicals: Streptozotocin (Sigma Co., USA), Citrate buffer pH4.5 (Sigma Co., USA), Normal saline, Sodium pentobarbital, FITC-Dx-150 (Sigma Co., USA).

3.2. Drug Cream Preparation

In the experimental protocol, the various doses of 10%, 100%, and 200% for PE, 0.5%, 5% and 10% for SIM were used and mixed in PMA2-base cream. In Protocol 1, the dried PE ethanol extract was weighted according to the calculation of 10%PE, 100%PE, 200%PE; the simvastatin was weighted according to the calculation of 0.5%SIM, 5%SIM and 10%SIM as well. Then the weighted PE extract was put in the glass beaker, the corresponding amount of PMA2 cream based on the calculation was added into the glass beaker, with small amount each time. After the PMA2 cream was added into the glass beaker, the PMA2 cream and PE extract or SIM powder were stirred to mix well till the mixed cream presented a uniformed light-yellow color (for PE). After that, another small amount of PMA2 cream was added to the glass beaker and repeated the mix step, till all the corresponding amount of PMA2 cream was added to the glass beaker and mixed well. Then the prepared 10%PE, 100%PE, 200%PE, 0.5%SIM, 5%SIM, and 10%SIM creams were kept in tightly closed light-proof brown glass bottles at 4°C. Before the drug administration, the creams were taken out and put in the room temperature. Only one batch of each dose cream of PE and SIM was prepared and used in Protocol 1. After the 100%PE and 5%SIM were chosen to be the optimal doses which were used in Protocol 2. 100%PE cream and 5%SIM cream were prepared as in Protocol 1. For the combined cream, the exact amount of dried PE extract and SIM powder were weighted according to the calculation in Protocol 1. Then mix the PE with PMA2 cream base first as described before, then the weighted SIM powder was added to the well-mixed PE-PMA2 cream little by little. Then the well mixed 100%PE, 5%SIM and combined cream were kept in tightly closed light-proof brown glass bottles in at 4°C. Only one batch of 100%PE, 5%SIM and combined cream was prepared and used in Protocol 2. 10 µl of each cream was topically applied to the wound area of each wound once a day for 4-day groups, 7-day groups and 14-day groups.

3.3. Animals

Male BALB/C mice (7-8 weeks, 20–25 g) were purchased from Nomura Siam International Company, Bangkok, Thailand. The experimental procedures and daily care were approved by the Animal Care and Use Committee (CU-ACUC), Faculty of Medicine, Chulalongkorn University. All the procedures were conducted according to the guideline of experimental animals by The National Research Council of Thailand. All mice were housed at $25 \pm 3^\circ\text{C}$, with access to standard chow and sterilized water ad libitum under a 12 h light-dark cycle. A total of 120 BALB/C mice are used in this project.

3.4. Induction of Diabetic Wound Model

Male BALB/C mice (7-8 weeks, 20–25 g) were intraperitoneally injected by streptozotocin (STZ) to induce diabetes according to the previous method [9, 187]. Briefly, animals were induced by intraperitoneal injection of STZ in citrate buffer, pH 4.5 (Sigma Chemical Co., USA) at a dose of 45 mg/kg daily for consecutive 5 days. Two weeks after the first day of STZ injection, the fasting blood glucose level was detected from tail vein blood for each mouse. If fasting blood glucose level was ≥ 200 mg/dL, then the mouse was considered to be a successful diabetic mice model [9, 188].

3.5. Wound Creation

After four weeks of successful diabetic mice model establishment, the mice were anesthetized by isoflurane and the bilateral full-thickness excision skin wounds were created on each side of the dorsal midline of the mice by ophthalmic scissors after shaving the hair. We modified the wound creation method from the reproducible excisional wound healing previously by Galiano R.D. and his colleagues [189]. Before the wounding surgery, all the equipment, including the plastic frames, suture thread, were sterilized in 70% alcohol, and the whole dorsum of the mouse was also sterilized by a piece of 70% alcohol cotton pad. Along the spinal line, 30 mm from the middle of the mouse ears, and 15 mm from the spinal line, on the dorsal skin of both

sides of each mouse vertebral column, two 6mm × 6mm square full-thickness wounds were made by removing of the full-thickness skin by ophthalmic scissors [9, 11-13]. Full-thickness skin wounds of the non-diabetic age-matching control animals were made in the same way. The major wound healing way in rodent wounds is contraction, other than re-epithelialization in the human wound healing process [189, 190]. To mimic the re-epithelialization process in human wound healing, after wounding, we used the plastic stretch frame sutured to keep the wound stretched to prevent contraction. The bilateral full-thickness excisional wound of the diabetic and control groups was shown in **Figure 6**. The wound skin collected from the left side of mouse was used for the measurement of MDA content, IL-6, and VEGF protein levels, while the right side of wound skin of mouse was used for measurement of re-epithelialization and neutrophil infiltration.

After wounding, normal saline was used to moisturize the wound (only on the wounding day), then the wound was treated by topical application of 10 µl vehicle of PMA2 base cream, 10%PE, 100%PE, 200%PE, 0.5%SIM, 5%SIM, 10%SIM, or combined cream. The topical application of each cream type as described in the experiment design Protocol 1.1, Protocol 1.2, and Protocol 2 was performed by using a 1 ml syringe with minimum scale of 0.01 ml and without needle. After drug application, the mice were observed for 30 min for its activity, then taken back to the cage with new wood shavings bedding.

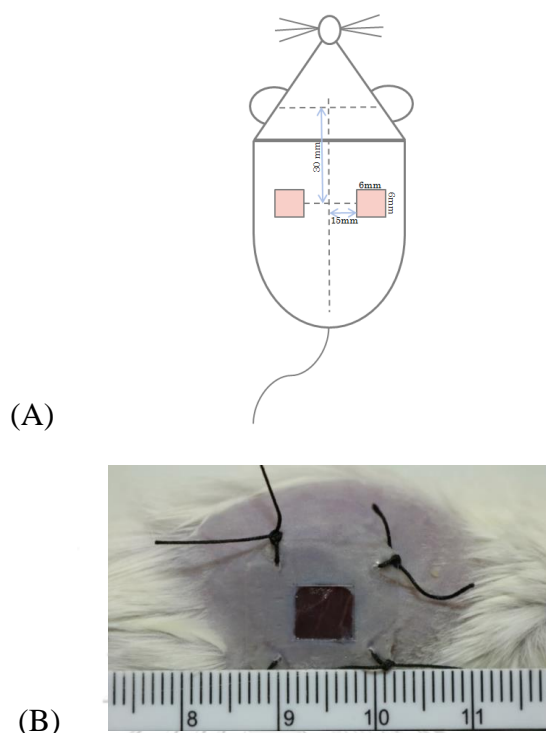


Figure 6. Wound Positions on Dorsal Skin of BALB/C Mouse.

(A). The positions of full-thickness bilateral wounds were made on both sides of the dorsum on each mouse; (B). At each wound site, the plastic stretch frame was sutured to keep the wound stretched and prevent contraction. The left side wound skin of mouse was used for measurement of MDA content, IL-6 and VEGF protein levels, while the right side of wound skin of mouse was used for measurement of re-epithelialization and neutrophil infiltration.

3.6. Experimental Design

3.6.1. To Study the Dose-Response of Simvastatin

20 male BALB/C mice were used in this study as shown in **Figure 7**. After two weeks of the STZ injection, all diabetic mice were processed according to the wound creation model as described previously and shown in **Figure 6**. To find out the most suitable dose of simvastatin, the wounded mice were divided into 4 groups: diabetic group (DM+Vehicle; n=5), diabetic mice treated with various doses of simvastatin cream; DM+0.5%SIM (10 μ l of PMA2 cream base contained 0.5% w/v SIM, n=5), DM+5%SIM (10 μ l of PMA2 cream base contained 5% w/v SIM, n=5), and DM+10%SIM (10 μ l of PMA2 cream base contained 10% w/v SIM, n=5), (Sigma Aldrich, USA). Each diabetic mouse was treated with 10 μ l cream topically once a day per wound. The most suitable dose of simvastatin was determined by the results

of the percentage of wound closure (%WC) and the percentage of capillary vascularity (%CV) on day 14.

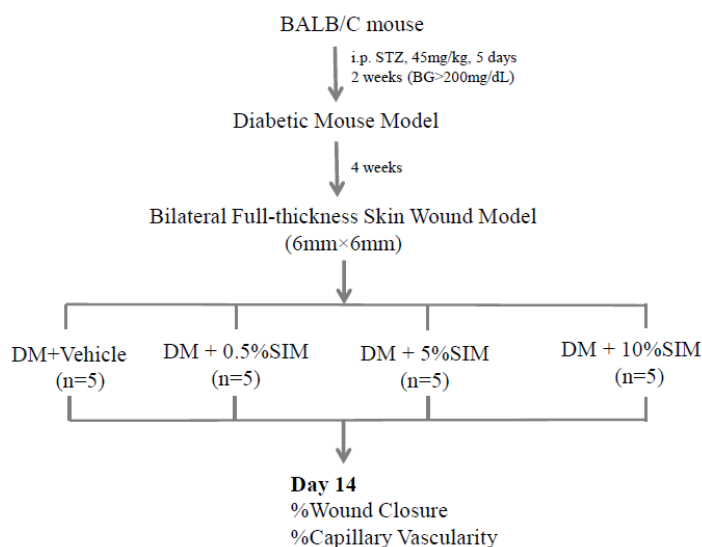


Figure 7. Experimental Design Used for the Study of Dose-Response of Simvastatin.

3.6.2. To Study the Dose-Response of PE

To find out the most suitable dose of PE, the wounded mice were divided into 4 groups: diabetic group (DM+Vehicle; n=5), diabetic mice treated with various doses of PE cream; DM+10%PE (10 μ l of PMA2 cream base contained 10% w/v PE, n=5), DM+100%PE (10 μ l of PMA2 cream base contained 100% w/v PE, n=5), and DM+200%PE (10 μ l of PMA2 cream base contained 200% w/v PE, n=5), (Sigma Aldrich, USA). Each diabetic mouse was treated with 10 μ l cream topically once a day per wound. The most suitable dose of PE was determined by the results of the percentage of wound closure (%WC) and the percentage of capillary vascularity (%CV) on day 14. The details are shown in **Figure 8**.

On day 14, the percentage of wound closure (%WC) was evaluated by equation presented in **Figure 10**. On day 14, the percentage of capillary vascularity (%CV) was calculated by equation presented in **Figure 13**.

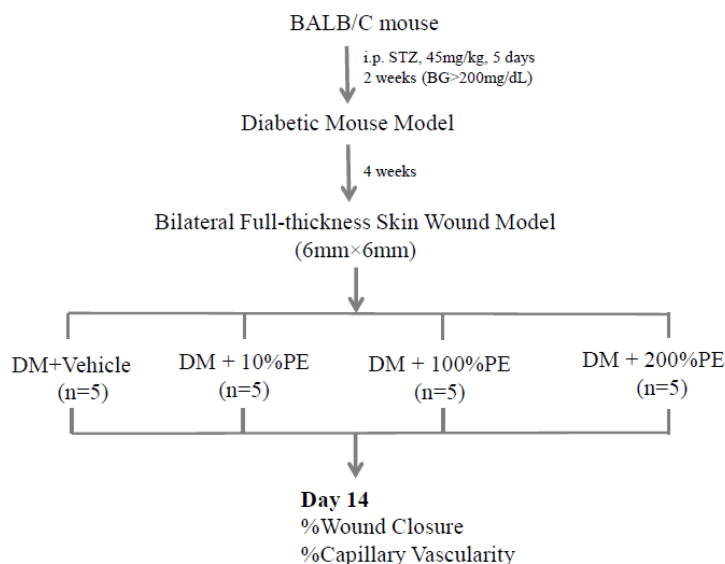


Figure 8. Experimental Design Used for The Study of Dose-Response of PE.

3.6.3. To Study the Effects of Combination of PE and Simvastatin on Diabetic Wound Healing in Mice

60 male BALB/C mice were used in this study. After wounding, animals were divided into 4 groups (DM+Vehicle; n=5), diabetic mice treated with the most suitable dose of simvastatin (DM+5%SIM, n=5), diabetic mice treated with the most suitable dose of PE (DM+100%PE, n=5), and diabetic mice treated with a mixture of simvastatin and PE (DM+Combine, 5%SIM +100%PE in PMA2 based cream, n=5), as shown in **Figure 9**. 100%PE was chosen to be the most suitable dose based on the %WC and %CV from Protocol 1, as shown in **Figure 24 (A-B)**. 100%PE increased significantly ($p<0.05$) both %WC and %CV on day 14. However, 200%PE showed increased %CV significantly ($p<0.05$) on day 14, with only tendency ($p=0.146$) of increasing %WC on day 14. For simvastatin, 5%SIM and 10%SIM increased both %WC and %CV significantly ($p<0.05$) on day 14, as shown in **Figure 25**. To lower the harmful systematic side effects of simvastatin, 5%SIM was chosen to be the most suitable dose for Protocol 2. All groups received 10 μ l cream topically once a day per wound.

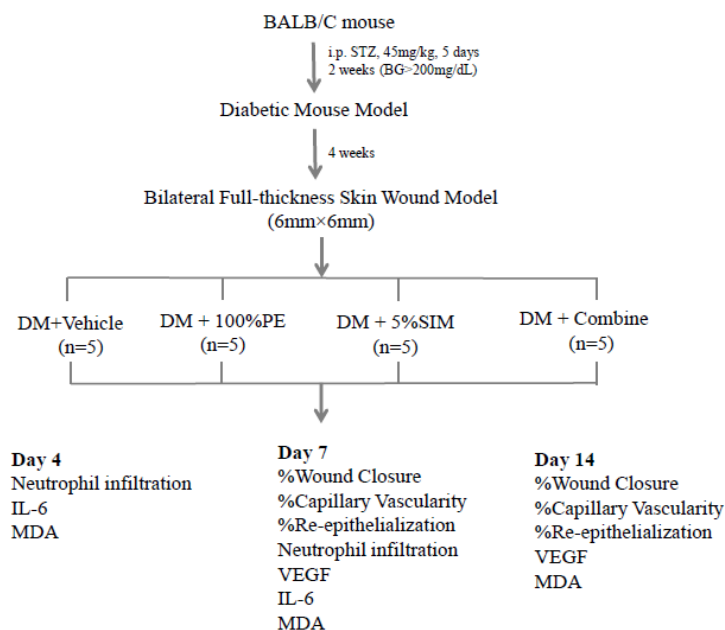


Figure 9. Experimental Design Used for The Study of The Effects of Combination of PE and SIM on Diabetic Wound Healing in Mice.

3.7. Measurement of Parameters

3.7.1. Percentage of Wound Closure (%WC)

In this study, all parameters were measured at two time-points, on day 7 and day 14, post-wound creation. To determine the effects of simvastatin and PE on the diabetic wound, the percentage of wound closure was used. On the experimental day, after the animal was anesthetized by intraperitoneal injection of sodium pentobarbital at a dosage of 45 mg/kg, the image of each wound area was taken by microscope (Model Nikon SMZ800, Japan).

As shown in **Figure 11 (A-E)**, the wound area was determined from the taken microscopic wound images. Firstly, by using Image-Pro Plus 6.1 Program, the RGB color image was enhanced through the brightness adjustment menu (42-46 level), the contrast adjustment menu (69 level), the gamma adjustment menu (9.7 level). After the enhancement process, the boundary of the “unhealed area” was indicated in the original RGB color image. Then this enhanced RGB color image was converted to a grayscale image as shown in **Figure 11 (B)**. In **Figure 11 (C-D)**, by using the

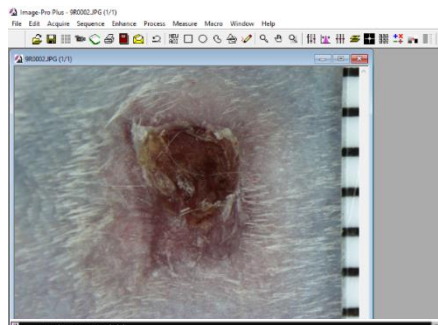
segmentation function from the curve line tool menu in the Image-Pro Plus 6.1 Software. The area marked with the yellow, red, and dark color is called the “unhealed” wound area. The procedures measuring the “unhealed” area are described in **Figure 11 (A-E)**. Then the percentage of wound closure (%WC) was calculated by using the equation shown in **Figure 10**.

$$\text{Percentage of wound closure (\%WC)} = \frac{(\text{Area of Original Wound} - \text{Area of Actual Wound}) \times 100}{\text{Area of Original Wound}}$$

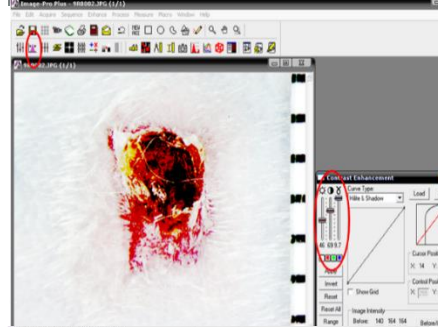
Figure 10. Equation of Calculation of Percentage of Wound Closure (%WC).



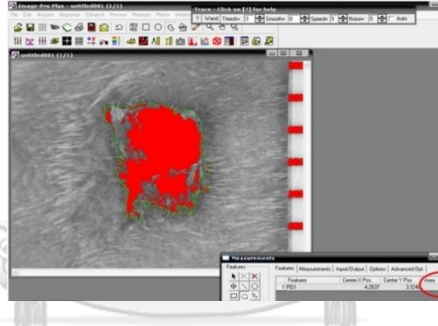
(A)



(B)



(C)



จุฬาลงกรณ์มหาวิทยาลัย
CHULALONGKORN UNIVERSITY

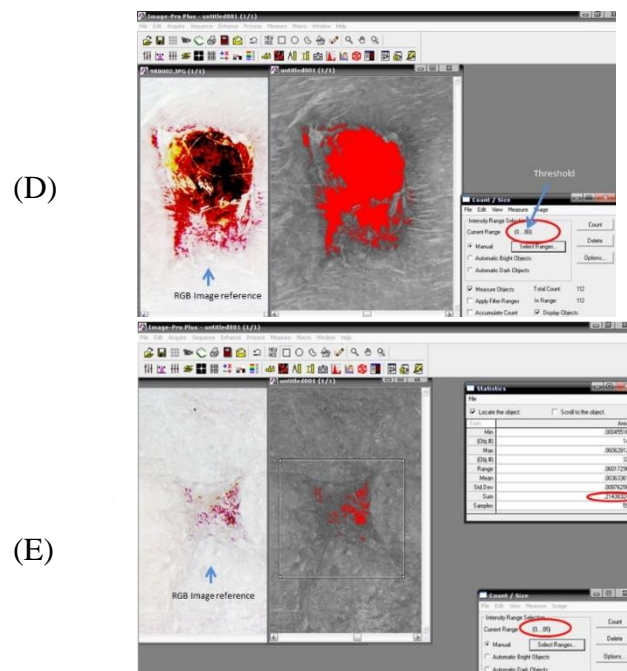


Figure 11. Wound Area Analysis by Using Image-Pro Plus Program (A-E).

(A). Original microscopic image of mouse wound from DM+Combine group on day 7 post-wounding; (B). By using Image-Pro Plus Program, the RGB colour image was enhanced through the brightness adjustment menu (42-46 level), the contrast adjustment menu (69 level), and the gamma adjustment menu (9.7 level), and then converted to grayscale 8 images; (C). By using the segmentation function and adjust the threshold value (77-87) to the unhealed area of each wound. When we used “pseudo-color labeled (red) the unhealed area selected by the threshold value could be compared to the original RGB colour image as the reference. This red colour area was then counted as the area of an unhealed wound. (D-E) Examples of wound area measurement were chosen from the wound area of day 7 and day 14 in DM+Combine groups.

จุฬาลงกรณ์มหาวิทยาลัย
CHULALONGKORN UNIVERSITY

3.7.2. Percentage of Capillary Vascularity (%CV)

After taken the microscopic images for wound area determination as described above, each mouse was anesthetized by intraperitoneal injection of sodium pentobarbital at a dosage of 55 mg/kg, then the jugular vein cannulation was performed to infuse 0.01 ml of 5% FITC-labeled dextran (MW= 250000, Sigma Chemical Co., USA) The capillary vascularity network of both wound sites was examined by fluorescence confocal microscope (ECLIPSE E800, Nikon) with a 10x objective lens on day 7 and day 14 post-wounding, as shown in **Figure 12**.

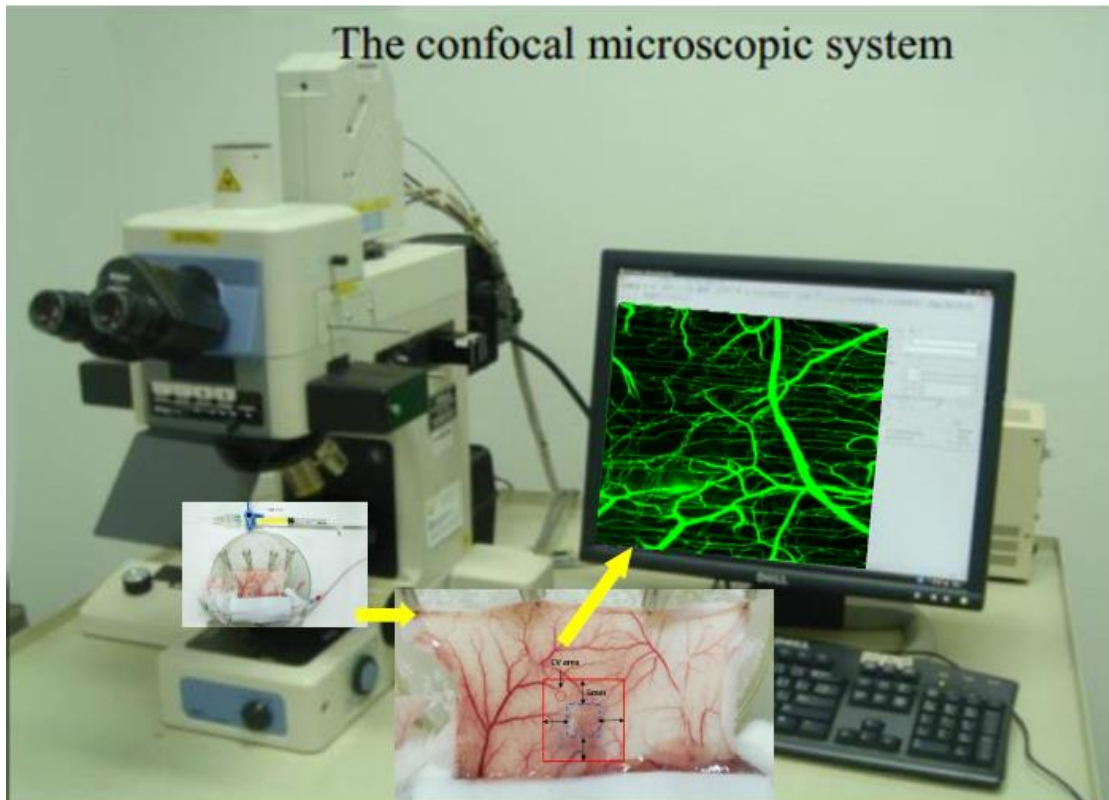


Figure 12. Microscopic Photography of Vascular Network of Wound Site.

The wound position was determined by depicting a square of 6mm×6mm when the wound was made before the opening of the dorsal skin by cutting. The areas around the wound edges (< 0.5 mm distance from the depicted wound position) were used to take the images which were used for calculating the percentage of capillary vascularity (%CV).

As shown in **Figure 14**, the example of AOI windows chosen from the confocal microscopic image is shown. The windows of a 40x40 pixel area of Interesting (AOI) were selected for measuring the percentage of capillary vascularity (%CV). 10-20 such AOI were chosen from the microscopic vasculature image, which avoids the big microvessles and contains only blood vessels less than 15 μm . Images from 4-5 mice, with 3-5 images each mouse were chosen for the percentage of capillary vascularity (%CV). The measurement process of the percentage of capillary vascularity (%CV) was shown in **Figure 15**. The principle of the percentage of capillary vascularity (%CV) based on the equation presented in **Figure 13** [191].

$$\text{Percentage of capillary vascularity (\%CV)} = \frac{\text{Number of Pixels within AOI Capillaries} \times 100}{\text{Total Number of Pixels within Entire AOI Frame}}$$

Figure 13. Equation of Calculation of Percentage of Capillary Vascularity (%CV).

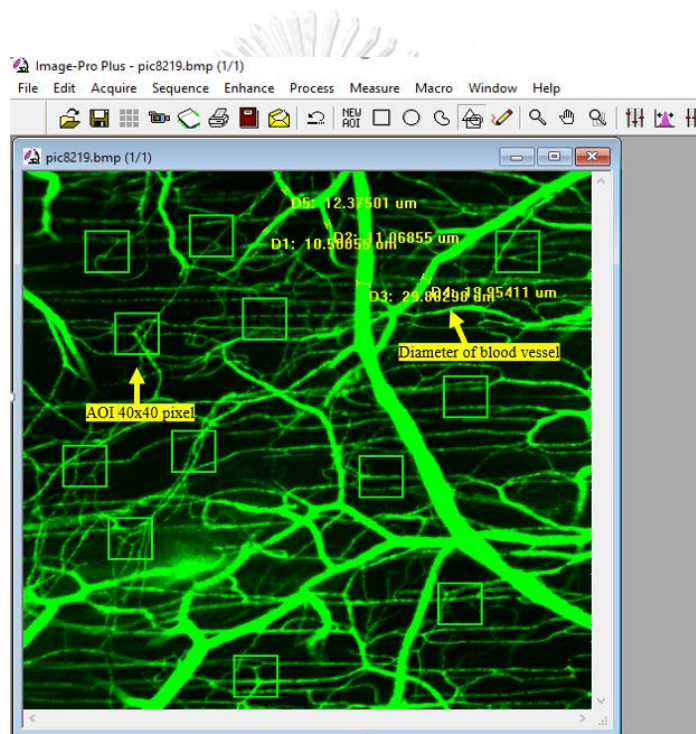


Figure 14. AOI Windows for Percentage of Capillary Vascularity (%CV) Analysis.

The windows of 40x40 pixel area of Interesting (AOI) were selected for measuring the percentage of capillary vascularity (%CV). 10-20 such AOI were chosen from the microscopic vasculature image, which avoids the big microvessles and contains only blood vessels less than 15 μm . In each group, images are chosen from 4-5 mice, with 3-5 images each mouse were chosen for measurement of the percentage of capillary vascularity (%CV); The example microscopic image was taken from DM+Combine day 7 group.

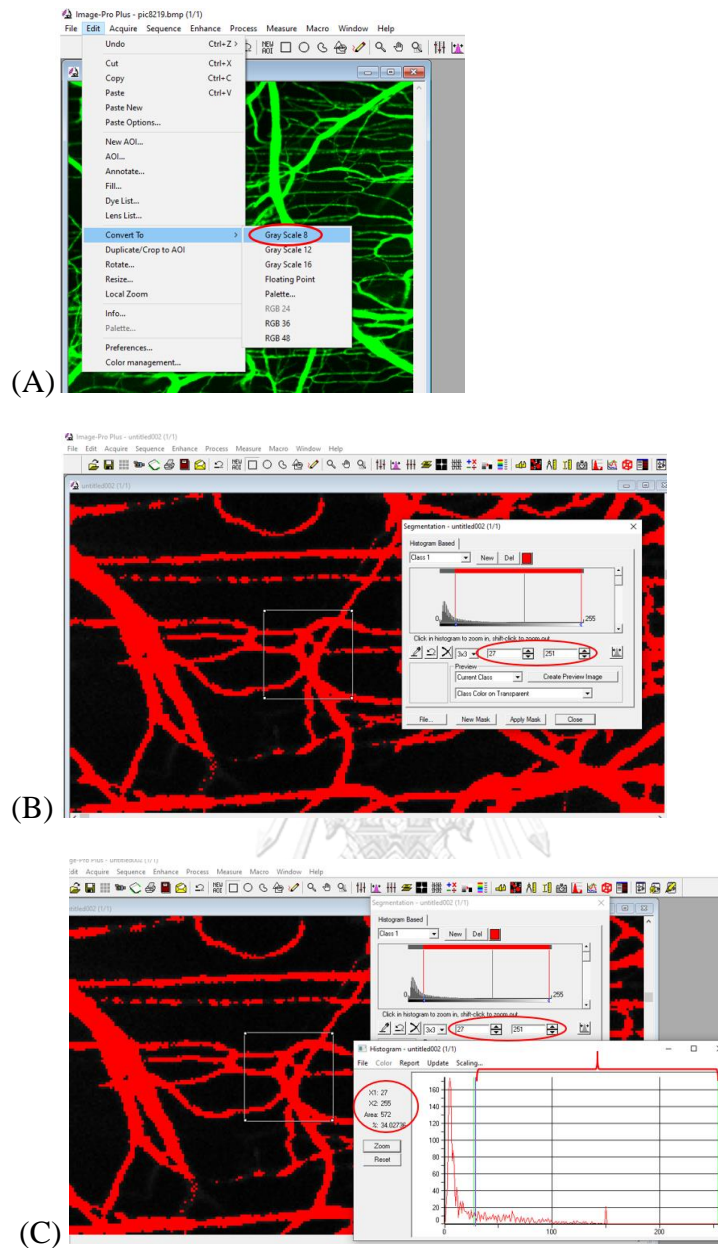


Figure 15. Demonstrating How the %CV Was Obtained from Each AOI.

(A). After choosing all the AOIs in one microscopic image, convert the image to greyscale 8 by using Image -Pro Plus Program 6.1; (B). Choose 1 AOI, use the segmentation function, and set the maximum histogram to 255, the minimum histogram value is chosen when the capillary vasculature is filled up by the red color, which indicates the outline and pixels inside capillary vasculature of AOI were determined; (C). Use the histogram graph scaling function to read the %CV data of the AOI calculated by Image-Pro Plus program 6.1.

3.7.3. Percentage of Re-Epithelialization (%RE)

Re-epithelialization was one of the major features that indicated the wound healing successful. Migration across the wound gap of keratinocytes at the wound edge across the wound gap starts the re-epithelialization process [192]. Re-epithelialization rate (ER) was used to determine how quickly new epithelial tissue grows from the edge of the wound.

After fluorescence micrographic images were taken, the tissue specimen at the right site of the wounded area was collected and fixed in 10% formaldehyde for 24 hours. The center of wound samples was cut and embedded in paraffin, as shown in **Figure 16**. From the paraffin-embedded tissue blocks, 5 μm sections were serially cut and stained with hematoxylin-eosin (H&E staining) for routine histology at the Department of Pathology, Faculty of Medicine, Chulalongkorn University. The H&E-stained sample slides will be used to measure re-epithelization by using Stereotype Microscopy (Nikon SM2800, Japan) and digital sight for microscope (Nikon DS-L2, Japan). Wound images used for judging the wound edge were taken under 400 \times magnification.

The thickness of the featured wound edge was increased with the proliferated epidermis, which is comprised of numerous layers of keratinocytes of special morphology. The basal keratinocytes at the wound edge are arranged to be a regimented single layer of cuboidal or low columnar cells [193]. The re-epithelialization degree were analyzed by using the method modified from Somchaichana J. et al. [194]. The length of the curved line from the wound edge to the epithelium tongue (curved line 1 and curved line 2), and the wound gap between the epithelium tongues (curved line 3) was also measured, as shown in **Figure 16**. The total length of the curved lines of the new epithelium was calculated by the equation presented in **Figure 17**.

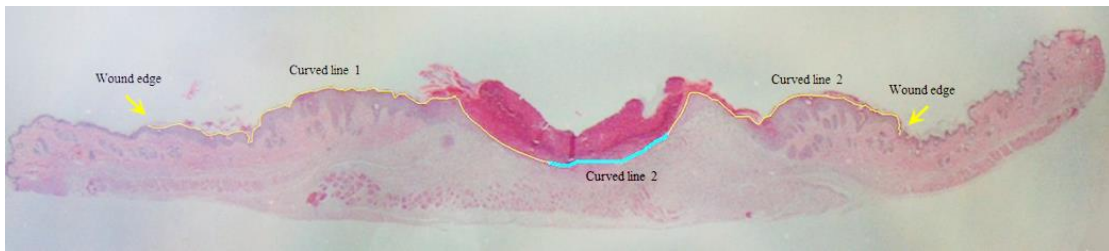


Figure 16. Measurement of Re-epithelialization of Wound Tissue.

The yellow arrows indicate the wound edges at day 0 when making the wound; The yellow curves are the new epithelialium; The blue curve is the unhealed gap of the wound; This H&E-stained slide image was taken under 10× magnification.

$$\% \text{ Re-epithelialization} = \frac{\text{Distance covered by epithelium}}{\text{Distance between the two wound edges}} \times 100\%$$

Figure 17. Equation of Calculation of Percentage of Re-epithelialization.

3.7.4. Measurement of Neutrophil Infiltration

Neutrophil infiltration is a feature of the prolonged inflammation stage in diabetic wound healing. Banded, segmented, and mature neutrophils were counted in the neutrophil infiltration measurement process based on the neutrophil development progress and morphology [195].

After fluorescence micrographic images were taken, the tissue specimen at the right site of the wounded area was collected and fixed in 10% formaldehyde for 24 hours. The centers of wound samples were cut and embedded in paraffin, as shown in **Figure 16**. From the paraffin-embedded tissue blocks, 5 μm sections were serially cut and stained with hematoxylin-eosin (H&E staining) for routine histology at the Department of Pathology, Faculty of Medicine, Chulalongkorn University. The H&E-stained sample slides were used to measure neutrophil infiltration by using Stereotype Microscopy (Nikon SM2800, Japan) and digital sight for microscope (Nikon DS-L2, Japan). Wound images used for judging the wound edge were taken under 400×

magnification. The first slide image used for the neutrophil infiltrated count was taken from the wound edge.

The micrographic images for neutrophil infiltration in the dermis part were taken from one wound edge position to the other wound edge position. At each position of the wound skin specimen slide, two micrographic images were taken, one next to the dermis-epidermis edge, and the other one far away from the dermis-epidermis. If the dermis part is narrow, then only one microscopic picture is taken at the position. The cells in hair follicles were not included in the total cells of each wound slide. The number of neutrophils of a total of 1000 cells from the dermis part of the wound skin H&E staining slides was evaluated, 7-15 slides each wound were used in the neutrophil number counting by using Image-Pro II 6.1 software. **Figure 18** shows the counted infiltrated neutrophils from the slide.

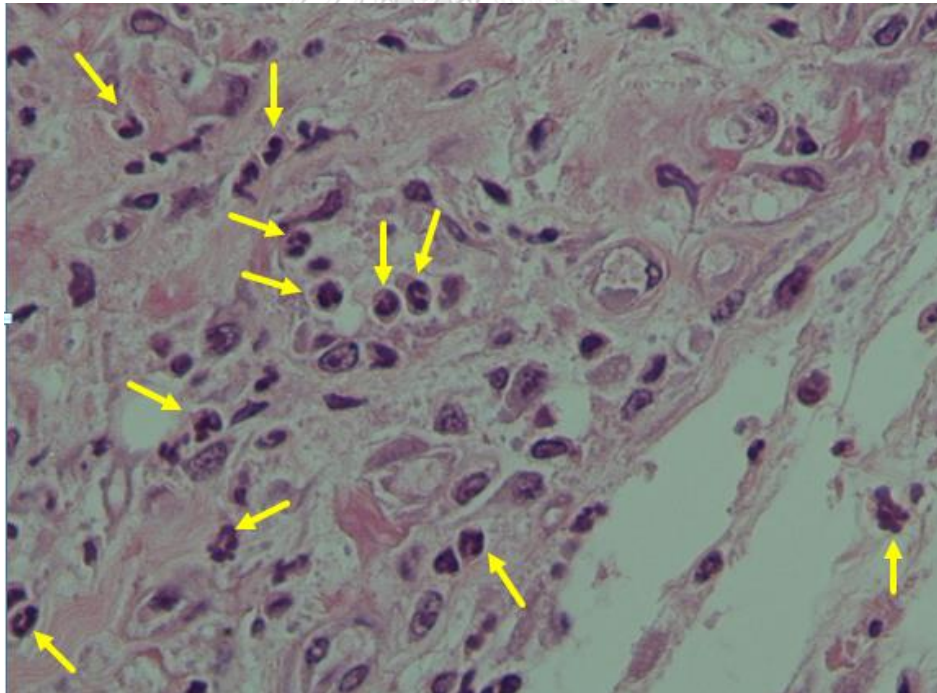


Figure 18. Neutrophil Infiltration Micrograph.

The cells pointed marked by arrows are banded, segmented, and mature neutrophils that were counted in the neutrophil infiltration measurement process based on the neutrophil development progress and morphology; This H&E-stained slide image was taken under 400× magnification.

3.7.5. Immunoassays and TBARS Assay

3.7.5.1. Wound Skin Sample Supernatant Preparation

Firstly, on the time-point of day 4, 7, and 14, the left side wound skin of each mouse (10mm×10mm) was collected in an Eppendorf tube after capillary vascularity micrographic images were taken and moved to be kept at -80°C. On the homogenizing day, the wound skin tissue (10mm×10mm) was taken out into an ice bath to make the wound skin tissue soft, then the 10mm×10mm wound skin tissue was cut to keep only the 6mm×6mm square wound area, which is the same area as the wound creation. The skin wound sample weight was measured by analytical laboratory balance (ME104T, Mettler-Toledo GmbH, Switzerland). Then the 6mm×6mm wound skin sample was chopped in a glass surface dish on an ice bath. When the wound skin sample was chopped to very small minced-granules with liquid, it was transferred to a 1.5 ml Eppendorf tube, 10 times of the homogenate solution was added to the Eppendorf tube according to each sample weight, and vortexed on a vortex mixer (Model KMC-1300V, Vision scientific Co. Ltd., Thailand) till the chopped sample was homogeneously distributed in the Eppendorf tube. Then it was kept in the ice bath. Each lot, 30 minutes after the last wound skin sample was chopped and vortexed. The protein from sample homogenates was extracted by using the supersonic extraction method (Model VCX750, Sonics & Materials Inc., USA). Each sample homogenate was extracted three times, each time 15 seconds, with an interval time of 10 seconds. Then the sample homogenates were spun down with a laboratory centrifuge (Model Sorvall Legend X1R centrifuge, Thermo Fisher Scientific, Germany) at speed of 10,000 rpm at 4 °C. After that, according to the volume of each sample supernatant, the supernatant was transferred by pipette into several 1.0 ml Eppendorf tubes to keep at -80°C for later use. Each assay used a new tube sample supernatant.

3.7.5.2. Total Protein Content Measurement

Abcam's BCA Protein Quantification Kit was used in this project to determine the concentration of total proteins in the wound skin sample supernatant. The principle of the assay is that protein can reduce copper (Cu^{2+}) salt to a cuprous state. The Cu^{2+} ion

form can be complexed with the bicinchoninic acid reagent to form a blue compound with strong absorbance at 562 nm. The absorbance OD is positively proportional to the total protein concentration in the sample.

Briefly, the procedure is presented as below: first, samples' supernatant was taken from -80°C to an ice bath. Before the BCA assay, sample dilution is tried before the real measurement, according to the trial result, proper dilution ratios for each time point were chosen. For the total protein assay BCA, day 14 samples were diluted from 1 to 4, day 7 samples were diluted from 1 to 8, day 4 samples were diluted from 1 to 10. Label eight tubes from A to H. Each tube was prepared with 100 μl BSA solution with different concentrations by using the working solution. A was the BSA stock with no dilution with protein concentration 2000 $\mu\text{g/ml}$, H was only the working solution with protein concentration 0. Other protein concentration solutions were prepared by the method of dilution to make standard solutions of 2000, 1500, 1000, 750, 500, 250, 125, 0 $\mu\text{g/ml}$ protein standard solution, as described in Abcam's BCA Protein Quantification Kit Protocol. Keep the standard solutions in an ice bath. Then for day 7 groups, 6.25 μl sample supernatant, and 43.75 μl was added to new Eppendorf tube, vortex to homogenate the supernatant in working solution. For day 14 groups, 12.50 μl sample supernatant, and 37.50 μl was added to new Eppendorf tube, vortex to homogenate the supernatant in working solution, kept in the ice bath. Then 9 μl of each standard solution and liquid sample supernatant was added to duplicated wells of 96 well plate. Then add 4 μl compatibility reagent to each well, cover the 96-well plate with sticky plastic film to shake on an orbital shaker for 1 minute, and then incubate 15 minutes at 37°C . Then at room temperature, 260 μl Reagent A and Reagent B mixture was added to each well. Covered with sticky plastic film, the 96-well plate was shaken for 1 minute, and then incubated for 5 minutes at room temperature. The sticky plastic film was removed, and the bottom of the 96-well plate was cleaned, then the OD values were read out by a colorimetric microplate reader (Model860, BIO-RAD). The protein concentration of each sample was calculated from the standard curve, expressed as mg/ml.

3.7.5.3. Measurement of Tissue MDA

Lipid peroxides, derived from PUFAs, are unstable and decompose to form a complex series of compounds, which include reactive carbonyl compounds, such as MDA, which is a product of lipid peroxidation, taken as the biomarker of lipid peroxidation and an indicator of oxidative stress in cells and tissues [196].

Lipid peroxidation is the oxidative degradation of lipids. Lipid peroxidation consists of three major steps: initiation, propagation, and termination by a free radical chain reaction mechanism. Polyunsaturated fatty acids are usually the lipid substrates to be oxidized in the initial phase, which could donate hydrogen atoms to the activated oxygen species like singlet oxygen ($^1\text{O}_2$), $\text{O}_2^{\bullet-}$, or $\text{HO}\bullet$, to produce a highly reactive carbon-centered lipid radical ($\text{L}\bullet$). For polyunsaturated fatty acids contain double bonds between methylene bridges, which could set hydrogen atoms free or offset under the existence of activated oxygen species with unpaired electrons. The initial phase could also happen when the pre-existing lipid hydroperoxides breakdown by transition metals. In the second phase of propagation in lipid peroxidation, molecular oxygen could react with the reactive carbon-centered lipid radical to generate lipid peroxy radical ($\text{LOO}\bullet$) by diffusion. Further, this peroxy radical could reduce DNA and proteins by attracting the electron close to itself to produce lipid hydroperoxides (LOOH), the main oxidant product. In the context of oxidative stress, after reaction with endogenous antioxidants, excessive lipid peroxy radicals could steal electrons from other lipid molecules, producing another highly reactive carbon-centered lipid radical ($\text{L}\bullet$). This regenerated lipid radical proceeds the propagation phase to carry on the radical chain. On the other hand, the lipid hydroperoxide (LOOH) can undergo the Fenton reaction to produce reactive alkoxy radicals when iron or other metal catalysts exist. In these ways, the radical chain reactions are amplified under the lack of endogenous antioxidants. The end products of ROOH degradation are aldehydes and hydrocarbons. For ROS have a very short half-life and are difficult to detect, the end-products of ROS-induced lipid peroxidation are taken as the index of oxidative stress, such as MDA [197-199]. Lipids are the susceptible targets of ROS-induced oxidation, for the abundant double bonds in the molecular structures. Lipid peroxidation degree

is taken to measure the oxidative stress. The most well-studied biomarkers of lipid peroxidation are isoprostanes (IsoPs) and malondialdehyde (MDA). Also, there are other biomarkers include oxysterols, oxidation resistance assays, lipid hydroperoxides, and fluorescent products of lipid peroxidation [200]. As a biomarker, current methods measuring IsoPs content are impractical for large-scale GC/MS screening, which is still the gold standard of IsoPs quantification, or not so accurate which needs further validation by immunoassay kits. So far, there is no evidence supporting the link between IsoPs and clinical outcomes yet [200-203].

Now there are several commercially available ELISA kits detecting MDA content with good performance and improved accuracy. Studies showed that MDA promised a good clinical marker of progression of CAD and carotid [200, 204-207]. Diabetic patients usually have lipid metabolism dysfunction. Lipid peroxidation is involved in many chronic diseases, including diabetes [66]. The measurement of thiobarbituric acid reactive substances (TBARS) is a common method for the evaluation of lipid peroxidation. TBARS assay is the most widely employed assay used to determine lipid peroxidation. The principle is that MDA and TBA can form a pink-colored MDA-TBA adduct under high-temperature (90-100°C). The reaction is shown in

Figure 19.

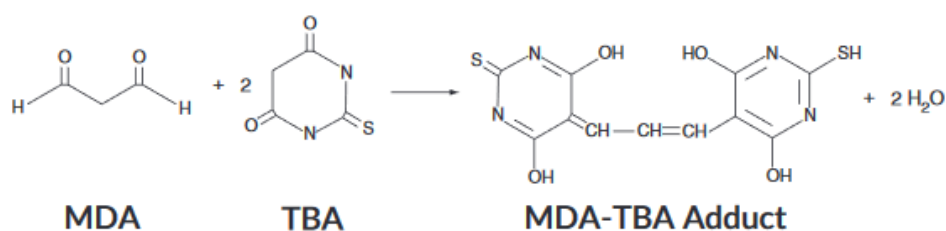


Figure 19. The Reaction of MDA and TBA to Form MDA-TBA Adduct.

To measure the lipid peroxidation in wound skin tissue, TBARS assay kit (Cayman Chemical Co. USA) was used in this project. Eppendorf tubes with caps were prepared. 50 µl of each sample and the standard solution were added to the tube. Then add 50 µl of SDS solution to the tube and vortex to mix homogeneously. After that 2 ml of the color reagent was added to each tube, mix homogeneously by vertex. The tubes were put upright in a steel holder with caps half tightly closed, boiled in

vigorously boiling water for 1 hour. Then the tubes were taken out and incubate on ice for 10 minutes. After that, all the tubes are centrifuged for 10 minutes at 10,000 rpm at 4°C. After centrifuge, all the tubes were stabled at room temperature for 30 minutes to make solutions in tube clear. Then 150 µl of each standard and sample solution was loaded to 96-well plate. The OD value was read by a colorimetric microplate reader (Model 860, BIO-RAD), setting the wavelength at 540 nm. The content of MDA has been expressed in the unit of nmol/mg total protein. All standard solutions and samples were duplicated in the 96-well plate.

3.7.5.4. Measurement of Tissue VEGF

VEGF (Vascular Endothelial Growth Factor) is a potent mediator of both angiogenesis and vasculogenesis. It is required for regulating the proliferation, migration, and survival of embryonic endothelial cells and during wound healing. For protocol 2, on day 7 and 14, the diabetic wound skin tissue sample supernatants were used in the VEGF immunoassay. Mouse VEGF quantitative ELISA kit (R&D System, Inc., USA) was used to measure mouse VEGF protein content in this project. This assay employs the quantitative sandwich enzyme immunoassay method. The principle is described in **Figure 20**. Firstly, microplate well was coated with a polyclonal antibody specific for mouse VEGF; Secondly, the sample solution was added, any VEGF antigen present is bounded to the VEGF antibody; Thirdly, an Enzyme-linked polyclonal VEGF antibody was added, binding VEGF antigen; Fourthly, after washing away unbounded VEGF antibody-enzyme reagent, Substrate was added to yield a blue compound under enzyme catalysis. The blue compound turns yellow when stop solution was added.

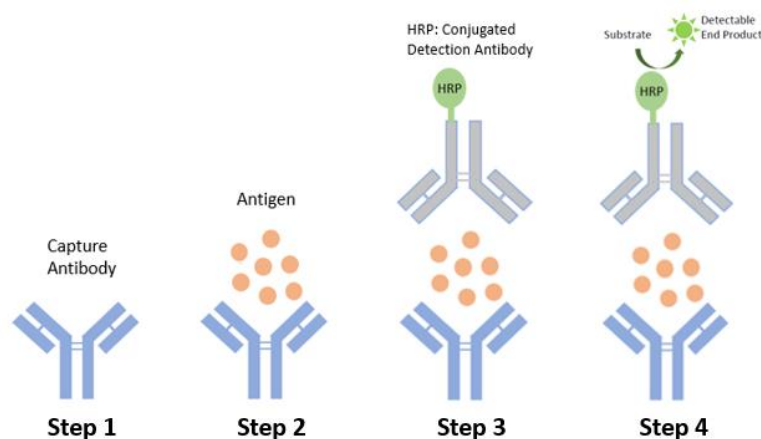


Figure 20. Principle of Sandwich ELISA.

Step1. Coating capture antibody; Step2. Add sample containing antigen; Step3. Add detecting antibody; Step4. Add substrate to get the detectable end product.

All reagents, mouse VEGF standard solutions, and sample solutions were prepared as described in the chemical part. 50 μl assay diluent RD1N was added to each well center of the pre-coated plate well. Then 50 μl of each standard, sample solution was added to each well. Mix by gently tapping the plate frame for 1minute. Cover with adhesive strip provided and incubate for 2 hours at room temperature. Then the liquid was poured out from the plate well and wash each well 5 times by wash buffer, with each well 400 μl each time. The wash buffer was then removed thoroughly and 100 μl mouse VEGF conjugate was added to each well. The plate was covered with sticky plastic film and incubated for another 2 hours at room temperature. Then the wash step was repeated 5 times as described. 100 μl substrate solution then was added to each well, incubated for 30 minutes at room temperature, with protection from light. Finally, 100 μl stop solution was added to each well and gently tap the plate frame to mix well. Then the OD value of each well solution was read by a colorimetric microplate reader (Model860, BIO-RAD), setting the measure wavelength at 450 nm and reference wavelength at 570 nm. The content of VEGF was expressed in the unit of pg/mg total protein. All standard solutions and samples were duplicated in the well plate.

3.7.5.5. Measurement of Tissue IL-6

For protocol 2, on day 4 and 7, the diabetic wound skin tissue sample supernatants were used in the IL-6 immunoassay. Mouse IL-6 quantitative ELISA kit (R&D System, Inc., USA) was used to measure mouse IL-6 protein content in this project. This assay employed the quantitative sandwich enzyme immunoassay method.

All reagents, mouse IL-6 standard solutions, and sample solutions were prepared as described in the chemical part. 50 μ l assay diluent RD1-14 was added to each well center of the pre-coated plate well. Then 50 μ l of each standard, sample solution was added to each well, mixed by gently tapping the plate frame for 1minute. The plate then was covered with adhesive strip provided and incubates for 2 hours at room temperature. Then the liquid was poured out from the plate well and washed 5 times by wash buffer for each well, with each well 400 μ l each time. The wash buffer was removed thoroughly and 100 μ l mouse IL-6 conjugate was added to each well. The plate was covered with sticky plastic film and incubated for another 2 hours at room temperature. Then the wash step was repeated 5 times as described. 100 μ l substrate solution was added to each well, incubated for 30 minutes at room temperature, with protection from light. Finally, 100 μ l stop solution was added to each well and plate frame was gently tapped to mix. Then the OD value of each well solution was read by a colorimetric microplate reader (Model860, BIO-RAD), setting the measure wavelength at 450 nm and reference wavelength at 570 nm. The content of IL-6 was expressed in the unit of pg/mg total protein. All standard solutions and samples were duplicated in the well plate.

3.8. Statistics

All data were presented as the mean \pm standard errors of mean (SEM). One-way ANOVA was used for the comparison between groups, followed by the least significant difference (LSD) post-hoc test using SPSS software, version 22. The correlation analysis was conducted by using the two-tailed Pearson's correlation. Statistical significance was accepted when p - value less than 0.05 ($p < 0.05$).

CHAPTER IV

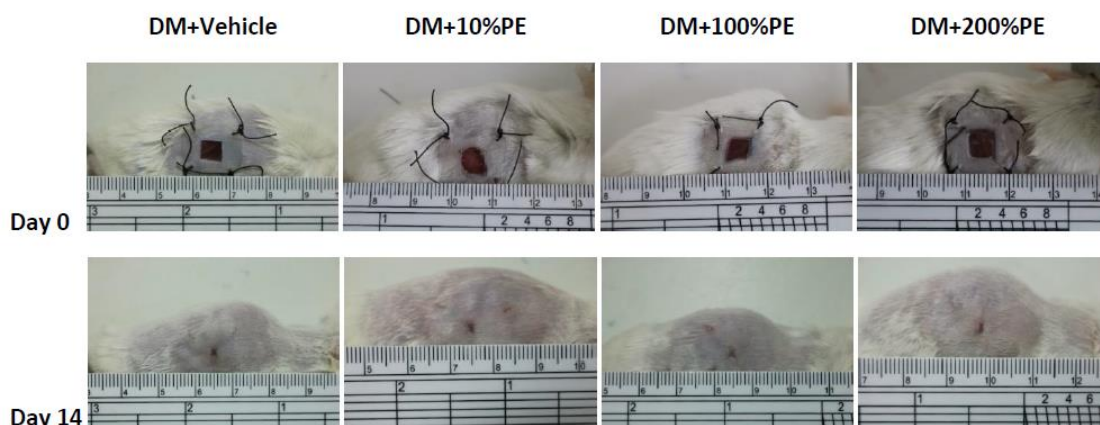
RESULTS

This chapter shows the results of two major parts of results. In the first part, the objectives were to study the dose-responses of Simvastatin and PE on %WC and %CV in 14-day DM groups (DM+10%PE group, DM+100%PE group, DM+200%PE group, DM+0.5%SIM group, DM+5%SIM group, DM+10%SIM). In the second part, the objectives were to evaluate the effects of combined treatment of PE and Simvastatin on diabetic wound.



4.1. Results of the Dose-Response of Simvastatin and PE on Wound Closure (%WC) and Capillary Vascularity (%CV)

(A).



(B).

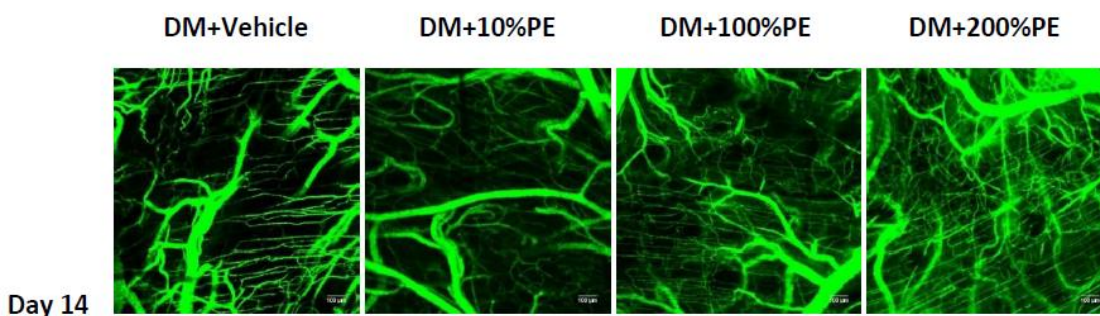


Figure 21. Wound Area Images and Confocal Microscopic Images of Areas Around Full-thickness Dorsal Skin Wound in STZ-induced Diabetic BALB/C Mouse Model in Protocol 1 from PE Treatment Groups.

(A). Wound area images at day 0 and day 14; Wound area images presented here were from the same wound on day 0 and day 14; (B). Confocal microscopic images of areas around full-thickness dorsal skin wound on day 14. The clear pictures most represent the average %CV were chosen from each group in Protocol 1 from PE treatment groups.

Table 5. Percentage of Wound Closure (%WC) of Every Group in Various Doses of PE (DM+10%PE, DM+100%PE, and DM+200%PE groups) on Day 14 in Protocol 1

(All data were expressed as mean \pm SEM)

Groups	n	% WC
DM+Vehicle	4	94.83% \pm 1.37%
DM+10%PE	4	97.52% \pm 0.72% ^{ns}
DM+100%PE	4	99.09% \pm 0.35%*
DM+200%PE	4	96.83% \pm 0.89% ^{ns}

ns=not significant, compared with DM+Vehicle group;

* p <0.05, compared with DM+Vehicle group.

Table 6. Percentage of Capillary Vascularity (%CV) of Every Group in Various Doses of PE (DM+10%PE, DM+100%PE, and DM+200%PE groups) on Day 14 in Protocol 1

(All data were expressed as mean \pm SEM)

Groups	n	% CV
DM+Vehicle	4	36.30% \pm 0.71%
DM+10%PE	4	38.50% \pm 0.75%*
DM+100%PE	4	39.40% \pm 0.72%*
DM+200%PE	4	40.75% \pm 0.54%*,#

ns=not significant, compared with DM+Vehicle group;

* p <0.05, compared with DM+Vehicle group;

p <0.05, compared with DM+10%PE group.

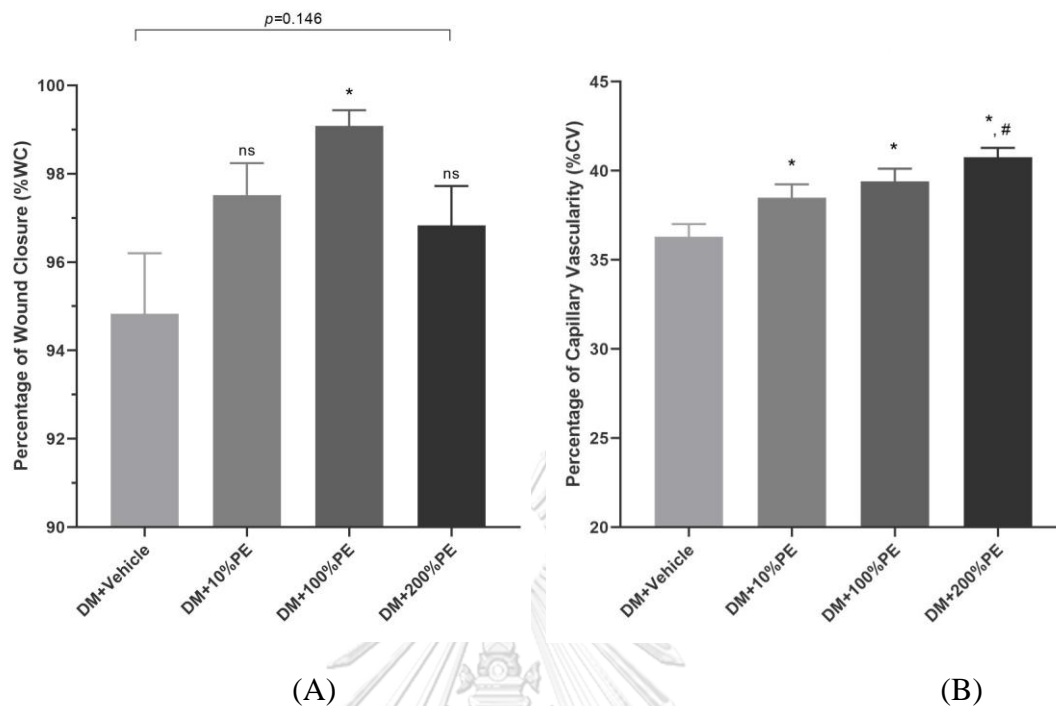


Figure 22. Percentage of Wound Closure (%WC) and Capillary Vascularity (%CV) of Every Group in Various Doses of PE (DM+10%PE, DM+100%PE, and DM+200%PE groups) on Day 14 in Protocol 1. (All data were expressed as mean \pm SEM)

ns=not significant, compared with DM+Vehicle group;

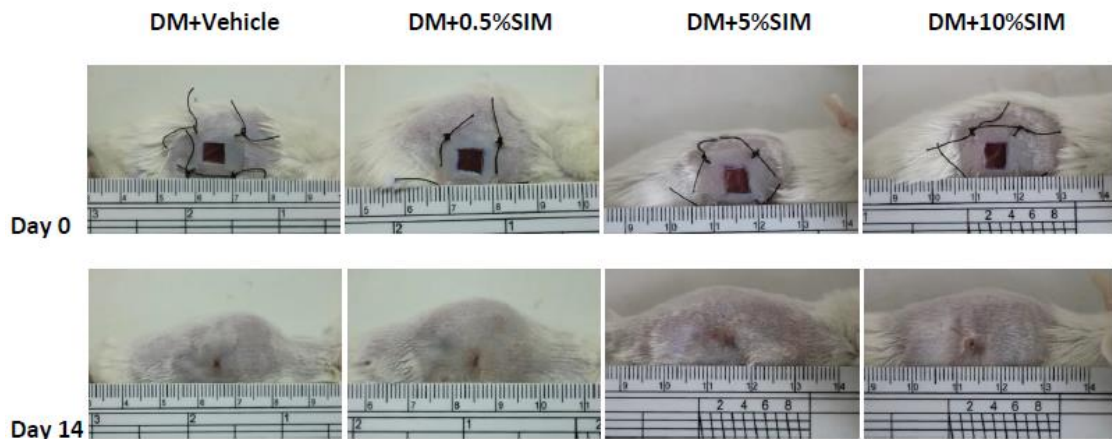
* $p<0.05$, compared with DM+Vehicle group;

$p<0.05$, compared with DM+10%PE group;

Table 5, **Table 6**, and **Figure 22** show the results of the percentage of wound closure (%WC) and capillary vascularity (%CV) of every group in the various doses of PE (DM+10%PE, DM+100%PE, and DM+200%PE groups) on day 14 in Protocol 1. For the results of percentage of wound closure (%WC), only DM+100%PE group has significant difference ($p<0.05$) when compared with DM+Vehicle group on day 14. All of the results of the percentage of capillary vascularity (%CV), DM+10%PE group, DM+100%PE group, and DM+200%PE group have significant difference when compared with DM+Vehicle group on day14, with $p<0.05$, respectively. DM+200%PE group has significant difference ($p<0.05$) when compared with DM+10%PE group on day14. This means that only DM+100%PE group could enhance both of percentage of wound closure (%WC) and capillary vascularity (%CV)

significantly when compared with DM+Vehicle group on day 14 post-wounding in diabetic wounds in mice.

(A).



(B).

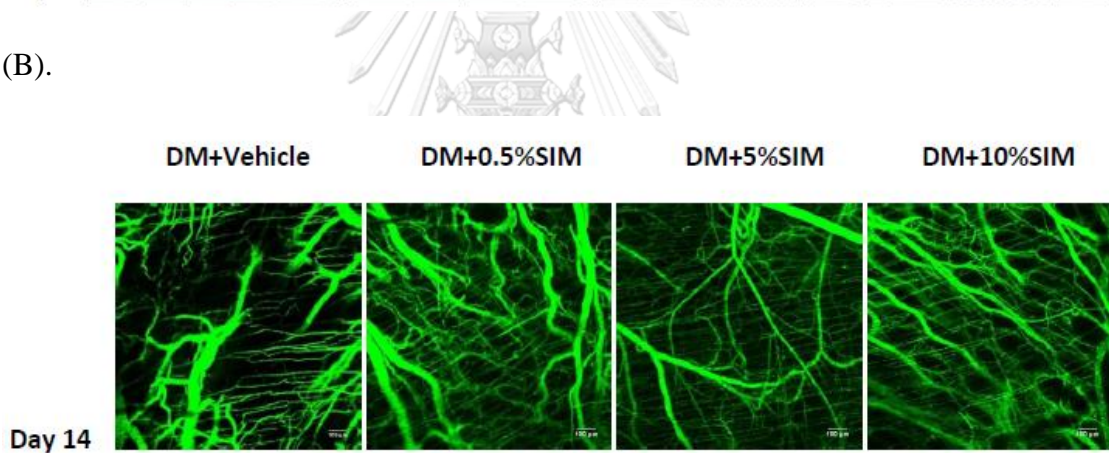


Figure 23. Wound Area Images and Confocal Microscopic Images of Areas Around Full-thickness Dorsal Skin Wound in STZ-induced Diabetic BALB/C Mouse Model in Protocol 1 from SIM Treatment Groups.

(A). Wound area images on day 0 and day 14; Wound area images presented here were from the same wound on day 0 and day 14; (B). Confocal microscopic images of areas around full-thickness dorsal skin wound on day 14. The clear pictures most represent the average %CV were chosen from each group in Protocol 1 from SIM treatment groups.

Table 7. Percentage of Wound Closure (% WC) of Every Group in Various Doses of SIM (DM+0.5%SIM, DM+5%SIM, and DM+10%SIM groups) on Day 14 in Protocol 1

(All data were expressed as mean \pm SEM)

Groups	n	% WC
DM+Vehicle	4	94.83% \pm 1.37%
DM+0.5%SIM	4	97.01% \pm 0.83% ^{ns}
DM+5%SIM	4	99.07% \pm 0.35% [*]
DM+10%SIM	4	99.36% \pm 0.43% [*]

ns=not significant, compared with DM+Vehicle group;

* p <0.05, compared with DM+Vehicle group.

Table 8. Percentage of Capillary Vascularity (% CV) of Every Group in Various Doses of SIM (DM+0.5%SIM, DM+5%SIM, and DM+10%SIM groups) on Day 14 in Protocol 1

(All data were expressed as mean \pm SEM)

Groups	n	% CV
DM+Vehicle	4	36.30% \pm 0.71%
DM+0.5%SIM	4	38.49% \pm 0.25% ^{ns}
DM+5%SIM	4	39.31% \pm 1.36% [*]
DM+10%SIM	4	41.27% \pm 0.90% ^{*,#}

ns=not significant, compared with DM+Vehicle group;

* p <0.05, compared with DM+Vehicle group;

p <0.05, compared with DM+0.5%SIM group.

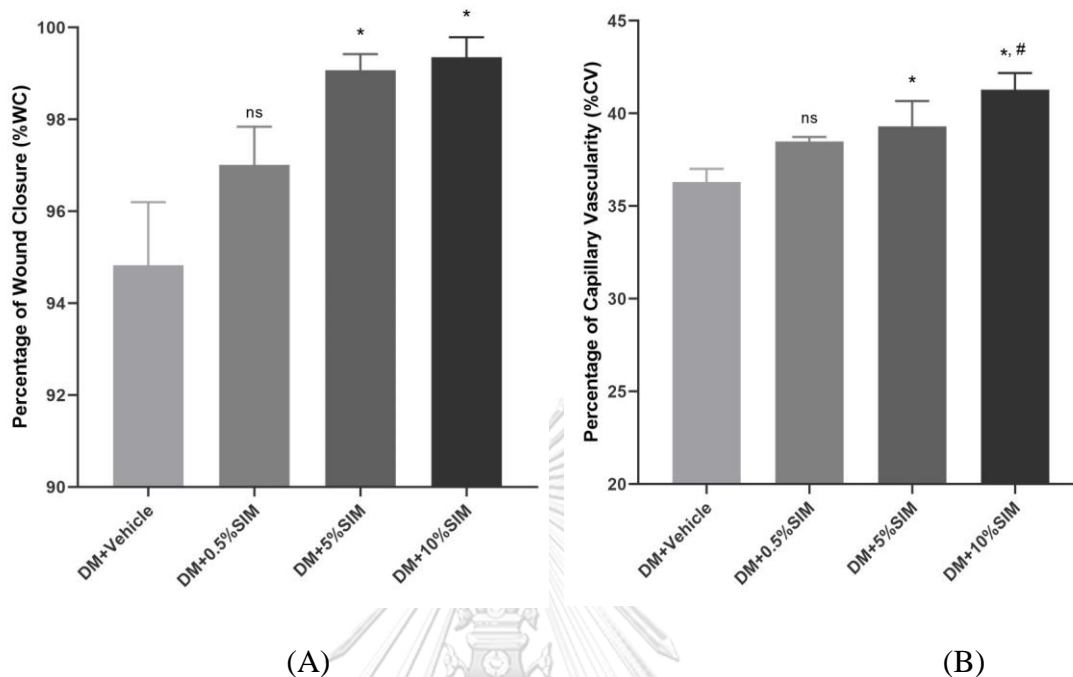


Figure 24. Percentage of Wound Closure (%WC) and Capillary Vascularity (%CV) of Every Group in Various Doses of SIM (DM+0.5%SIM, DM+5%SIM, and DM+10%SIM groups) on Day 14 in Protocol 1. (All data were expressed as mean \pm SEM)

ns=not significant, compared with DM+Vehicle group;

* $p < 0.05$, compared with DM+Vehicle group;

$p < 0.05$, compared with DM+0.5%SIM group;

จุฬาลงกรณ์มหาวิทยาลัย
CHULALONGKORN UNIVERSITY

Table 7, Table 8, and Figure 24 showed the results of the percentage of wound closure (%WC) and capillary vascularity (%CV) of every group in the various doses of SIM (DM+0.5%SIM, DM+5%SIM, and DM+10%SIM groups) on day 14 in Protocol 1. For the results of percentage of wound closure (%WC), DM+5%SIM group and DM+10%SIM group have significant difference ($p < 0.05$) when compared with DM+Vehicle group on day 14. The results of the percentage of capillary vascularity (%CV), DM+5%SIM group and DM+10%SIM group have significant differences when compared with DM+Vehicle group on day 14, with $p < 0.05$, respectively. DM+10%SIM group has significant difference ($p < 0.05$) when compared

with DM+0.5%SIM group on day 14. This means that only DM+5%SIM group and DM+10%SIM group could enhance both of percentage of wound closure (%WC) and capillary vascularity (%CV) significantly when compared with DM+Vehicle group on day 14 post-wounding in diabetic wounds in mice.

4.1. Correlation of Doses and Percentage of Wound Closure (%WC) and Capillary Vascularity (%CV) in Protocol 1

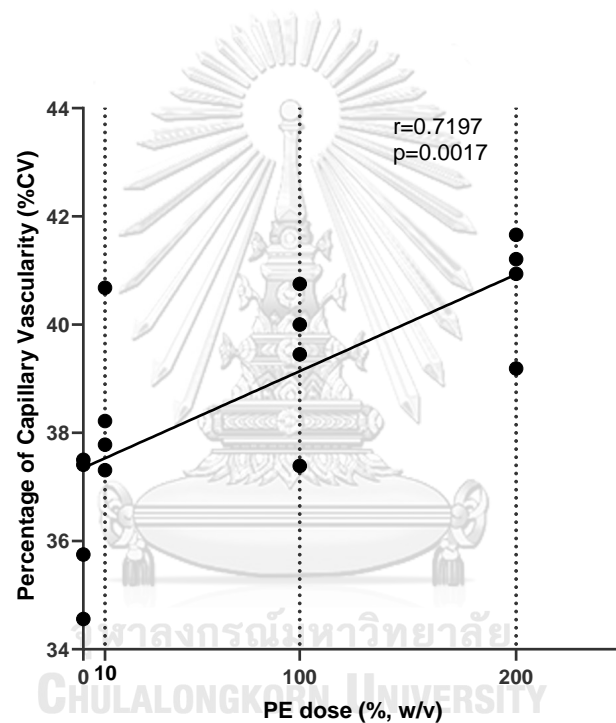


Figure 25. Pearson's Correlation Analysis between Data Sets of %CV and PE Doses on Day 14 in Protocol 1. (Details of each data set were shown in Appendix 8)
 $(Y = 0.0179 * X + 37.35, R^2 = 0.5180, \text{Pearson's correlation coefficient } r = 0.7197, p = 0.0017)$

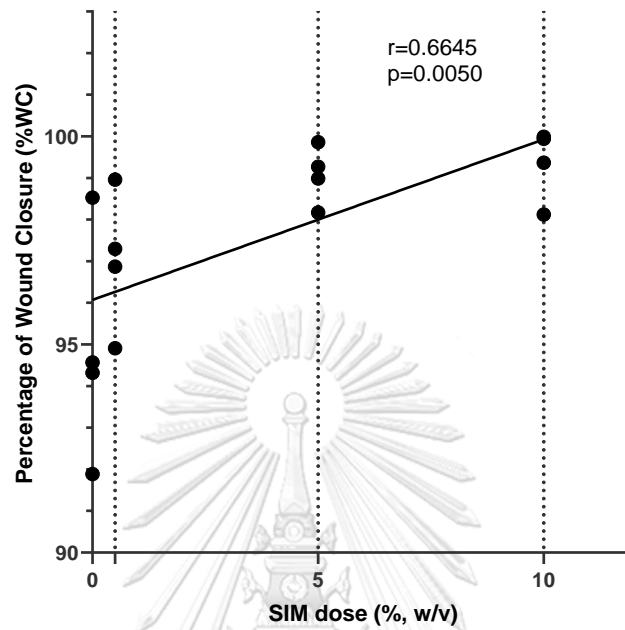


Figure 26. Pearson's Correlation Analysis between Data Sets of %WC and SIM Doses on Day 14 in Protocol 1. (Details of each data set were shown in Appendix 9)
 ($Y=0.3875 \cdot X+96.07$, $R^2=0.4415$, Pearson's correlation coefficient $r=0.6645$, $p=0.0050$)

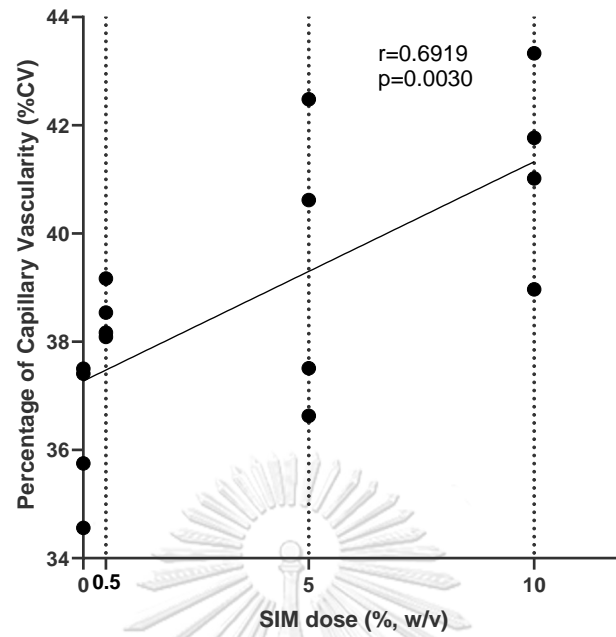


Figure 27. Pearson's Correlation Analysis between Data Sets of %CV and SIM Doses on Day 14 in Protocol 1. (Details of each data set were shown in Appendix 10)
 $(Y = 0.4053 \cdot X + 37.27, R^2=0.4787, \text{Pearson's correlation coefficient } r=0.6919, p=0.0030)$

4.2. Protocol 2

In the second part, the objectives were to evaluate the effects of combined treatment of PE and simvastatin on diabetic wound. In addition, in this part, the study had been designed to find out the possible pathway(s) of the combination of topical application PES and simvastatin whether they involve in anti-inflammation, anti-oxidative stress, and anti-angiogenesis or not.

4.2.1. Results of Physiological Parameters in Protocol 2

4.2.1.1. Result of Percentage of Body Weight Change (%BW) in Protocol 2

The body weight (BW) of each mouse in each group was weighted on the wounding day and the experiment day on day0, 4, 7, and 14. The data of %BW change is shown in **Table 9**, the graph is shown in **Figure 28** accordingly.

Table 9. Percentage of Body Weight Change (%BW) of Experimental Mice on Day 4, 7, and 14 in Protocol 2

(All data were expressed as mean \pm SEM)

Groups	Day4		Day7		Day14	
	n	%BW	n	%BW	n	%BW
CON+Vehicle	/	/	/	/	4	4.20% \pm 1.13%
DM+Vehicle	5	-0.91% \pm 1.98%	5	-1.39% \pm 2.17%	5	-2.20% \pm 2.93% ^{NS}
DM+100%PE	5	-0.24% \pm 1.19% ^{ns}	5	-4.43% \pm 2.54% ^{ns}	5	-8.67% \pm 1.48% ^{#, ns}
DM+5%SIM	5	-3.22% \pm 2.03% ^{ns}	5	-8.16% \pm 2.55% ^{ns}	4	0.74% \pm 3.41% ^{NS, ns}
DM+Combine	5	-1.65% \pm 0.98% ^{ns}	5	-8.71% \pm 1.63% [*]	5	-5.13% \pm 2.27% ^{#, ns}

ns=not significant, compared with DM+Vehicle group;

* p <0.05, compared with DM+Vehicle group;

p <0.05, compared with CON+Vehicle group;

NS= not significant, compared with CON+Vehicle group;

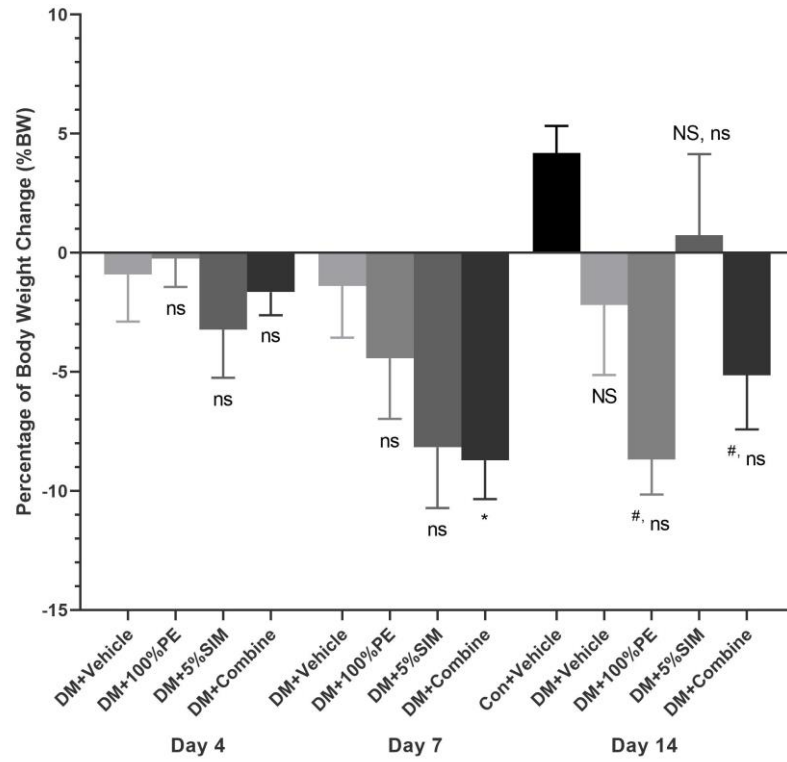


Figure 28. Percentage of Body Weight Change (%BW) of Experimental Mice Measured on Day 4, 7, and 14 in Protocol 2. (All data were expressed as mean \pm SEM)

ns=not significant, compared with DM+Vehicle group;

* p <0.05, compared with DM+Vehicle group;

p <0.05, compared with CON+Vehicle group;

NS= not significant, compared with CON+Vehicle group;

4.2.1.2. Results of Fasting Blood Glucose in Protocol 2

Four weeks after the first injection of STZ, the fasting blood glucose level (FBG) was detected from the tail vein blood sample from each mouse. If fasting blood glucose level was $> 200\text{mg/dL}$, then it was considered to be a successful diabetic mice model [9, 186]. After successful diabetic mice model establishment, the fasting blood glucose level (FBG) was assessed again from every group on day 4, 7, and 14 post-wounding. **Table 10** and **Figure 29** show the data and graph of FBG on day 14 in Protocol 2. FBG data of all diabetic mice in Protocol 2 was higher than 200mg/dL .

Table 10. Fasting Blood Glucose (FBG) Levels of Experimental Mice on Day 4, 7, and 14 in Protocol 2

(All data were expressed as mean \pm SEM)

Groups	n	Day4		Day7		Day14	
		n	FBG (mg/dL)	n	FBG (mg/dL)	n	FBG (mg/dL)
CON+Vehicle	/	/	/	/	/	4	76 \pm 19
DM+Vehicle	5	5	436 \pm 31	5	432 \pm 47	5	299 \pm 34 [#]
DM+100%PE	5	5	334 \pm 36 [*]	5	396 \pm 40 ^{ns}	5	464 \pm 82 ^{#, ns}
DM+5%SIM	5	5	282 \pm 17 [*]	5	310 \pm 42 ^{ns}	5	393 \pm 73 ^{#, ns}
DM+Combine	5	5	322 \pm 21 [*]	5	459 \pm 38 ^{ns}	5	451 \pm 78 ^{#, ns}

ns=not significant, compared with DM+Vehicle group;

* $p < 0.05$, compared with DM+Vehicle group;

$p < 0.05$, compared with CON+Vehicle group.

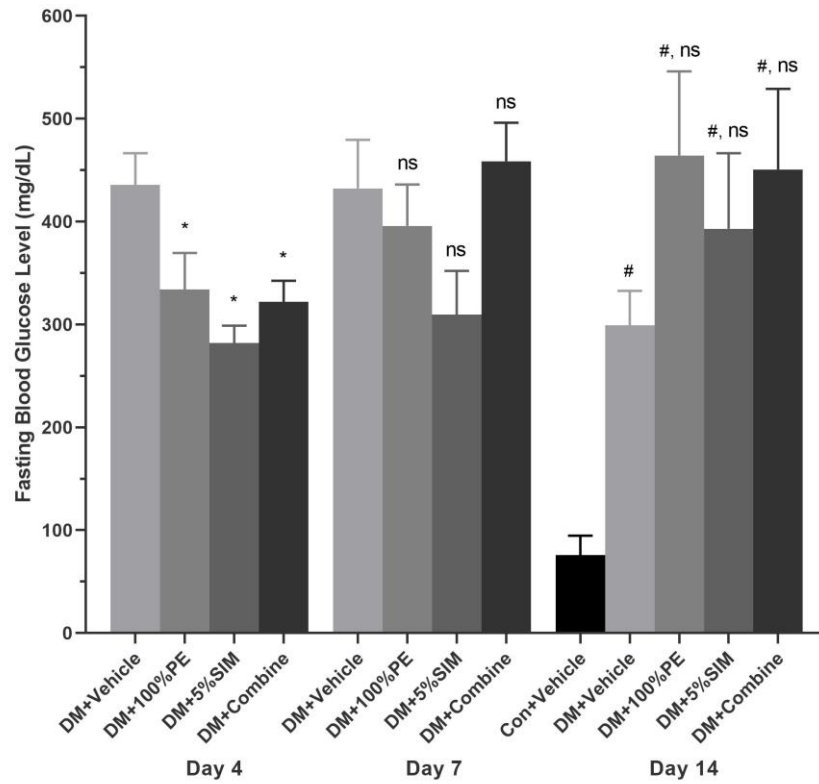


Figure 29. Fasting Blood Glucose (FBG) Levels of Experimental Mice on Day 14 in Protocol 1. (All data were expressed as mean \pm SEM)

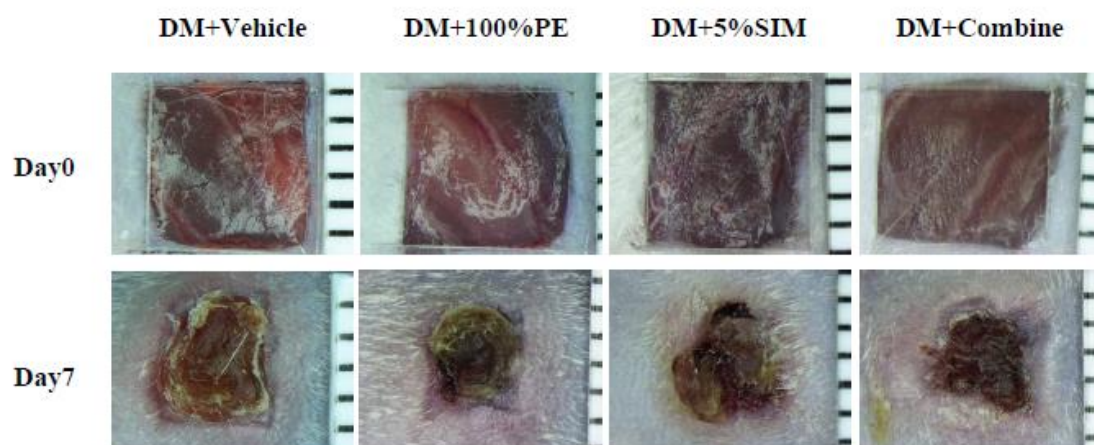
ns=not significant, compared with DM+Vehicle group;

* p <0.05, compared with DM+Vehicle group;

p <0.05, compared with CON+Vehicle group.

4.2.2. Effects of combined treatment of PE and Simvastatin on Percentage of Wound Closure (%WC) and capillary vascularity (%CV)

(A).



(B).

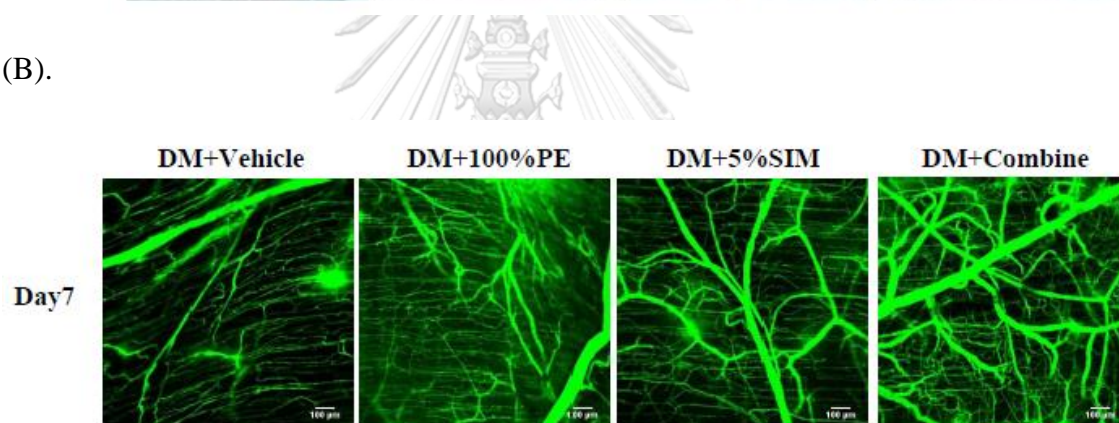
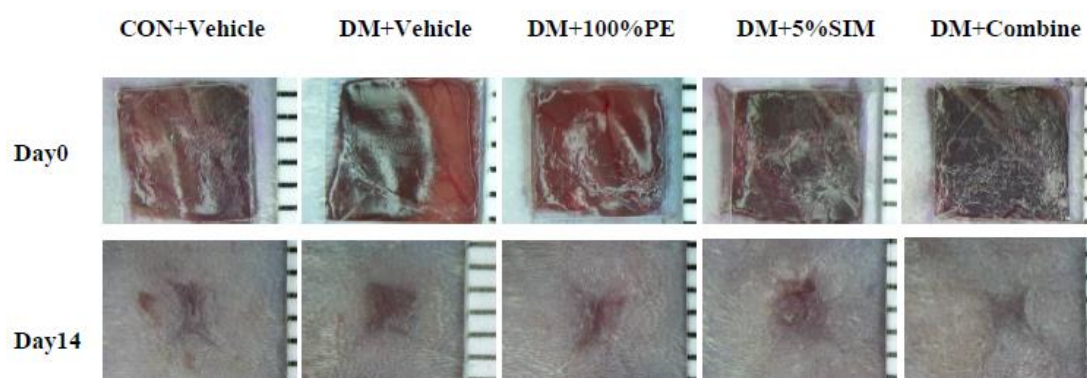


Figure 30. Wound Area Images and Confocal Microscopic Images of Areas Around Full-thickness Dorsal Skin Wound in STZ-induced Diabetic BALB/C Mouse Model on Day 7 in Protocol 2.

(A). Wound area images on day 0 and day 7; (B). Confocal microscopic images of areas around full-thickness dorsal skin wound on day 7. Wound area images presented here were from the same wound on day 0 and day 7. The clear pictures most represent the average %CV were chosen from each group.

(A).



(B).

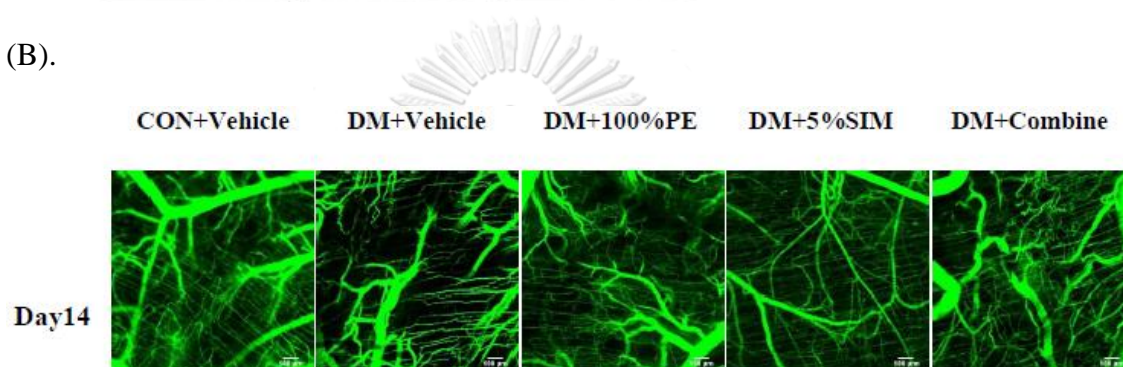


Figure 31. Wound Area Images and Confocal Microscopic Images of Areas Around Full-thickness Dorsal Skin Wound in STZ-induced Diabetic BALB/C Mouse Model on Day 14 in Protocol 2.

(A). Wound area images on day 0 and day 14; (B). Confocal microscopic images of areas around full-thickness dorsal skin wound on day 14. Wound area images presented here were from the same wound on day 0 and day 14. The clear pictures most represent the average %CV were chosen from each group.

Table 11. Results of Percentage of Wound Closure (%WC) of Groups on Day 7 in Protocol 2

(All data were expressed as mean \pm SEM)

Groups	n	%WC
DM+Vehicle	4	54.80% \pm 9.00%
DM+100%PE	5	57.01% \pm 5.11% ^{ns}
DM+5%SIM	6	59.03% \pm 5.11% ^{ns}
DM+Combine	6	69.88% \pm 4.90% ^{ns}

ns=not significant, compared with DM+Vehicle group.

Table 12. Results of Percentage of Capillary Vascularity (%CV) of Groups on Day 7 in Protocol 2

(All data were expressed as mean \pm SEM)

Groups	n	%CV
DM+Vehicle	4	35.77% \pm 1.29%
DM+100%PE	5	40.44% \pm 0.78%*
DM+5%SIM	6	40.58% \pm 0.91%*
DM+Combine	6	41.84% \pm 1.20%*

* p <0.05, compared with DM+Vehicle group.

Table 13. Results of Percentage of Wound Closure (% WC) of Groups on Day14
in Protocol 2

(All data were expressed as mean \pm SEM)

Groups	n	% WC
CON+Vehicle	3	99.27% \pm 0.13%
DM+Vehicle	4	94.83% \pm 1.37% [#]
DM+100%PE	5	98.75% \pm 0.20% [*]
DM+5%SIM	5	99.01% \pm 0.28% [*]
DM+Combine	5	99.33% \pm 0.09% ^{*, NS}

*p<0.05, compared with DM+Vehicle group;
#p<0.05, compared with CON+Vehicle group;
NS=not significant, compared with CON+Vehicle group.

Table 14. Results of Percentage of Capillary Vascularity (% CV) of Groups on Day 14
in Protocol 2

(All data were expressed as mean \pm SEM)

Groups	n	% CV
CON+Vehicle	3	40.68% \pm 1.19%
DM+Vehicle	4	36.30% \pm 0.71% [#]
DM+100%PE	5	39.38% \pm 1.43% ^{NS}
DM+5%SIM	5	38.52% \pm 1.32% ^{NS}
DM+Combine	5	40.49% \pm 0.86% ^{*, NS}

*p<0.05, compared with DM+Vehicle group;
#p<0.05, compared with CON+Vehicle group;
NS=not significant, compared with CON+Vehicle group.

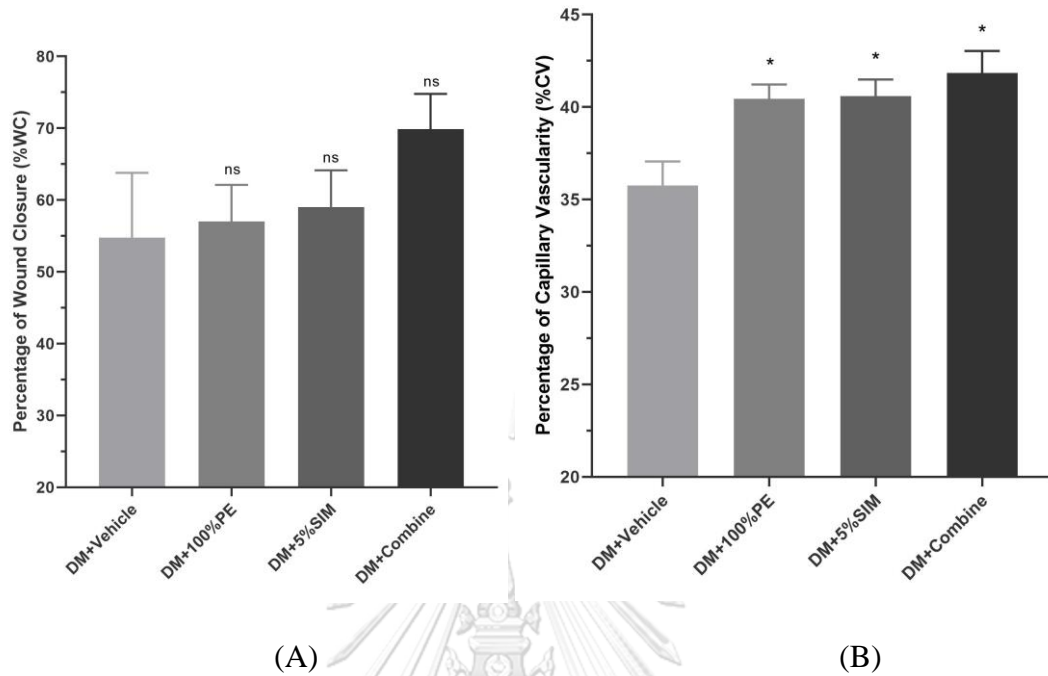


Figure 32. Percentage of Wound Closure (%WC) and Capillary Vascularity (%CV) of Groups on Day 7 in Protocol 2. (All data were expressed as mean ± SEM)

ns=not significant, compared with DM+Vehicle group;

* $p < 0.05$, compared with DM+Vehicle group.

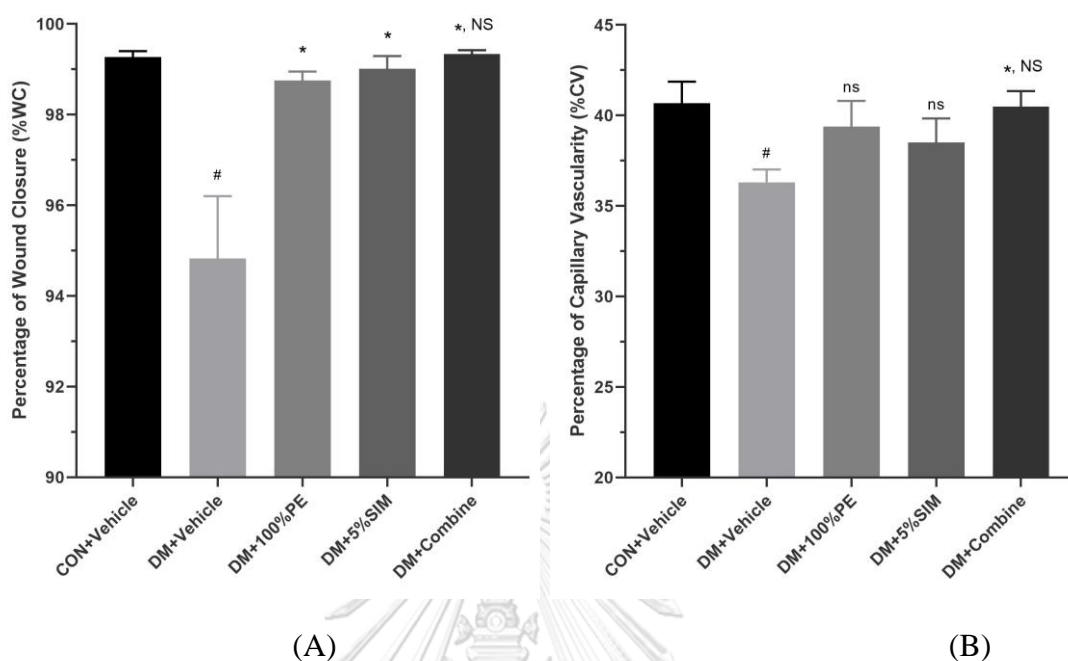


Figure 33. Percentage of Wound Closure (%WC) and Capillary Vascularity (%CV) of Groups on Day 14 in Protocol 2. (All data were expressed as mean \pm SEM)

* $p < 0.05$, compared with DM+Vehicle group;

$p < 0.05$, compared with CON+Vehicle group;

NS=not significant, compared with CON+Vehicle group.

Table 11 shows the results of the percentage of wound closure (%WC) in all groups on day 7 in protocol 2. None of the treatment groups has significant difference when compared with DM+Vehicle on day 7. However, DM+Combine group had tendency to increase %WC on day 7. **Table 12** shows the results of the percentage of capillary vascularity (%CV) in all groups on day 7 in protocol 2. DM+100%PE group, DM+5%SIM group, and DM+Combine group all have increased percentage of capillary vascularity (%CV) significantly ($p < 0.05$, respectively) when compared with DM+Vehicle group on day 7. DM+Combine group increased the percentage of capillary vascularity (%CV) most among these three treatment groups. It suggests that the combination of PE and simvastatin has a combined effect on increasing wound capillary vascularity on day 7 in diabetic mice. **Figure 32** shows the graphs of the percentage of wound closure (%WC) and percentage of capillary vascularity (%CV) on day 7 in Protocol 2.

Table 13 shows the data of the percentage of wound closure (%WC) of groups on day 14. The results of percentage of wound closure (%WC) showed that each of the treatment groups and CON+Vehicle group has significant difference ($p<0.05$) when compared with DM+Vehicle group on day 14 in Protocol 2. There is no significant difference between DM+Combine group and CON+Vehicle group. This suggests that combined treatment of PE and simvastatin could restore the %WC to that of the non-diabetic CON+Vehicle group level. **Table 14** shows the data of the percentage of capillary vascularity (%CV) of groups on day 14 in Protocol 2. The results of the percentage of capillary vascularity (%CV) show that DM+Combine group had significant difference ($p<0.05$) when compared with DM+Vehicle group on day 14. However, there was no significant difference between groups of DM+Combine and CON+Vehicle on day 14. This suggests that combined treatment of PE and simvastatin could restore the %CV to that of the non-diabetic CON+Vehicle group level. **Figure 33** shows the graphs of the percentage of wound closure (%WC) and percentage of capillary vascularity (%CV) on day14.



4.2.3. Effects of Combined Treatment of PE and Simvastatin on VEGF Protein Level

Table 15 showed the data of tissue VEGF protein level (pg/mg total protein) at wound site on day 7 and day 14 in Protocol 2. **Figure 36** shows the graph of VEGF

protein level (pg/mg total protein) in all groups on day 7 and day 14 in Protocol 2. The results showed that VEGF protein levels (pg/mg total protein) of DM+Combine group were upregulated comparing to DM+Vehicle group, both on day 7 and day 14. This indicated that combined drug treatment can upregulate wound VEGF protein level both on day 7 and day 14.

Table 15. VEGF Protein Level (pg/mg total protein) of Wound Site on Day 7 and Day 14 in Protocol 2

(All data were expressed as mean ± SEM)

Groups	Day 7		Day 14	
	n	VEGF Protein Level (pg/mg)	n	VEGF Protein Level (pg/mg)
DM+Vehicle	4	183.1 ± 12.8	4	76.5 ± 12.0
DM+100%PE	4	138.1 ± 39.9 ^{ns}	4	95.8 ± 6.9 ^{ns}
DM+5%SIM	4	213.3 ± 18.0 ^{ns}	4	103.2 ± 8.8 ^{ns}
DM+Combine	4	260.8 ± 18.5*	4	113.3 ± 15.2*

ns=not significant, compared with DM+Vehicle group;

* $p < 0.05$, compared with DM+Vehicle group;

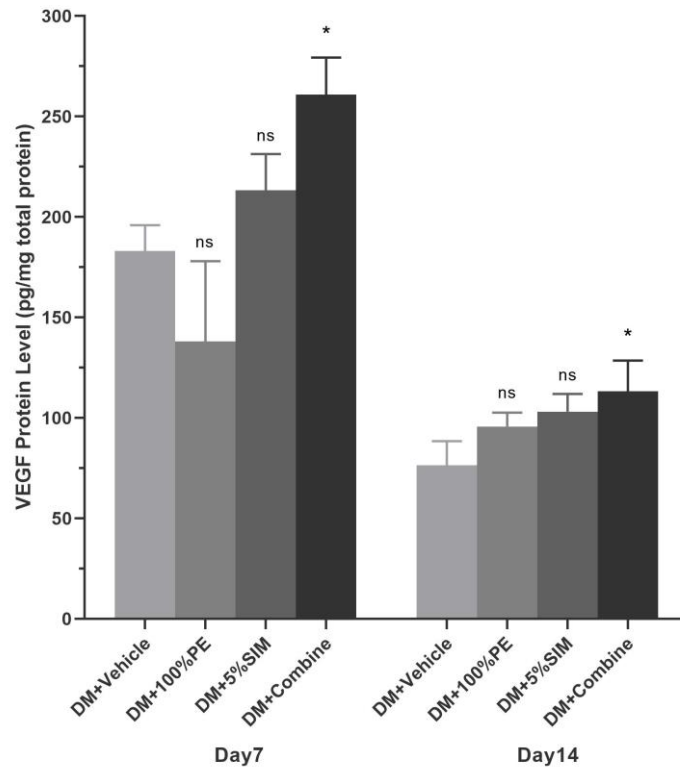


Figure 34. VEGF protein level (pg/mg total protein) of Wound Site on Day 7 and Day 14 in Protocol 2. (All data were expressed as mean \pm SEM)

ns=not significant, compared with DM+Vehicle group;

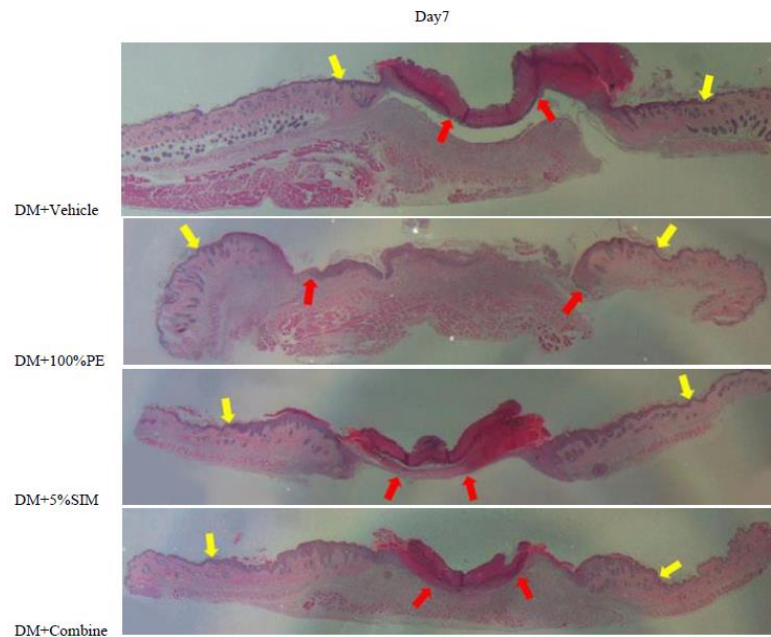
* p <0.05, compared with DM+Vehicle group;

4.2.4. Effects of Combined Treatment of PE and Simvastatin on Percentage of Re-Epithelialization (%RE)

Figure 35 (A-B) showed the images of re-epithelialization of groups on day 7 and day 14 in Protocol 2. **Table 16** showed the data of the percentage of re-epithelialization at wound site (H&E staining, 400x magnification) on day 7 and day 14 in Protocol 2. **Figure 36** showed the graphs of the percentage of re-epithelialization at wound site (H&E staining, 400x magnification) on day 7 and day 14 in Protocol 2. The results showed that the percentage of re-epithelialization of DM+Combine group at wound site was not upregulated significantly either on day 7 or day 14.



(A).



(B).

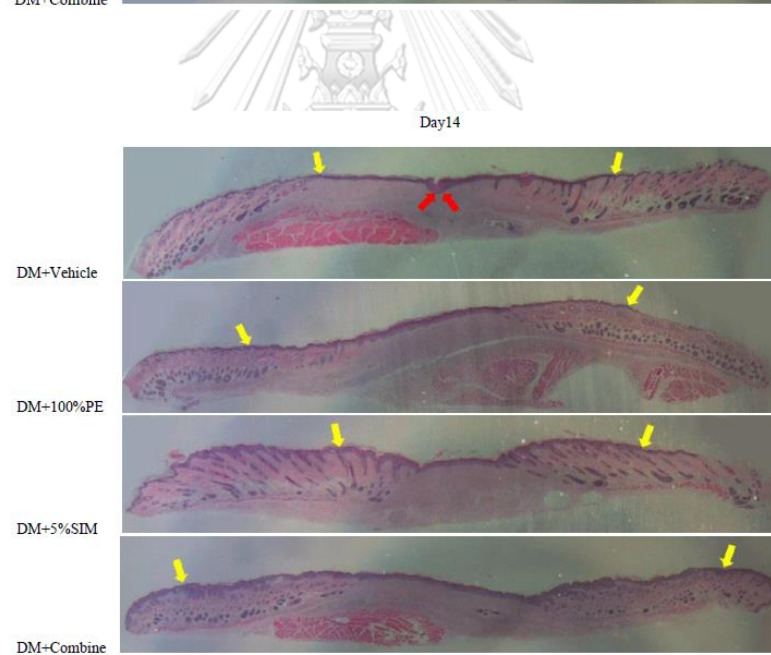


Figure 35. Images of Re-Epithelialization of Groups on Day 7 and Day 14 in Protocol 2.

(A). Images of re-epithelialization of each group on day 7; (B). Images of re-epithelialization of each group on day 14; The images shown were taken under 10× magnification; Wound images used for judging the wound edge were taken under 400× magnification, not shown.

Table 16. Percentage of Wound Re-epithelialization (%RE) at Wound Site (H&E staining, 400x magnificence) on Day 7 and Day 14 in Protocol 2

(All data were expressed as mean \pm SEM)

Groups	Day7		Day14	
	n	Re-epithelialization (%RE)	n	Re-epithelialization (%RE)
DM+Vehicle	4	86.34% \pm 6.39%	5	99.12% \pm 0.88%
DM+100%PE	4	61.00% \pm 13.04%*	5	100.00% \pm 0.00% ^{ns}
DM+5%SIM	5	83.94% \pm 6.40% ^{ns}	5	100.00% \pm 0.00% ^{ns}
DM+Combine	5	91.19% \pm 3.96% ^{ns}	5	100.00% \pm 0.00% ^{ns}

ns=not significant, compared with DM+Vehicle group;

* p <0.05, compared with DM+Vehicle group.

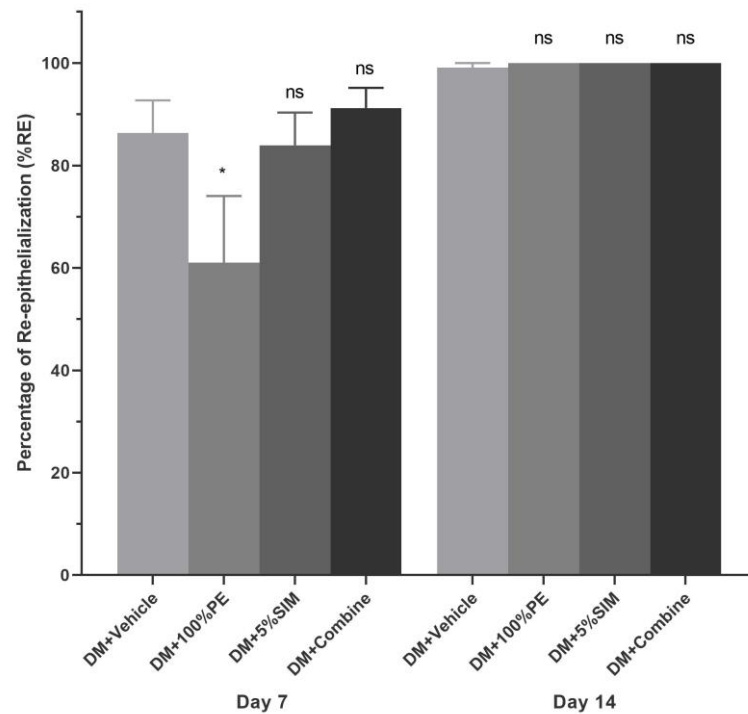


Figure 36. Percentage of Re-Epithelialization at Wound Site (H&E staining, 400x magnification) on Day 7 and Day 14 in Protocol 2.

(All data were expressed as mean \pm SEM)

ns=not significant, compared with DM+Vehicle group;

* $p < 0.05$, compared with DM+Vehicle group.

4.2.5. Effects of Combined Treatment of PE and Simvastatin on Neutrophil Infiltration

Figure 37 showed the images of infiltrated neutrophils at wound site of groups on day 4 and day 7 in Protocol 2. **Table 17** showed the number of infiltrated neutrophils at the wound site (H&E staining, 400x magnification) on day 4, and day 7 in Protocol 2. **Figure 38** showed the graph of wound number of infiltrated neutrophils (H&E staining, 400x magnification) on day 4 and day 7 in Protocol 2. The results showed that neutrophil infiltration count was downregulated significantly ($p < 0.05$) in each of the treatment groups significantly on day 4. The neutrophil infiltration count was downregulated significantly ($p < 0.05$) in DM+5%SIM group, and DM+Combine group on day 7. This indicated that combined drug treatment can significantly downregulate the number of infiltrated neutrophils both on both day 4 and day 7 in diabetic mice.

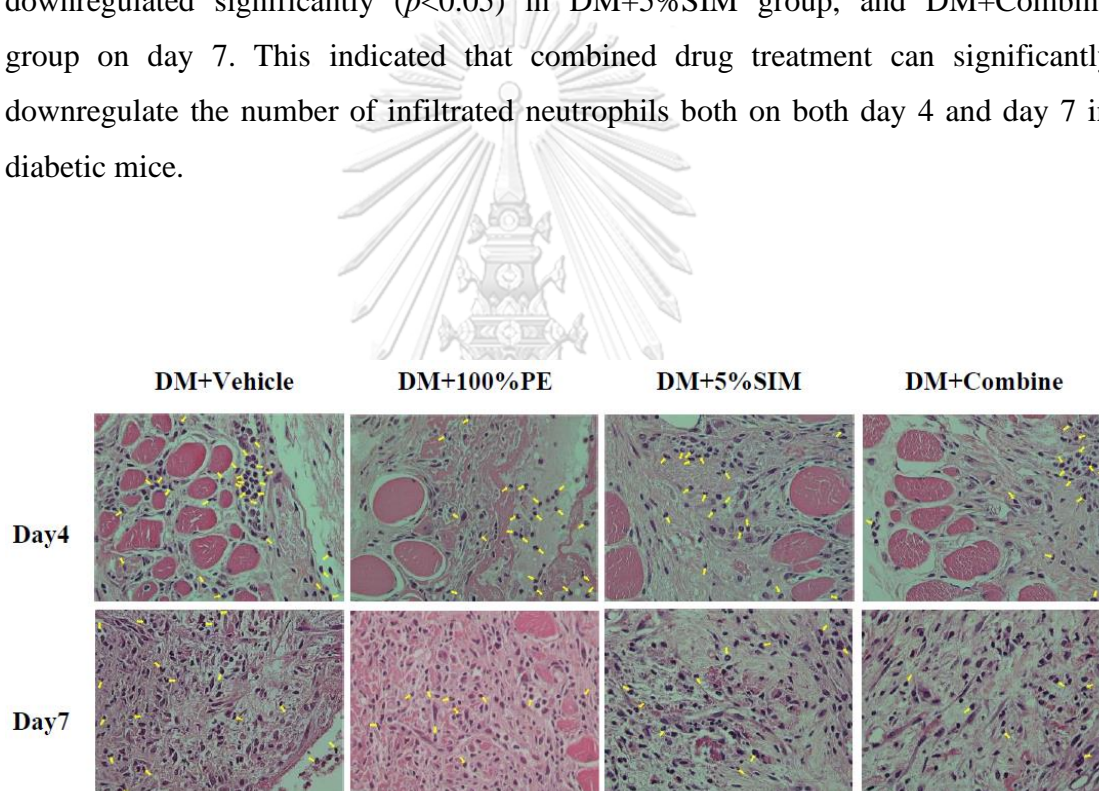


Figure 37. Images of Infiltrated Neutrophils of Each Group on Day 4 and Day 7 in Protocol 2.

The images shown here were taken under 400× magnification, the shape of neutrophils was judged by using the Image-Pro Plus program.

Table 17. Number of Infiltrated Neutrophils of Wound Site (H&E staining, 400x magnificence) on Day 4 and Day 7 in Protocol 2

(All data were expressed as mean \pm SEM)

Groups	Day 4		Day 7	
	n	Number of Infiltrated Neutrophils	n	Number of Infiltrated Neutrophils
DM+Vehicle	4	96 \pm 8	3	52 \pm 11
DM+100%PE	4	80 \pm 3*	5	38 \pm 2 ^{ns}
DM+5%SIM	5	68 \pm 4*	4	34 \pm 4*
DM+Combine	4	47 \pm 3*	4	23 \pm 2*

ns= not significant, compared with DM+Vehicle group;
* p <0.05, compared with DM+Vehicle group.

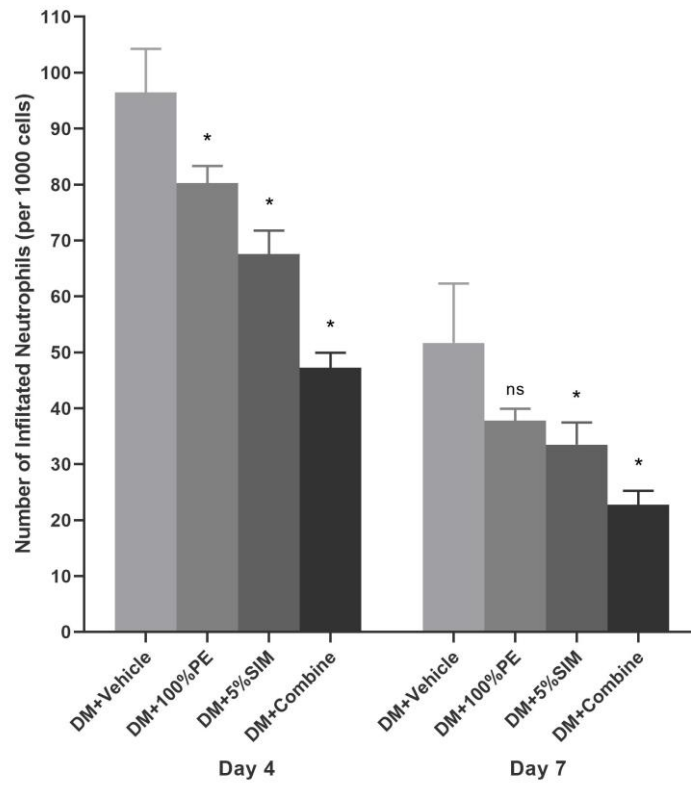


Figure 38. Number of Infiltrated Neutrophils of Wound Site (H&E staining, 400x magnificence) on Day 4 and Day 7 in Protocol 2.

(All data were expressed as mean \pm SEM)

ns= not significant, compared with DM+Vehicle group;

* $p < 0.05$, compared with DM+Vehicle group.

CHULALONGKORN UNIVERSITY

4.2.6. Effects of Combined Treatment of PE and Simvastatin on IL-6 Protein Level

Table 18 showed the data of IL-6 protein level (pg/mg total protein) of wound site on day 4 and day 7 in Protocol 2. **Figure 39** showed the graph of IL-6 protein expression (pg/mg total protein) of wound site on day 4 and day 7 in Protocol 2. The results showed that DM+Combine group had tendency to downregulate IL-6 protein levels (pg/mg total protein) both on day 4 ($p=0.248$) and day 7 ($p=0.127$), but without significant difference when compared with DM+Vehicle group, respectively.

Table 18. IL-6 protein level (pg/mg total protein) of Wound Site on Day 4 and Day 7 in Protocol 2

(All data were expressed as mean \pm SEM)

Groups	Day 4		Day 7	
	n	IL-6 Protein Level (pg/mg)	n	IL-6 Protein Level (pg/mg)
DM+Vehicle	4	470.4 \pm 61.6	4	145.3 \pm 27.8
DM+100%PE	5	441.1 \pm 37.0 ^{ns}	5	133.0 \pm 19.9 ^{ns}
DM+5%SIM	4	413.8 \pm 47.4 ^{ns}	5	132.6 \pm 16.1 ^{ns}
DM+Combine	5	386.5 \pm 50.6 ^{ns}	5	101.8 \pm 9.2 ^{ns}

ns=not significant, compared with DM+Vehicle group.

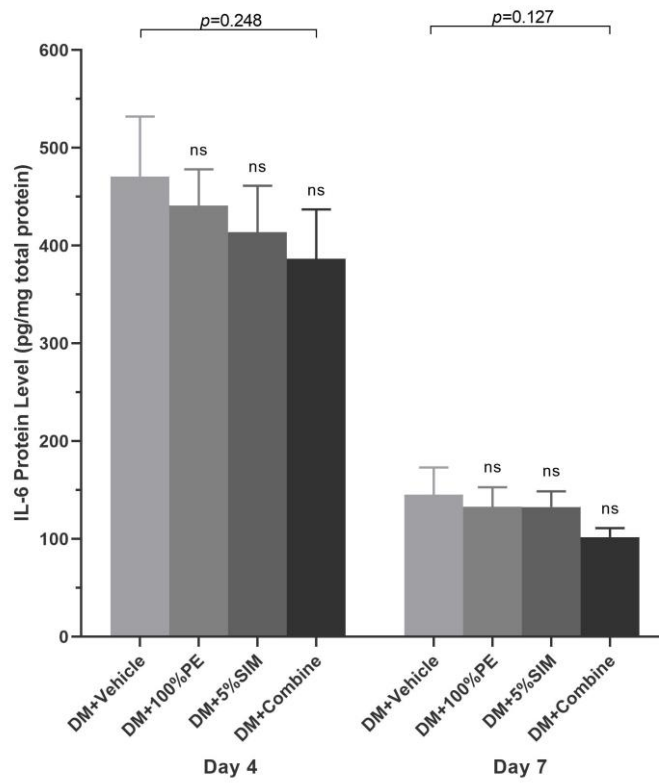


Figure 39. IL-6 Protein Expression (pg/mg total protein) of Wound Site on Day 4 and Day 7 in Protocol 2. (All data were expressed as mean \pm SEM)
 ns=not significant, compared with DM+Vehicle group.

4.2.7. Effects of Combined Treatment of PE and Simvastatin on Tissue MDA

Table 19 show MDA content (nmol/mg total protein) of wound site on day 4, day 7 and day 14 in Protocol 2. **Figure 40** shows the graph of MDA content (nmol/mg total protein) of wound site on day 4, day 7 and day 14 in Protocol 2. The results showed that MDA content was downregulated significantly ($p<0.05$) by DM+Combine group on day 4 and day 14. Even though not significantly, DM+Vehicle group had a tendency to downregulate MDA content on day 7, as shown in **Figure 40**. This indicated that combined drug treatment of PE and SIM has a combined effect in ameliorating the oxidative stress in diabetic mice wound on day 4 and day 14.

Table 19. MDA Content (nmol/mg total protein) of Wound Site on Day 4, Day 7, and Day14 in Protocol 2

(All data were expressed as mean \pm SEM)

Groups	Day 4		Day 7		Day 14	
	n	MDA Content (nmol/mg)	n	MDA Content (nmol/mg)	n	MDA Content (nmol/mg)
DM+Vehicle	4	1.84 \pm 0.34	5	2.82 \pm 1.57	4	7.23 \pm 0.82
DM+100%PE	5	0.73 \pm 0.12*	5	2.11 \pm 0.48 ^{ns}	4	5.97 \pm 1.83 ^{ns}
DM+5%SIM	5	1.23 \pm 0.21 ^{ns}	5	2.24 \pm 0.26 ^{ns}	4	4.54 \pm 1.06 ^{ns}
DM+Combine	4	1.01 \pm 0.20*	5	1.05 \pm 0.24 ^{ns}	3	1.38 \pm 0.22*

ns= not significant, compared with DM+Vehicle group;

* $p<0.05$, compared with DM+Vehicle group.

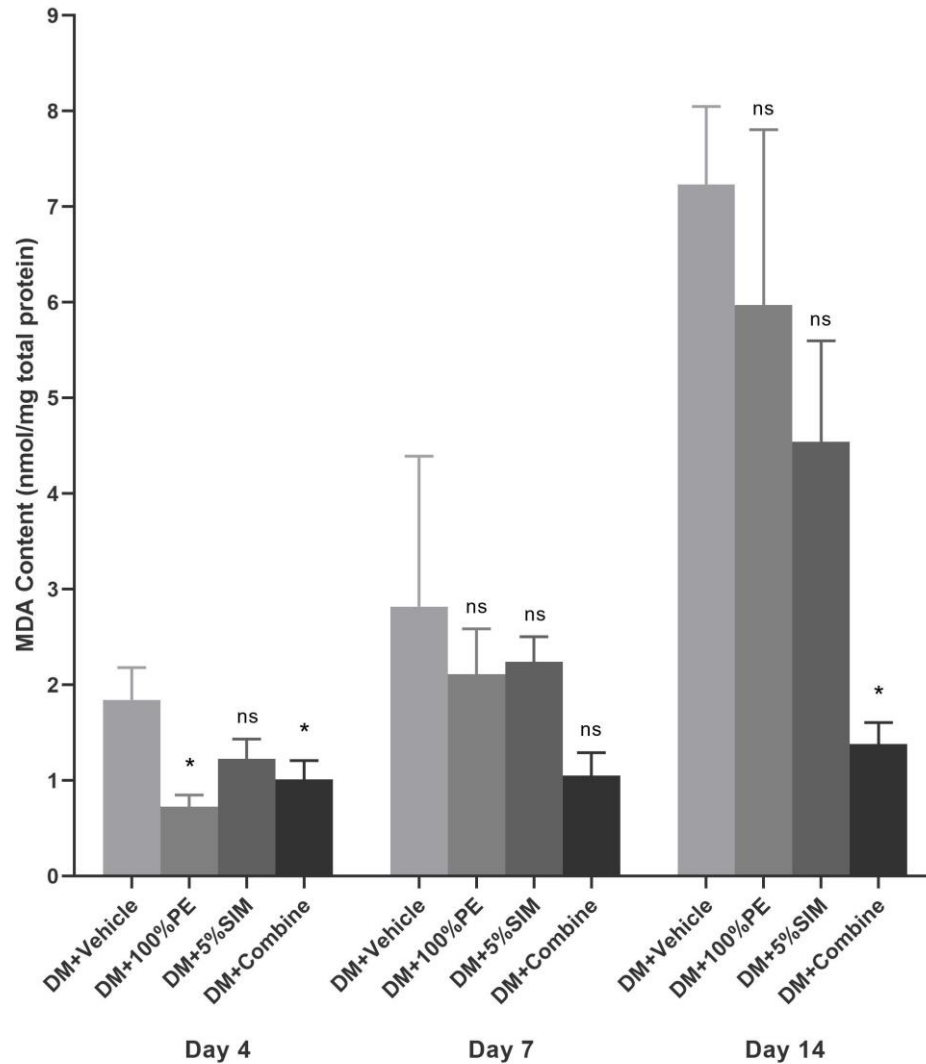


Figure 40. MDA Content (nmol/mg total protein) of Wound Site on Day 4, Day 7 and Day 14 in Protocol 2. (All data were expressed as mean \pm SEM)

ns= not significant, compared with DM+Vehicle group;

* $p < 0.05$, compared with DM+Vehicle group.

To conclude, the results and advantages of the combination treatment of PE and SIM on the parameters are shown in **Table 20**, **Table 21**, and **Table 22**.

Table 20. Summarization of Parameters on Day 4 in Protocol 2

(All data were expressed as mean \pm SEM)

Parameter	DM+Vehicle	DM+100%PE	DM+5%SIM	DM+Combine
IL-6	470.4 \pm 61.6	441.1 \pm 37.0 ↓	413.8 \pm 47.4 ↓	386.5 \pm 50.6 ↓
Infiltrated Neutrophils	96 \pm 8	80 \pm 3* ↓	68 \pm 4* ↓	47 \pm 3* ↓
MDA	1.84 \pm 0.34	0.73 \pm 0.12* ↓	1.23 \pm 0.21 ↓	1.01 \pm 0.20* ↓

* p <0.05, compared with DM+Vehicle group.

Table 21. Summarization of Parameters on Day 7 in Protocol 2

(All data were expressed as mean \pm SEM)

Parameter	DM+Vehicle	DM+100%PE	DM+5%SIM	DM+Combine
%WC	54.80% \pm 9.00%	57.01% \pm 5.11% ↑	59.03% \pm 5.11% ↑	69.88% \pm 4.90% ↑
%CV	35.77% \pm 1.29%	40.44% \pm 0.78%* ↑	40.58% \pm 0.91%* ↑	41.84% \pm 1.20%* ↑
VEGF	183.1 \pm 12.8	138.1 \pm 39.9 ↓	213.3 \pm 18.0 ↑	260.8 \pm 18.5* ↑
IL-6	145.3 \pm 27.8	133.0 \pm 19.9 ↓	132.6 \pm 16.1 ↓	101.8 \pm 9.2 ↓
Infiltrated Neutrophils	52 \pm 11	38 \pm 2 ↓	34 \pm 4* ↓	23 \pm 2* ↓
Re-epithelialization	86.34% \pm 6.39%	61.00% \pm 13.04% ↓	83.94% \pm 6.40% ↓	91.19% \pm 3.96% ↑
MDA	2.82 \pm 1.57	2.11 \pm 0.48 ↓	2.24 \pm 0.26 ↓	1.05 \pm 0.24 ↓

* p <0.05, compared with DM+Vehicle group.

Table 22. Summarization of Parameters on Day 14 in Protocol 2

(All data were expressed as mean \pm SEM)

Parameter	DM+Vehicle	DM+100%PE	DM+5%SIM	DM+Combine	CON+Vehicle
%WC	94.83% \pm 2.75%	98.75% \pm 0.45%* ↑	99.01% \pm 0.62%* ↑	99.33% \pm 0.20%* ↑	99.27% \pm 0.13%* ↑
%CV	36.30% \pm 0.71%	39.38% \pm 1.43% ↑	38.52% \pm 1.32% ↑	40.49% \pm 0.86%* ↑	39.33% \pm 1.19%* ↑
VEGF	76.5 \pm 12.0	95.8 \pm 6.9 ↑	103.2 \pm 8.6 ↑	113.3 \pm 15.2* ↑	/
Re-epithelialization	99.12% \pm 0.88%	100.00% \pm 0.00% ↑	100.00% \pm 0.00% ↑	100.00% \pm 0.00% ↑	/
MDA	7.23 \pm 0.82	5.97 \pm 1.83 ↓	4.54 \pm 1.06 ↓	1.38 \pm 0.22* ↓	/

* $p < 0.05$, compared with DM+Vehicle group.

4.2.8. Correlation Analysis between Parameters

4.2.8.1. Correlation Analysis of %WC and VEGF on Day 7

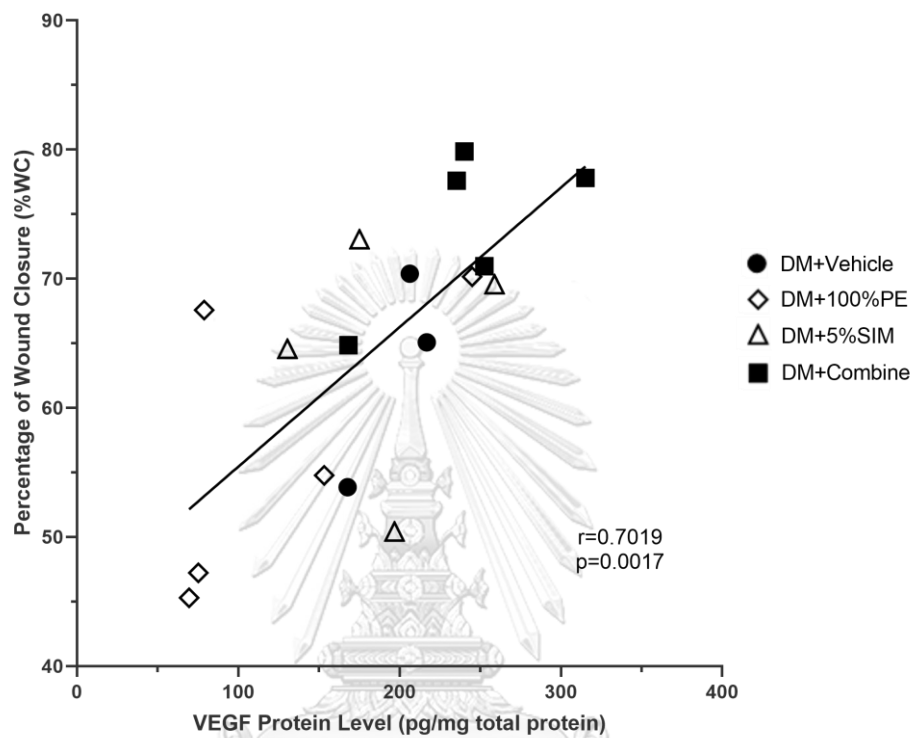


Figure 41. Pearson's Correlation Analysis between Data Sets of Percentage of Wound Closure (%WC) and VEGF Protein Level (pg/mg total protein) of Groups on Day 7. (Details of each data set were shown in Appendix 19)
 $(Y = 0.1081 * X + 44.64, R^2 = 0.4926, \text{Pearson's correlation coefficient } r = 0.7019, p = 0.0017)$

4.2.8.2. Correlation Analysis of %CV and VEGF on Day 7

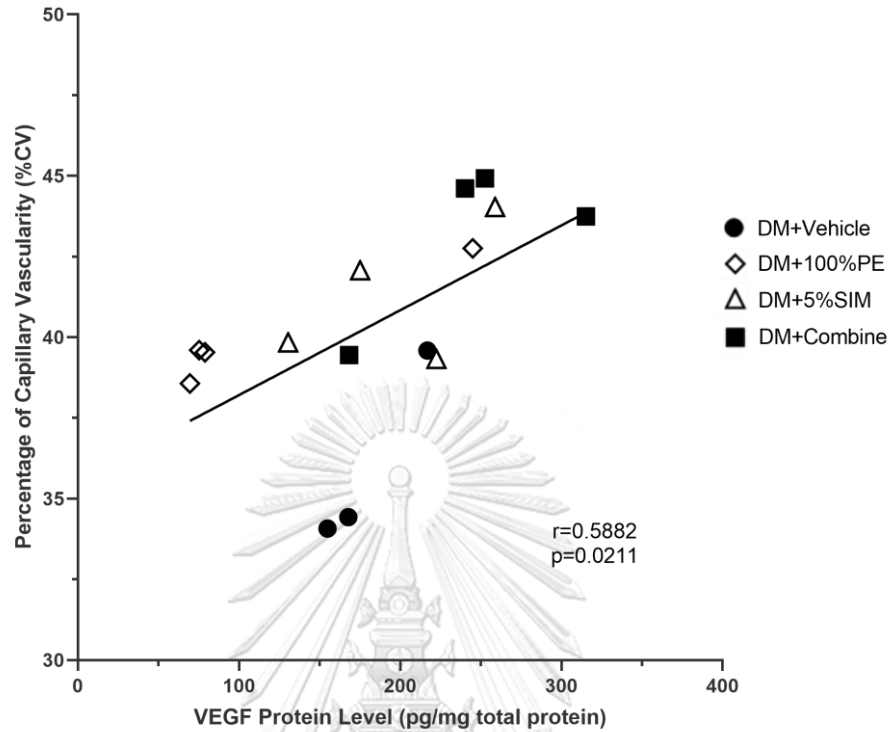


Figure 42. Pearson's Correlation Analysis between Data Sets of Percentage of Capillary Vascularity (%CV) and VEGF Protein Level (pg/mg total protein) of Groups on Day 7 in Protocol 2. (Details of each data set were shown in Appendix 20)
 $(Y = 0.0263 * X + 35.58, R^2 = 0.3460, \text{Pearson's correlation coefficient } r = 0.5882, p = 0.0211)$

4.2.8.3. Correlation Analysis of %WC and %CV on Day 7

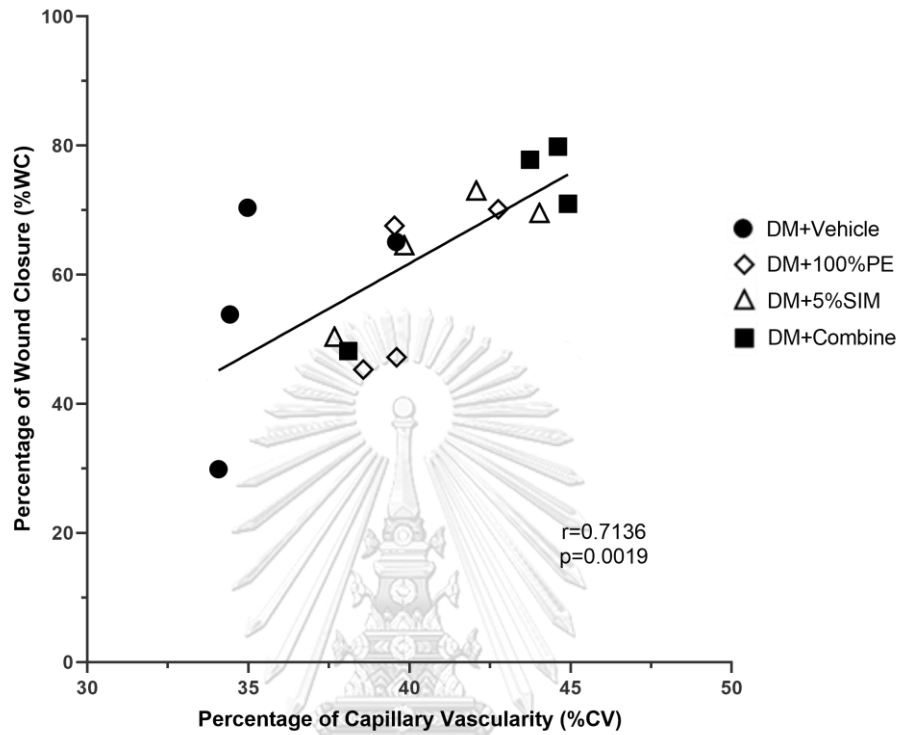


Figure 43. Pearson's Correlation Analysis between Data Sets of the Percentage of Wound Closure (%WC) and Percentage of Capillary Vascularity (%CV) of Groups on Day 7 in Protocol 2. (Details of each data set were shown in Appendix 13)
 $(Y = 2.7990 * X - 50.21, R^2 = 0.5092, \text{Pearson's correlation coefficient } r = 0.7136, p = 0.0019)$

CHULALONGKORN UNIVERSITY

4.2.8.4. Correlation Analysis of %WC and %CV on Day 14

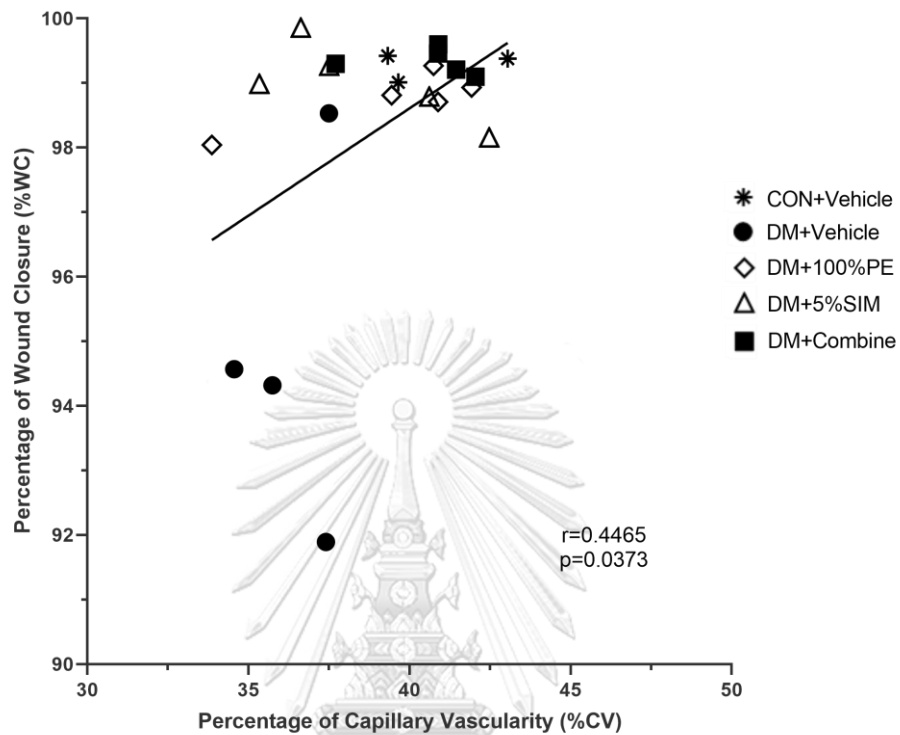


Figure 44. Pearson's Correlation Analysis between Data Sets of the Percentage of Wound Closure (%WC) and Percentage of Capillary Vascularity (%CV) of Groups on Day 14 in Protocol 2. (Details of each data set were shown in Appendix 16)
 $(Y = 0.3325 * X + 85.31, R^2 = 0.1993, \text{Pearson's correlation coefficient } r = 0.4465, p = 0.0373)$

4.2.8.5. Correlation Analysis of %WC and IL-6 Protein Level on Day 7

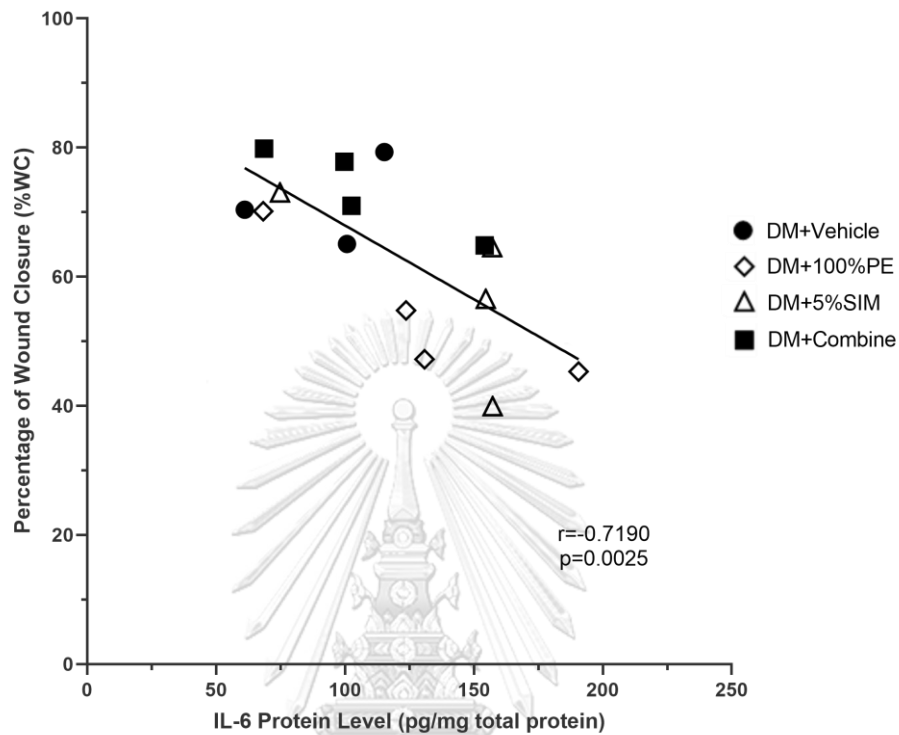


Figure 45. Pearson's Correlation Analysis between Data Sets of the Percentage of Wound Closure (%WC) and IL-6 Protein Level (pg/mg total protein) of Groups on Day 7 in Protocol 2. (Details of each data set were shown in Appendix 27)
 $(Y = -0.2289 * X + 90.84, R^2 = 0.5170, \text{Pearson's correlation coefficient } r = -0.7190, p = 0.0025)$

CHULALONGKORN UNIVERSITY

4.2.8.6. Correlation Analysis of %RE and VEGF Protein Level on Day 7

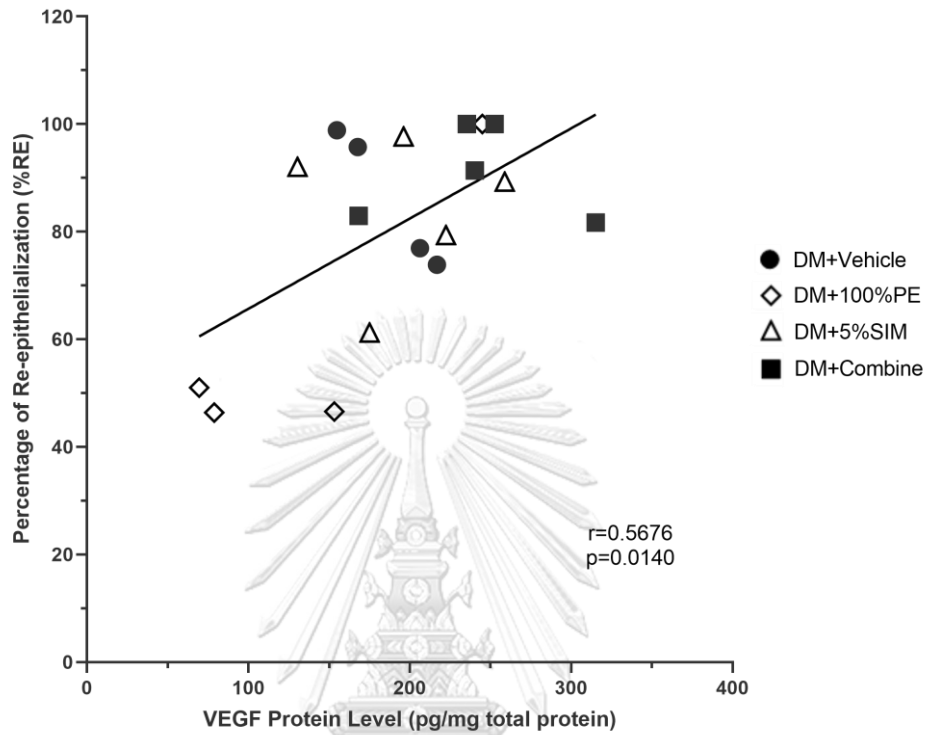


Figure 46. Pearson's Correlation Analysis between Data Sets of the Percentage of Re-Epithelialization (%RE) and VEGF Protein Level (pg/mg total protein) of Groups on Day 7 in Protocol 2. (Details of each data set were shown in Appendix 31)
($Y = 0.1677 * X + 48.89$, $R^2 = 0.3222$, Pearson's correlation coefficient $r = 0.5676$, $p = 0.0140$)

CHULALONGKORN UNIVERSITY

CHAPTER V

DISCUSSION

Diabetes mellitus (DM) is a group of metabolic disorders with hyperglycemia as its hallmark. DM is a prevalent medical problem throughout the world and continues to increase in number and significance due to lifestyle changes. It ranks the 7th cause of death-leading diseases in the US in 2015, with a total of 252,806 death taking diabetes as a contributing cause of death. It is estimated that the number of DM patients will triple by 2050, which will cause a major health and economic burden. Up to 15% of diabetic patients may suffer chronic non-healing diabetic foot ulcers (DFUs), with approximately 85% of persons with diabetes will end up with lower extremity amputations [1, 2]. Armstrong D.G. and his colleagues reported that one leg is lost due to diabetes every 30 seconds in the world [3]. The major underlying causes are noted to be peripheral neuropathy and ischemia from peripheral vascular disease [4, 5]. Peripheral arterial diseases are up to 8 times more common in diabetic patients. Inadequate blood supply at the foot injury may result in foot ulceration, potentially leading to limb amputation [1].

In diabetic wound, hyperglycemia can cause oxidative stress. Oxygen-free radicals like hydrogen peroxide (H_2O_2), superoxide radical (O_2^-), hydroxyl radical (OH^-), and nitric free radicals are overproduced, oxidant enzymes such as superoxide dismutase (SOD), catalase (CAT), glutathione peroxidase (GPx), glutathione (GSH) are downregulated, causing oxidative stress in peripheral vessels. Also, at the diabetic wound site, excessive inflammatory cells are infiltrated, such as neutrophils. The oxidative stress and inflammation at the diabetic wound site can disturb the wound healing process, leading to slow diabetic foot ulcer healing [6]. Control of risk factors, such as hyperglycemia, which induce endothelial malfunction, oxidative stress, diabetic neuropathy, and peripheral arterial diseases, could be the effective management approaches for diabetic foot ulcer [1, 7]. What's more, management of infection and revascularization also are gold standards for diabetic foot ulcer treatment besides diabetic control [1].

Since both simvastatin and PE showed antioxidant and anti-inflammation effects, which have potential benefits for diabetic wound healing. We aimed to find out whether the effects of the combination of topical application of PE and simvastatin and the possible pathway(s) that may involve their effects.

5.1. Results of Physiological Parameters

Table 9 and **Figure 28** showed the results of the percentage of body weight change (%BW) of each group on day 4, day 7, and day 14 in Protocol 2, when compared with the body weight at wounding day. The body weight change (%BW) of each mouse on day 4, day 7, and day 14 is shown in **Appendix 1-3**, respectively. Bodyweight loss is one of the features of clinical diabetic patients and diabetes animals. Under the diabetic condition, insufficient insulin prevents the blood glucose from transferring to energy for body use, but protein and fat for energy instead, leading to bodyweight loss. The change rates of mice bodyweight of the groups were all less than 20% during the treatment period on day 4, day 7, and day 14. On day 4, there was no significant difference among all the treatment groups when compared with DM+Vehicle group. On day 7, DM+Combine group had significant difference when compared with DM+Vehicle group, $p < 0.05$. On day 14, DM+Combine had significant difference when compared with CON+Vehicle group, $p < 0.05$. However, DM+Combine group has no significant difference when compared with DM+Vehicle group. This indicates that the significant body weight loss perhaps due to the diabetic situation in mice, not caused by the treatment. It has been proved that the bodyweight loss in the STZ-induced diabetic model is due to the harmful effects of STZ on DNA alkylation, inducing hyperglycemia and necrotic lesion properties [208].

Table 10 and **Figure 29** showed the Fasting Blood Glucose (FBG) levels of experimental mice measured on endpoint day (day 4, day 7, and day 14) groups in Protocol 2. The fasting blood glucose level of each mouse on day 4, day 7, and day 14 is shown in **Appendix 4-6**, respectively. All the average mean values and the fasting blood glucose level of each mouse in diabetic group were above 200mg/dL on day 4, day 7, and day 14. On day 4, FBG levels of all the treatment groups have significant

difference ($p < 0.05$) when compared with DM+Vehicle group. This perhaps relate to local absorbance of the PE and simvastatin, exerting their hypoglycemic effects in systematic circulation.

The method of multiple low-dose intraperitoneal injections of STZ was used in this study [9, 37]. Streptozotocin (STZ), a toxic glucose analogue, is toxic to pancreatic β -cells, leading to a decrease in insulin secretion and degranulation, accompanied by hyperglycemia. It is preferentially accumulated in pancreatic β -cells through GLUT2 glucose transporter. After taken into β -cells, STZ cracks into glucose and methyl-nitrosourea particles. Further, STZ could also inhibit glucose-induced insulin secretion by fragmenting mitochondrial DNA in β -cells, which is important on metabolic signaling function of STZ, resulting in hypoinsulinemia and hyperglycemia to induce the type I diabetic animal model [209]. Hypoinsulinemia then increases acyl-coenzyme A oxidase which can initiate β -oxidation of fatty acids, finally leading to lipid peroxidation. Further, increased lipid peroxidation results in raised levels of ROS, which can attack unsaturated fatty acids on the cell membrane, to enlarge lipid peroxidation and the development of diabetic complications in the end [26]. High blood glucose level may activate pathways of protein kinase C, increased activity of the polyol pathway, non-enzymatic glycation and oxidative stress, which finally lead to endothelial dysfunction within four weeks of the diabetic animal model [210]. For this reason, in the present study, the excisional full-thickness wound was made after four weeks of the diabetes. The results showed that fasting blood glucose (FBG) levels of all diabetic mice were significantly higher than the CON+Vehicle group on day 14 in Protocol 2. These results suggest the success of multiple low dose STZ-induced diabetic BALB/C mice model in this study.

Both simvastatin and PE could ameliorate a systematic hypoglycemic situation when orally administrated. In a most recent published research paper in 2019, simvastatin promoted hyperglycemia and glucose intolerance in high sucrose-induced pre-diabetic rats [14]. Clinically, simvastatin had been shown to increase fasting plasma glucose in long-term use in diabetic patients [211]. But till now, there is no evidence showing that topical application of simvastatin could increase blood glucose either in an animal model or in the clinical patient. It has been reported that systematic hypoglycemic

effects of various effective parts of PE have been discovered in diabetic animal models and clinical patients. In 2012, Nain P. and colleagues proposed that the hypoglycemic effect of leaf extract of PE may relate to its stimulation of insulin and restoration of metabolic activity [169]. It is believed that the beneficial effect of PE in controlling hyperglycemia was related to its antioxidative and anti-inflammatory properties from polyphenol and flavonoid chemicals. Kim et al. suggested that polyphenol-rich fractions of *E. officinalis* Gaertn. can attenuate the fructose-induced metabolic syndrome, significantly inhibited the increased serum and hepatic mitochondrial oxidative stress in 2010. Furthermore, protective potential of the In 2011, Akhtar and colleagues reported that high dose of orally taken PE fruit powder could decrease both postprandial blood glucose and fasting blood glucose in normal and type 2 diabetic patients, which probably due to the direct insulin-releasing effect from β -cells and indirect insulin-like effects which has been proved in type 2 diabetes animal models [170]. In 2014, Ansari and colleagues proposed that the hypoglycemic effect in STZ-induced type 2 diabetic rats may involve an extra-pancreatic effect since the serum insulin level did not increase [26]. In 2013, Pate S.S. and colleagues reported that oral administration of 100 mg/kg/day hydroalcoholic extract of PE significantly decreased serum glucose, increased serum insulin, and glucose metabolism in male Wistar rats [175]. Thus they proposed that the anti-diabetic activity of PE may due to increased sensitivity of peripheral tissue or a direct insulin-like property [175]. Further, there was also a report found out that there was a significant negative correlation between fasting blood glucose or HbA_{1c} levels and serum nitric oxide level in diabetic patients, but this is still in controversy [25, 212]. However, the hypoglycemic effect of topical application of PE on diabetic ulcer animal models or clinical patients has not yet been reported.

5.2. Protocol 1

5.2.1. Results of the Dose-Responses of Simvastatin and PE on Wound Closure (%WC) and Capillary Vascularity (%CV)

Diabetic wound has a prolonged healing time. Treatment of drugs with antioxidant and anti-inflammatory properties could enhance wound healing. In protocol 1, **Table 5 and Figure 22 (A)** showed the graph of the percentage of wound closure (%WC) of three doses of PE (DM+10%PE, DM+100%PE, and DM+200%PE groups) on day 14. From the results, DM+100%PE group has significant difference ($p < 0.05$) when compared with DM+Vehicle group on day 14. It means that DM+100%PE group could enhance the percentage of wound closure (%WC) significantly on day 14 in diabetic wounds in mice. In our study, %WC increased as PE dose increased from 10%PE to 100%PE, w/v. The wound-healing effect of PE in diabetic wound is tightly related to its anti-inflammatory and antioxidant properties based on the mounting evidence. However, the %WC in DM+200%PE group decreased, even lower than that in DM+10%PE group. The concentration gradient from drug formulation to the deeper inner skin site provides the driving force for the drug penetration through the skin barrier, which is determined by the saturation of the drug in the vehicle. Thus, usually, higher solubilized drug system has a larger driving force for drug transportation and more chemicals in molecular state reaches the deep skin tissue, resulting a better treatment effect. However, a drug in a super-saturated vehicle is in a metastable state may transform back to its stable form, thus changing the flux of the drug through skin and finally affect the treatment effect [213]. Moreover, multifaceted dynamic interactions between drug and host perhaps could explain this. Some medicinal herbs and especially active compounds act by gene expression [214, 215]. Further pharmacokinetics and pharmacodynamics research of the chemical constituents extracted from PE effective parts are needed to elucidate the dynamic processes of drug action to enhance our understanding of factors that influence pharmacological response [216].

Also, the pronounced reduction in wound area exhibited by PE (100% w/v) might be explained by the effect of PE on enhancing wound capillary vascularity. Likewise, in protocol 1, **Table 6 and Figure 22 (B)** showed the results of the capillary vascularity

(%CV) of every group in the various doses of PE (DM+10%PE, DM+100%PE, and DM+200%PE groups) on day 14. All DM+10%PE group, DM+100%PE group, and DM+200%PE group have significant difference when compared with DM+Vehicle group on day 14, with $p < 0.05$, respectively. There was also a positive relationship ($r=0.7197$) between %CV and PE concentration, with every 0.000179% capillary density increase for every 1% PE concentration increase in PMA2 cream base, within PE dose from 0 to 200%, w/v. The %CV increase could be explained around 51.80% by the increase of PE concentration increase in PMA2 cream base. These results support that PE has the effect on angiogenesis in diabetic wound, in a dose-dependent manner.

In present study, we found that at high doses of topical application of 100%PE and 200%PE improved wound vascularity in diabetic mice. The wound closure (%WC) and capillary vascularity (%CV) were significantly different between DM+Vehicle group and DM+100%PE group on 14 days after wound creation.

Besides the wound healing effects of PE shown in **Table 4**, by using the excision and incision wound models, Boakye YD et al. found that wounds treated with *Phyllanthus muellerianus* (PLE, 0.25, 0.5, and 1% w/w) cream increased wound contraction rate when compared to untreated wounds [217]. The outstanding wound healing effect of PE might due to its superior antioxidant and anti-inflammatory properties presented previously.

In protocol 1, **Figure 24 (A)** showed the graph of the linear regression of SIM dose and %WC on day 14 in Protocol 1. We found a moderate positive correlation ($r=0.6645$) between %WC and SIM concentration in PMA2 cream base, with every 0.003875% wound closure increase for every 1% w/v simvastatin concentration increase in PMA2 cream base. The %WC increase could be explained around 44.15% by the increase of SIM concentration increase in PMA2 cream base. **Figure 27** showed the graph of the linear regression of SIM dose and %CV on day 14 in Protocol 1. We also found a moderate positive correlation ($r=0.6919$) between %CV and SIM concentration, with every 0.004053% capillary density increase for every 1% SIM concentration increase in PMA2 cream base, within SIM dose from 0 to 10%,

w/v. The %CV increase could be explained around 47.87% by the increase of SIM concentration increase in PMA2 cream base.

Researchers have found out the pleiotropic effect of simvastatin on wound healing, as shown in **Table 1**. Moreover, previously in our lab, 0.25 mg/kg body weight simvastatin was orally given to diabetic BALB/c nude mice 7 days before the wound creation till the experiment endpoint. In this study, in DM+5%SIM (w/v) group, this dose equals 0.02 mg/kg body weight (25g body weight per mouse, each wound 10 μ l). This indicates that topical application of lower dose simvastatin may have a better effect than that of oral administration of higher dose simvastatin on wound closure on day 7 and day 14 post-wounding in diabetic mice.

The most traditional way of treatment of wound healing includes oral administration of drugs and hypodermic injections, which are quite unfriendly for systematic drug side effects, pain, requires professional assistance, and risk of disease transmission for hypodermic needle contamination. Topical application of drugs has benefits of easy administration with no pain, which could increase patients' compliance comparing to the way of oral administration, while reducing the gastrointestinal difficulties and reducing the unawareness of new wound made unexpectedly. Further, local management is the most common way for the diabetic deep cavity wound, which causes bone infections and subsequent amputation [218].

Topical application of drug could enhance the local drug concentration thus to empower the beneficial effect of simvastatin in wound healing, while avoiding the systematic side effects of simvastatin. PMA2 cream base provides an effective drug delivery system to help fat-soluble penetrate the skin tissue more effectively to the wound site [219]. When applied topically, simvastatin had its high solubility in PMA2 cream base and high penetration permeability with molecular weight less than 500 g/mol [220-222]. Therefore, it is highly reasonable to take simvastatin in PMA2 creams base in application treatment of diabetic wound. Simvastatin has been topically used to reduce skin inflammatory conditions, in animal wound model, human skin, clinical ulcer patients, by its antiinflammation, antioxidant effect, angiogenesis effect [11-13, 223-225]. PE is a medicinal plant with cascading antioxidant properties. PE owns singlet oxygen quenching, superoxide anion radical

quenching and hydroxyl radical quenching, enzyme and non-enzymatic antioxidants abilities in the wound tissues, as presented above [178].

Nowadays, both simvastatin and PE have been used in research with other drugs in wound healing. Development and physicochemical characterization of alginate composite film loaded with simvastatin has a potential wound healing effect [226]. Simvastatin exhibited synergistic activity with conventional topical antimicrobials, such as fusidic acid, mupirocin, daptomycin, and retapamulin, against various clinical isolates of multidrug-resistant strains of *S. aureus* [227]. PE extract was also in combination with other drugs in research. It has been shown that PE extract was combined with epigallocatechin-3-gallate (EGCG) significantly downregulated MDA content and plasma FRAP in diabetic patients [171]. *Emblica officinalis* was also used in combination with insulin in experimental diabetic neuropathy [174].

Topical application of combined antioxidants and simvastatin in the treatment of diabetic wound healing has several profits. Firstly, the combination can reduce the unwanted systematic side effects of simvastatin when taken orally and high dose side effects when topically applied. Previously, a combination of simvastatin and antioxidant has been proved to reduce cerebral vascular endothelial inflammatory conditions in a rat traumatic brain injury [228]. Therefore, it is promising to combine low dose simvastatin with PE in treatment of diabetic wound.

The concept of drug dose equivalence is applied in isobolographic analysis, which is basis for assessing synergy and dose combination strategy optimization of two drugs with multiple mechanisms of actions. But till now there has no research on drug plasma concentrations of PE and simvastatin for the bioavailability analysis [229]. The isobole graph is based on each drug's dose-effect. For the constitutive drug in the combination, we care about the dose pair that give the specific effect. As for PE and simvastatin drug pair to exert a specific effect, their doses may vary of considerable magnitude. We assumed that the model in our study fits the straight line isobole. As shown in **Figure 47** and **Figure 48**, the diagonal line connecting intercepts A and B is termed the "additive" isobole [230]. The additive isobole for the specific effect is a straight line with intercepts A_i and B_i when the potency ratio is constant. So the dose pair in the drug combination is not related to their amount, only related to the dose

they make the same effect [230]. In this study, in the DM+Combine group, the amount of drug ratio of PE and simvastatin is 100 mg/kg: 0.2 mg/kg=500 times. Such high drug amount ratio has been reported before. One example is the experimental combination of cocaine and buprenorphine on the rotational behavior of the nigraly lesioned rat, when the effect is set at 150 times above the saline control in 4h, which effect was produced by 10.0 mg/kg cocaine alone and by 0.0175 mg/kg buprenorphine alone, the biggest drug dose ration is about 570 times of cocaine to buprenorphine [231]. The amount of the drug in combination could be flexible at high dose ratio, according to the isobologram theory.

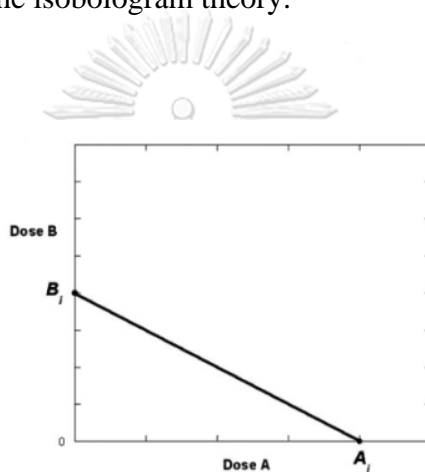


Figure 47. Isoble Additivity Graph

จุฬาลงกรณ์มหาวิทยาลัย
CHULAI

$$\frac{a}{A_i} + \frac{b}{B_i} = 1$$

(0 ≤ a ≤ A_i, 0 ≤ b ≤ B_i)

Figure 48. Equation of Additive Isoble

However, whether PE and SIM combination model fits the straight line isobole or not is still unknown yet. This isobolographic theory provides us a basis for further research on exact additive effect of PE and SIM in developing the fixed dose combination [230].

A research published in 2008 showed that intraperitoneally injection of 5 mg/kg simvastatin could enhance diabetic mice wound [10]. Previous research in our lab also proved that, oral administration of 0.25 mg/kg simvastatin could improve wound healing at diabetic wound [9]. By using different route of administration, the topical application of 0.5% (g/g) simvastatin-based cream has been proved to be effective in the treatment of chronic vascular cutaneous ulcers in clinical patients [224]. Topical application of 0.5% (mg/mg) simvastatin enhanced wound healing in diabetic mouse, with increased VEGF-C at day 4 and day 7, and promoted angiogenesis [12]. In addition, topical treatment of 10mg/ml simvastatin has been proved to increase dermal wound healing in infected rat wound [11]. Topical application of 2% concentration of simvastatin could enhance wound closure rate in full-thickness rat wound [225]. Most recently, another study in 2016 by Wang C.C. and colleagues showed that infected cutaneous wounds of rats had good response to topical treatment of 62.5 µg/ml simvastatin [13].

5.3. Protocol 2

5.3.1. Effects of Combined Treatment of PE and Simvastatin on Percentage of Wound Closure (%WC) and Capillary Cascularity (%CV)

Table 4 in the literature review part showed the available evidence of PE effect in wound healing and skincare. In present study, we carried out the first topical combination of simvastatin and a natural plant medicine on diabetic wound healing in mice model. As shown in **Table 5**, **Table 6**, **Table 7**, and **Table 8**, we measured %WC, %CV of three doses of SIM and PE on day14 post-wounding in Protocol 1. The dose-response of SIM and PE with %CV were also measured on day14 post-wounding. The middle doses of 100%PE (w/v) and 5%SIM (w/v) were chosen to be the optimal doses used in Protocol 2 of the experimental setting, based on the consideration of the unacceptable toxicity of too high dose and low efficacy of too low dose [232].

In Protocol 2, **Figure 32 (A)** and **Figure 33 (A)** showed the data of the percentage of wound closure (%WC) of groups on day 7 and day 14. Combine treatment

increased %WC on day 14 significantly ($p<0.05$), while on day 7 combine treatment only showed a tendency in increasing %WC in diabetic wound. This indicated that combine treatment can increase wound healing on day 14 in diabetic wound. Combine treatment increased %CV on both day 7 and day 14 significantly ($p<0.05$) in diabetic wound, as shown in **Figure 32 (B)** and **Figure 33 (B)**, which indicated that combine treatment can increase angiogenesis in diabetic wound both on day 7 and day 14.

Further, on day 7 post-wounding, we found a strong positive correlation ($r=0.7136$) between %WC and %CV, with every 0.027990% wound closure increase for every 1% of capillary vascularity increases in wound tissue. The %WC increase could be explained around 50.92% by the increase of capillary vascularity, as shown in **Figure 43**. The correlation between %WC and %CV on day 7 post-wounding was much stronger than that of day 14, as shown in **Figure 44**, but still with significance ($p<0.05$). This indicated that improving angiogenesis on day 7 post-wounding may benefit to diabetic wound healing.

In all groups, the plastic frames were removed from the wound on day 4 or day 5. However, the time of the frames kept fixed at the wound area is controversial in research published. Swine cutaneous model is the gold standard model in wound healing research animal model. Because pig skin wound heals through re-epithelialization with similar response like human being, which is distinct from small rodent animals [233, 234]. So that, the animal skin wound model in present study was modified from splinted wound model, in which a silicon ring is fixed around the wound to prevent contraction. The plastic frame mimics the silicone ring fixed to wound area to prevent mice skin contraction to maintain re-epithelialization being the major factor contributing to wound healing to the greatest extent as in human skin wound healing.

5.3.2. Effects of Combined Treatment of PE and Simvastatin on VEGF Protein Level

As shown in **Figure 3** in the literature review part, the pathophysiology features of diabetic wound healing, VEGF was downregulated in diabetic wound healing [12]. While the evidence showed that both VEGF mRNA and protein levels were severely decreased in diabetic animal models and clinical diabetic patient foot ulcers [12, 105,

107-109]. Upregulation of expression of VEGF protein in animal cutaneous wound model could increase angiogenesis and wound healing in both nondiabetic and diabetic mice model [12, 110]. Topical application of VEGF could enhance angiogenesis in diabetic mice wound [111]. A previous study in our lab had shown that oral administration of simvastatin-upregulated VEGF protein expression in diabetic wound model significantly on day 7 when compared with DM+Vehicle group [9]. One research published in 2008 showed that intraperitoneal injection of simvastatin can enhance angiogenesis, with both increased VEGF mRNA level and protein level in diabetic cutaneous mice model [10]. Topical application of simvastatin enhanced wound healing in diabetic mouse, with increased VEGF-C and angiogenesis on day 4 and day 7 [12]. Topical application of simvastatin could also improve the volume densities of vessels in rat wound [225]. Clinically, simvastatin enhanced VEGF in twenty-two hypercholesterolemic patients treated with simvastatin 20 mg/day for four weeks [235, 236].

PE fruit extract was proved to increase endothelial wound healing and sprouting *in vitro* cell model [38]. Gallic acid-enriched fraction of *Phyllanthus emblica* L. reduced the ulcerative damage on day 7 in indomethacin-induced gastric ulceration in mice, with the number of microvessels and tissue VEGF level upregulated in the treatment group [237]. Dried extract of PE fruit juice significantly enhanced endothelial wound closure, endothelial sprouting, and VEGF mRNA expression *in vitro* human umbilical vein endothelial cell model through its anti-oxidant effect [38]. However, the *in vitro* study using the age-related macular degeneration trans-mitochondrial cell lines reported that *Emblica Officinalis* (EO) significantly improved live cell number and mitochondrial membrane potential, reduced apoptosis and oxidative stress, down-regulated VEGF, and up-regulated PGC-1 α [238]. Low level of ROS could cause VEGF activation, thereby triggering angiogenesis and subsequent choroidal neovascularization in wet age-related macular degeneration [239, 240]. In the study, they found out that EO decreased the VEGF gene levels in age-related macular degeneration cybrids, suggesting that EO might help in reducing VEGF-induced neovascularization in age-related macular degeneration. This data was consistent with reports by Lu et al. wherein an EO preparation inhibited VEGF-induced angiogenesis

via suppression of VEGF receptor activity [241]. In present study, on day 14 post-wounding, DM+100%PE group showed higher capillary vascularity than DM+Vehicle group, as shown in **Figure 33 (B)**, which inferred that perhaps PE could stimulate other growth factors which play the dominant role in regulating angiogenesis apart from VEGF at the wound site in diabetic mice.

Besides, gallic acid, the enriched content in PE extract was reported to able to enhance angiogenesis in ulcer healing by increasing HGF protein level, PGE₂ synthesis, tissue NO content and von Willebrand factor VIII [237]. Appropriate amount of ROS is essential for VEGF expression and angiogenesis in endothelial cells [242]. However, the outstanding free radical scavenging ability of PE may suddenly reduce ROS level to influence VEGF expression in endothelial cells, as shown by the MDA content in wound as shown in **Figure 40**, which may explain why DM+100%PE group had low VEGF protein level on day 7 post-wounding as shown in **Figure 34**. However, the high dose of PE could deliver benefit to increase VEGF in diabetic condition as shown in the study of Lim and co-workers in 2016, in which they showed administration of 300 mg/kg EO to Sprague-Dawley (SD) rats was effective to reduce pro-inflammatory cytokine levels after 15 days treatment [243]. In diabetic studies, human subjects were given oral concentrations of EO at 1 g/mL, 2 g/mL, and 3 g/mL in water to improve high-density lipoprotein-cholesterol and reduce low-density lipoprotein-cholesterol levels [170].

In our study, the mice received 100%PE (w/v) in protocol 2, this dose equals to 0.4 mg/kg body weight in mice (mouse body weigh=25g). This PE dose in the topical application was much lower than the dose (orally) used in the above reports. Topical application of drug at the wound site could enhance the local drug concentration by the PMA2 base crease, a fat-soluble penetration beneficial drug delivery system [219]. PE has fluent polyphenolic constituents, phenolic compounds from olive leaves have been proved to improve wound healing in diabetic mouse, with VEGF protein level significantly increased on day 3 and day 7 [110]. Usually, during 3 to 7 days after wound, VEGF reaches the maximum protein level to increase early stage of angiogenesis, such as vasodilation, cell migration and proliferation, and vascular permeability. As the microenvironment of wound ameliorates, VEGF inducers like

hypoxia decreases, or other angiogenesis factors took pivotal role in angiogenesis by making VEGF protein level decrease gradually after about one week of wounding [104].

Furthermore, in **Figure 41** showed the Pearson's Correlation Analysis between percentage of wound closure (%WC) and VEGF protein level, the strong positive correlation ($r=0.7019$) was indicated on day 7 post-wounding. With every 0.001081% wound closure increase for every 1 pg/mg total protein VEGF protein level increase in wound tissue. The increased %WC could be explained around 49.26% by the increase of VEGF protein level increase. Moreover, as shown in **Figure 42**, on day 7 post-wounding, we found a moderate positive correlation ($r=0.5882$) between %CV and VEGF level, with every 0.000263% wound closure increase for every 1pg/mg total protein VEGF protein level increase in wound tissue. The %CV increase could be explained around 34.60% by the increase of VEGF protein level increase.

In present study, the results showed that topical application of combined PE and simvastatin enhanced both capillary density and VEGF protein level both on day 7 and day 14, as shown in **Figure 34**. Increasement of VEGF protein level and angiogenesis could provide oxygen and needed nutrients during the formation of granulation tissue in wound healing [244]. The VEGF protein level may be upregulated through eNOS/NO pathway. Babaei et al. had proved that excessive expression of endothelial NO synthase (eNOS) induced angiogenesis in a co-culture model [245, 246]. Modulating eNOS activity is encouraging in adjusting angiogenesis in immunodeficient mice [247]. Gallic acid enriched fraction of PE improved indomethacin-induced gastric ulcer healing via arginine catabolism related eNOS-dependent pathway, while promoting VEGF expression [237]. The gallic acid enriched fraction may promote VEGF expression through ADP-induced platelet aggregation and α -granule related VEGF pathway [248]. Further, PE extract could increase wound closure through induced ERK1/2 related collagen synthesis [28], this may be due to the ascorbic acid in PE extract. Simvastatin enhanced eNOS mRNA expression and protein levels in cultured endothelial cells pre-conditioned with steady laminar flow [249]. Also, simvastatin was proved to modulate resistance arterial contractile function through AMPK/phospho-eNOS(Ser1177)/NO-dependent pathway

[250]. Recently, simvastatin was also reported for its lipid-lowering-independent effect on wound healing, through effects of reducing inflammation and upregulation of VEGF production, angiogenesis, re-epithelialization in wound healing [9-13].

5.3.3. Effects of Combined Treatment of PE and Simvastatin on Percentage of Re-Epithelialization (%RE)

Increase of percentage of re-epithelialization help wound healing. Re-epithelialization is one of the major features that indicates the wound healing successful. Migration of keratinocytes at the wound edge across the wound gap starts the re-epithelialization process[192]. Percentage of re-epithelialization was used to determine the degree of new epithelial tissue grows from the edge of the wound. Evidence showed that both simvastatin and PE have re-epithelialization promotion effects in wound healing. Intraperitoneally injection of simvastatin could enhance epidermal regeneration in diabetic mice wound model [10]. Topical application and subdermal injection of simvastatin were proved to be effective in re-epithelialization in split-thickness in rat wound through its anti-inflammation and fibroblast proliferation promoting properties [225, 251]. The extract of *E. officinalis* enhanced the growth of human keratinocytes in culture [252]. It inferred that PE has great potential in enhancing diabetic wound healing probably through its antioxidant and anti-inflammatory effects.

The combination of PE and simvastatin showed benefit for re-epithelialization. The percentage of re-epithelialization of DM+Combine group at wound site was upregulated when compared to DM+Vehicle group on day 7, even though with no significant difference, as shown in **Figure 36**. On day 14, all groups had completed re-epithelialization except for DM+Vehicle group. There was no significant difference between any of the treatment group when compared with DM+Vehicle group on day 14.

Interestingly, on day 7 post-wounding, in DM+100%PE group, re-epithelialization decreased as VEGF protein level decreased the same group, as shown in **Figure 34** and **Figure 36**. Also, as shown in **Figure 46**, on day 7 post-wounding, there was a moderate positive correlation (Pearson correlation coefficient $r=0.5676$, $p=0.0140$) between VEGF protein level and percentage of wound re-epithelialization, which

could be explained by the non-angiogenic effect of VEGF on wound re-epithelialization related to keratinocyte and fibroblast migration [253, 254]. This phenomenon is perhaps related to PE effects of ROS scavenging property and VEGFR-2. Definite amount of ROS stimulate keratinocyte proliferation and migration to facilitate re-epithelialization in wound healing [69]. Further, keratinocyte proliferation and migration could also be induced by VEGF-E through VEGFR-2, which means that re-epithelialization could also be influenced by VEGF expression [255]. Thus, the outstanding free radical scavenging ability of PE may suddenly reduces ROS level and subsequent VEGF expression may explain the downregulated re-epithelialization in DM+100%PE group on day 7 post-wounding. Ingredients like propylene, glycerin, and caprylic/capric triglyceride in PMA2 cream base are the most common used humectants. Keeping moisture is an effective treatment in wound healing. Especially, glycerin can degrade the corneodesmosome, which could help drug local absorption at wound site [232]. This may partly explain the good result of %RE in DM+Vehicle group on day 7 compared to other treatment groups significantly ($p < 0.05$) (**Figure 36**). However, the final outcomes of %WC and %CV (**Figure 32** and **Figure 33**) still differentiated between PMA2 Vehicle treatment and combine treatment.

5.3.4. Effects of Combined Treatment of PE and Simvastatin on Neutrophil Infiltration

Inflammation constitutes a part of the acute response in injury, resulting in a coordinated influx of neutrophils at the wound site. Good aspects of neutrophils at wound site lies in that neutrophils can produce antimicrobial peptides, ROS, and proteases to combat microbes invading the wound and causing inflammation. Also, neutrophil infiltration may be induced by IL-6 related endothelial permeability. However, active neutrophils are observed for an extended period in chronic wounds. In chronic wounds, active neutrophils produce excessive protease which leading to growth factors inactivation and over degradation of extracellular matrix not helpful for cell migration and wound closure. Large bulk of evidences have shown that excessive neutrophil activity can increase the damage at the wound site, leading to prolonged inflammation and tissue damage [36]. In 1984, Briggaman et al. reported that too much neutrophils infiltrated at the wound site could potentially interfere with

re-epithelialization and the formation of a new basement membrane in the dermo-epidermal junction by keratinocytes [256]. There was very few research published about simvastatin effect on neutrophil infiltration in diabetic wound healing. Cowled PA et al. demonstrated that simvastatin can inhibit neutrophil infiltration in IRI-induced skeletal muscle [257]. Simvastatin also inhibited smoke-induced neutrophilic inflammation in airway epithelium [258]. Further, simvastatin showed antineutrophil effect by curtailing PMN-endothelium interaction [259]. In a carrageenan-induced footpad oedema in rat, simvastatin reduced extensive PNM leukocytes infiltration with eosinophiles, basophiles and lymphocytes at the local inflammation site [260]. Only previous study in our lab showed that simvastatin reduced infiltrated neutrophils in diabetic wound [5]. As shown in **Figure 1**, the normal pathophysiology of wound healing, neutrophil influx will peak at day 2 after wounding, and then decrease continuously till the inflammation was resolved [261]. However, in diabetic condition, the inflammation stage was prolonged and caused the delayed wound healing (**Figure 2**). Local inflammation was strictly associated with neutrophil infiltration. After clearance of the pathogens at the wound, neutrophils undergo apoptosis and finally engulfed by macrophages to resolve the inflammation [54]. In chronic wound, after day 12, the normal pathophysiology of wound healing will go into remodeling stage, in which the inflammation will be almost resolved [43, 262]. Thus, on day 14, the number of neutrophils infiltration was not commonly measured at this stage of remodeling.

So far, there has been no research work published about PE effect on neutrophil infiltration in diabetic cutaneous wound model. However, bioactive constituents extracted from PE have been proved for their anti-inflammatory effects. For example, gallic acid in enriched fraction of *Phyllanthus emblica* Linn. could significantly reduce the mucosal myeloperoxidase (MPO) activity in ulcerated mice [237]. Myeloperoxidase (MPO) is a peroxidase enzyme most abundantly expressed in neutrophil granulocytes, which can be taken as index of neutrophil amount.

In addition, the reduction of infiltrated neutrophils also contributes to the reduced oxidative stress since neutrophils are a rich source of ROS. Low infiltrated neutrophil numbers were in accordance with the wound tissue MDA content on day 4, day 7 and

day 14 in the combined treatment group, as shown in **Figure 38** and **Figure 40**. The combined treatment of PE and SIM demonstrated the better effects on both MDA content and number of infiltrated neutrophils on both day 4 and day 7 post-wounding.

5.3.5. Effects of Combined Treatment of PE and Simvastatin on IL-6 Protein Level

Inflammation constitutes a part of the acute response in injury, resulting in pro-inflammatory cytokines level changes at the wound site. Hyperglycemia could produce excessive ROS, which could increase the overexpression of pro-inflammatory cytokine IL-6 [34]. In diabetic animal model, it also showed that higher level of IL-6 and delayed wound healing [35]. Also in diabetic patients, IL-6 protein level and the circulating acute-phase proteins levels were significantly higher than those without foot ulcers [99]. This indicated that IL-6 has a detrimental effect on diabetic wound healing. Upregulation of IL-6 protein expression was accompanied with hyperglycemia in macrophage cells isolated from both normal mice and diabetic mice [97]. These observations suggested that IL-6 has crucial roles in wound healing, probably by regulating leukocyte infiltration, angiogenesis, and collagen accumulation. So that, targeting reduction in inflammation related neutrophil infiltration and IL-6 protein level could be an effective to reduce inflammation in order to improve wound healing [54].

Both PE and simvastatin have anti-inflammatory effects. So far, there has been no research work published about PE effect on IL-6 protein level in diabetic cutaneous wound model. Bioactive constituents extracted from PE, as shown in **Table 3** in literature review part, have been proved their anti-inflammatory effects by downregulating pro-inflammatory cytokines such as IL-6. A most recent study published in 2020 showed that, fraction c1 (containing mainly fisetin and gallic acid) and c2 from ethanol extract of dried fruits of PE could reduce IL-6 protein level in LPS-stimulated RAW264.7 mice macrophages [168].

Beside IL-6, PE also showed effect in anti-inflammation by inhibiting other pro-inflammatory cytokines. In 2007, Bhattacharya S. and colleagues reported that purified fraction of PE, pure gallic acid, significantly reduced the serum levels of IL-1 β and TNF- α at indomethacin-induced gastric lesions in rats [263]. Later in 2010,

ethanolic extract of amla efficiently reduced pro-inflammatory cytokine TNF- α and IL-1 β levels and upregulated anti-inflammatory cytokine (IL-10) concentration in NSAID-induced ulcer in albino mice [264]. Aqueous extract of PE decreased proinflammatory cytokines (TNF- α , IL-1 β and TGF- β 1) both in the serum and sciatic nerve of diabetic neuropathy rats [174]. Downregulation of IL-6 protein expression by simvastatin was also observed both in animal model and clinical patients [138, 150]. In our lab, increasement of IL-6 level was observed in diabetic wound before (not published). Also, other inflammatory cytokines decreasement such as TNF- α and IL-1 β has been reported by simvastatin topical application in cutaneous wound [11].

In the present study, the results showed that DM+Combine group had tendency to downregulate IL-6 protein levels (pg/mg total protein) both on day 4 ($p=0.248$) and day 7 ($p=0.127$), but without significant difference when compared with DM+Vehicle group, respectively, better than the single treatment by PE or SIM cream on day 4 and day 7, as shown in **Figure 39**.

Also, on both day7 and day14 post-wounding, topical application of the combined cream of PE and simvastatin improved wound closure in diabetic wound. Moreover, in this study, on day 7 post-wounding, there is a strong negative correlation (Pearson $r = -0.7190$, $p=0.0025$) between %WC and IL-6 protein level, as shown in **Figure 45**, with every 0.002289% wound closure increase for every 1 pg/mg total protein IL-6 protein level increase in wound tissue. The %WC increase could be explained around 51.70% by the increase of IL-6 protein level increase. This indicated that the tendency of combine treatment in downregulating IL-6 protein level could contribute to diabetic wound healing in mice both on day 4 and day 7.

The transcription factor NF- κ B is a pivotal mediator in inflammatory responses. It regulates pro-inflammatory cytokines including IL-6 in innate immune cells [265]. Further, STAT3 and ERK1/2 were also involved in wound healing that could be regulated by IL-6/IL-6R system [82, 266, 267]. Reduction of STAT3 and ERK1/2 activation could ameliorate inflammation status and enhance wound healing [267-270]. Rutin has been shown to down regulate cytokine expressions in IL-6/STAT3 pathway in CCl₄-induced hepatotoxicity in rats [271]. Also rutin ameliorated condition in UVB-irradiated mouse skin by reversing STAT3 phosphorylation [272].

In alcohol-induced liver injury mice model, quercetin with anti-inflammatory property prevented liver inflammation by decreasing IL-6, STAT3 and other inflammatory related cytokines through targeting of PI3K/Akt/NF- κ B and STAT3 signalling pathway [273]. Simvastatin downregulated ERK1/2 phosphorylation in LPS-induced inflammation in rat dopaminergic neurons [274]. Simvastatin also inhibited vascular inflammation response via interfering with the ERK1/2 signal pathway in rat vascular smooth muscle cells [275]. Further, simvastatin also reversed ERK1/2 activation in ischemia inflammatory status in rat model [276]. Activation of ERK1/2 was also reported to contribute to epithelial wound healing through induction of cell proliferation and migration [277].

5.3.6. Effects of Combined Treatment of PE and Simvastatin on Tissue MDA

ROS plays important role in animal and human physiology, but excessive free radicals play important role in inducing the oxidative stress at the diabetic wound. During diabetic wound healing, the wound site is rich in oxidants oxidized by excessive ROS, such as hydrogen peroxide, mostly contributed by neutrophils and macrophages. AGEs are a set of heterogeneous molecules that produced from nonenzymatic reaction of reducing sugars with amino groups of lipids, DNA and proteins. They are the end products of oxidation. During abnormal metabolism process, such as hyperglycemic, hyperlipidemic and excessive oxidative stress conditions, the AGEs accumulate gradually. They are also believed to play a direct causative role in the vascular complications of diseases [278]. Under hyperglycemia condition, oxidative stress is increased by excessive generation of ROS. The main mechanisms include diabetes influenced NADPH (polyol) pathway flux, mitochondrial electron transport chain, activation of protein kinase C. These pathways are explained in detail here. Firstly, NADPH (polyol) pathway is a major contributor to ROS production, even though not directly. Under hyperglycemic condition, aldose reductase has a high affinity for glucose. In diabetic situation, glucose is converted to sorbitol by aldose in an NADPH dependent manner, which is an essential cofactor of the glutathione production. The excessive glucose leads to the overproduction of sorbitol, with an overall consumption of NADPH, leading to an overall redox imbalance in cells called oxidative stress [279, 280]. In addition, superoxide radicals

can be produced by biochemical reactions catalyzed by xanthine oxidase, NADPH oxidase and cytochrome450. The NADPH is an electron transporter to change oxygen to superoxide anion, which has been found in phagocytes like macrophages, monocytes and neutrophils [280]. The identified Nox/Duox family proteins of the NADPH oxidase exert different functions in various tissues and cells. In wounded and inflamed tissue, large amounts of ROS, especially highly reactive superoxide radical anion, are produced by the NADPH oxidase enzyme complex, especially in highly inflamed cells by respiratory burst [61, 62]. In inflammation, p67phox, p47phox and p40phox cytosolic proteins are transferred to plasma membrane where they interact with a non-active heterodimer called b558 to activate NADPH oxidase to produce superoxide anions [281]. Secondly, mitochondrial electron transport chain is another prominent source of ROS production. Mitochondrial electron transport chain continuously converts a small proportion of molecular oxygen into superoxide anion in all mammalian cells by semi-ubiquinone compound. Then superoxide anion is changed to hydrogen peroxide by SOD. This chain is composed of four complexes, complex I, complex II, complex III and complex IV [279]. In normal physiological situation, glycolysis produces NADH and pyruvate. NADH is an electron donor to mitochondrial electron transport chain while pyruvate attend the citric acid cycle to produces NADH and FADH, which also contribute to ATP production. In STZ-induced rats, cytosolic mitochondrial NAD⁺/NADH ratio has been significantly reduced [282, 283]. NADH offer electron to complex I while FADH₂ to complex II. Then complex I and complex II both then transfer electrons to ubiquinone through Fe-S centers including endogenous antioxidatives such as GSH, vitamin C, vitamin E, carotenoids and et al. [280]. Then ubiquinone passes the electron to complex III, cytochrome C, complex IV and then to molecular oxygen to generate superoxide at cell membrane. The details are described in the following. The electron transfer accompanied energy enables protons go across the cell membrane, which creates a voltage across the inner and outer mitochondrial membrane and synthesizes ATP. In diabetes, more glucose enters citric acid cycle and provide more electrons to the mitochondrial electron transport chain. Once the mitochondrial electron transport chain got enough electrons it reaches the voltage threshold, the electrons start to gather at complex III. Then these electrons are donated to molecular oxygen, which

turns out to be superoxide anions on the cell membrane [279]. In diabetes, targeting mitochondrial has effect on diabetes and diabetic complications. Thirdly, protein kinase C activation is also the known mechanism of ROS production. The sorbitol mechanism form the NADPH (polyol) pathway can induce PKC activation. PKC activation can directly result in excessive ROS production through NF- κ B activation and diverse NADPH oxidases under diabetic situation. Most PKC isoforms can be activated by the lipid second messenger DAG, the synthesis of which could be increased due to glycerol 3-phosphate, the reduced form of dihydroxyacetone phosphate, the increased glycolytic intermediate in case of hyperglycemia. In addition, hyperglycemia also activate PKC through AGE receptors and the free radicals from the NADPH (polyol) pathway. Different PKC isoforms activated could induced various cell signaling pathways. It has been reported that PKC- α is an activator of NADPH oxidase, which could be inhibited by antioxidant α -tocopherol. Further, PKC- α and PKC- δ are related to the Toll-like receptor induction through NADPH oxidase in hyperglycemia condition. Further, PKC activation also could inhibit endothelial nitric oxide synthase (eNOS) to reduce nitric oxide production. Also, PKC also benefits to matrix protein accumulation through protein increase of TGF- β 1, fibronectin and type IV collagen through nitric oxide inhibition. All these pathways which directly produce ROS or indirectly activation of other pathways finally contribute to oxidative stress under hyperglycemia situation [279]. Fourthly, in diabetic situation, hyperglycemia can lead to oxidative stress through the high production of advanced glycated end products (AGEs). By creating Schiff base, AGEs are formed through the covalent bond of aldehyde or ketone groups of reducing sugar to the free amino groups of proteins. Then Amadori Rearrangement begins to form a more stable ketoamine, which then converted to AGEs directly or be oxidized to reactive carbonyl intermediates. Glucose can also be oxidized to form reactive carbonyl intermediates through intermediates of glyoxal and methylglyoxal. These carbonyl intermediates then undergo a series of chemical rearrangements to produce stable AGEs. Then AGEs and their cell surface receptor called RAGE are to induce cell signals into the cells in various tissues. One sequence is the production of ROS through NADPH oxidase system in cells. Fifthly, nitric oxide is another contributor to ROS concentration and formation of reactive nitrogen intermediates (RNIs). Nitric

oxide is produced through the activity of nitric oxide synthase (NOS). It can be calcium-dependent or constitutively expressed in different isoforms. Excessive NO causes deleterious effect in diabetes. Highly reactive peroxynitrite, which has high prooxidant property, could be generated from the combination of nitric oxide combines with superoxide radical [279]. Intracellular ROS concentration could be measured by using the redox couples such as $\text{NADP}^+/\text{NADPH}$, $\text{GSSG}/2\text{GSH}$, $\text{Cys}(\text{SH})_2/\text{CySS}$ and $\text{TrxSS}/\text{Trx}(\text{SH})_2$ [279].

Diabetic wound could produce ROS mainly through NADPH (polyol) pathway flux under hyperglycemia [280]. Besides, neutrophil respiratory burst was also indicated as one of the major sources of excessive ROS, such as hydrogen peroxide and superoxide anion, through NADPH dependent pathway [284]. The excessive ROS react with DNA, lipids and proteins to produce AGEs, the end products of oxidative stress [66, 67, 285]. Furthermore, the elevation of malondialdehyde (MDA, an important lipid peroxidation indicator) content and decrease of GPx were also observed in diabetic patients [25]. As shown in **Figure 40**, the tissue MDA was used as an indicator for excessive ROS was significantly increased in diabetic wounds.

Reduction of oxidative stress and inflammation status at wound site could increase wound closure dramatically. Simvastatin has been proved to exert its antioxidant effect in recent years in both animal models and clinical patients [286, 287]. In a rat bipolar mania model, treatment of simvastatin reduced elevated TBARS content, while preventing the reduction enzyme activities of CAT, GSH-Px, SOD in brain area [288]. Also, in hypercholesteremic patients, simvastatin reduced the levels of circulating MDA content [289]. Oral administration of simvastatin treatment reduced plasma MDA content in rat [286]. In an endotoxemic lung tissue model, simvastatin decreased TBARS levels significantly [290]. A meta-analysis carried out in 2019 also showed that simvastatin downregulated circulating MDA level in end-stage renal disease, type 2 diabetes, coronary artery disease, hypercholesterolaemia, metabolic syndrome and chronic kidney disease patients [287]. Further, a recent research published in 2019 showed that simvastatin caused significant decrease in lipid peroxidation and restored SOD and GPx activity to baseline value in a non-alcoholic steatohepatitis experimental model [291].

PE extract contains polyphenolic compounds, such as gallic acid, ellagic acid which exert antioxidant, anti-inflammation and wound healing property [25, 160-163, 183]. The wound healing property of PE extract most probably due to the free radical scavenging ability of its polyphenols [160, 161, 164, 165, 183]. Many chemical constituents extracted from PE have shown outstanding antioxidant effect in various models, such as gallic acid, ellagic acid, ascorbic acid, emblicanin A, emblicanin B, corilagin, punigluconin, pedunculagin, chebulagic acid, phyllanemblinin A, phyllanemobilin B, quercetin, phyllanthin fisetin and other chemical under research, as shown in **Table 3** in literature review part. The low molecular tannins of PE have broad-spectrum antioxidant activity in quenching singlet oxygen, quencher for superoxide anion and hydroxyl radicals. Methanolic extract of coarse PE fruit powder showed good free radical scavenging ability and excellent total antioxidant capacity *in vitro* assays [159]. Evidence showed that PE extract antioxidant is an excellent singlet-oxygen quencher for superoxide anion and hydroxyl radicals, better than Vitamin C, Vitamin E and Trolox C [177, 180-182]. In 2016, Yamamoto and colleagues reported that after polyphenol enriched water extract of Amla fruit treatment decreased ROS levels in a murine skeletal muscle cell line [292]. In type 1 diabetic rats, oral administration of polyphenol enriched hydroalcoholic extract of PE fruit treatment reduced lipid peroxidation and increased antioxidant parameters in the liver homogenates [175]. PE leaves extract increased reduced glutathione, glutathione peroxidase, superoxide dismutase, catalase, and decreased LPO level in the liver and kidney of diabetic rats [169]. Triphala (dried fruits of *Terminalia chebula*, *Terminalia bellirica*, and *Phyllanthus emblica*) showed effect on improvement of wound closure, with significant upregulated level of collagen, hexosamine, uronic acid, and SOD at wound site [293]. Both rutin and quercetin are key chemical components in exerting the wound healing effect *in vitro* model, which are also major components of PE [294]. Another study also showed that rutin has ROS scavenging activity in a cell model [295]. Aqueous solution of dry powder of PE fruit juice showed antioxidant effect in FRAP assay *in vitro* cell model [38]. Besides the extracts from PE, other effective bioactive chemicals of the same chemical category extracted from other medicinal plants also showed strong antioxidant effect and wound healing benefits. Crude ethanol extract of *Chromolaena odorata* leaves, which contains mainly

phenolic acids and compound of lipophilic flavonoid aglycones, has been proved to have beneficial to human cutaneous wound healing *in vitro* through exerting antioxidant effect [296]. Rutin and triglycoside of quercetin extracted from *Allophylus spicatus*, *Philenoptera cyanescens*, *Melanthera scandens*, *Ocimum gratissimum*, and *Jasminum dichotomum* have wound healing activity *in vitro*. In addition, rutin containing extract of *Croton bonplandianum* leaves showed antioxidant effect *in vitro* DPPH scavenging and reduce nitric oxide [297].

In diabetic rat model, PE extract decreased MDA content and restored other endogenous antioxidant enzymes, such as GSH, SOD and CAT [166]. Pingali et al. proved that orally taken aqueous extract of PE downregulated MDA content in type 2 diabetic patients [25]. Moreover, the MDA result shown in **Figure 40** also confirmed that the treatment of PE alone also exerts its antioxidant effect by downregulating MDA content in diabetic wound in mice, especially on day 4. Growing evidence showed that antioxidant-targeting therapy can improve the healing process in chronic wounds [69]. Sumitra et al. proved that alcoholic extract of *Phyllanthus emblica* Linn. fruits decreased MDA content at the wound site while increasing wound contraction speed, tensile strength, total collagen in granulation tissue in the rat wound model [28]. Pleiotropic effect of simvastatin of antioxidant has been found in recent research. Orally taken simvastatin downregulated circulating MDA content in hypercholesteremic and type 2 diabetic patients [287, 289]. Also, studies showed that oral administration of simvastatin improved oxidative stress by reducing MDA content in both animal and clinical patients [35, 36]. Our results shown in **Figure 40** were in accordance with the above evidence. The combined treatment of PE and SIM had better effect than the single treatment of PE or SIM alone on decreasing MDA content on day 4, 7, and 14 post-wounding. In a STZ-induced diabetic mice model, activation of Nrf2 pathway improved diabetic wound healing by ameliorating oxidative stress in Nrf2(-/-) mice [298]. PE reduced oxidative stress through ROS-Nrf2 signaling pathway in HepG2 cell line and murine skeletal muscle cell line [292, 299]. Also, simvastatin had been proved to ameliorate oxidative stress via Nrf2 in liver and kidney diseases [291, 300]. The above evidence supports that Nrf2 perhaps play a key role in regulating oxidative stress in cutaneous wound healing. However, whether

topical application of combined PE and simvastatin exert antioxidative stress effect in diabetic wound healing through ROS-Nrf2 signaling pathway still needs further study.

Therefore, it is proposed that the antioxidant effect of *Phyllanthus emblica* Linn. is the key mechanism of improving diabetic wound angiogenesis and wound healing. To sum up, based on previous discussion, both hyperglycemia and infiltrated neutrophils produce excessive ROS in diabetic wound. PE did not decrease BG, but decreased number of infiltrated neutrophils, the hydroxyls from the polyphenols, flavonoids and other active chemical ingredients extracted from PE (as listed in **Chapter of Literature Review**) donate electrons to ROS to scavenge the excessive ROS in diabetic wound. Also, PE decreased infiltrated neutrophils on day 4.

Drug combination therapy has a higher treatment rate, fewer side effects, and slower development of drug resistance, with higher patient compliance and less economic investment as presented in the literature review part [29, 30]. Recent new research of drug combination also showed the high potential of medicinal plants in wound healing treatment [31, 32]. Our research is the first report to demonstrate that combination of simvastatin with a medicinal plant has a magnificent antioxidant effect in the treatment of diabetic wound healing. Both simvastatin and PE wound healing promoting effects were based on their antioxidant and anti-inflammatory properties. **In Figure 49**, the proposed mechanism of topical application of PE and simvastatin was shown.

5.4. Proposed Potential Mechanisms

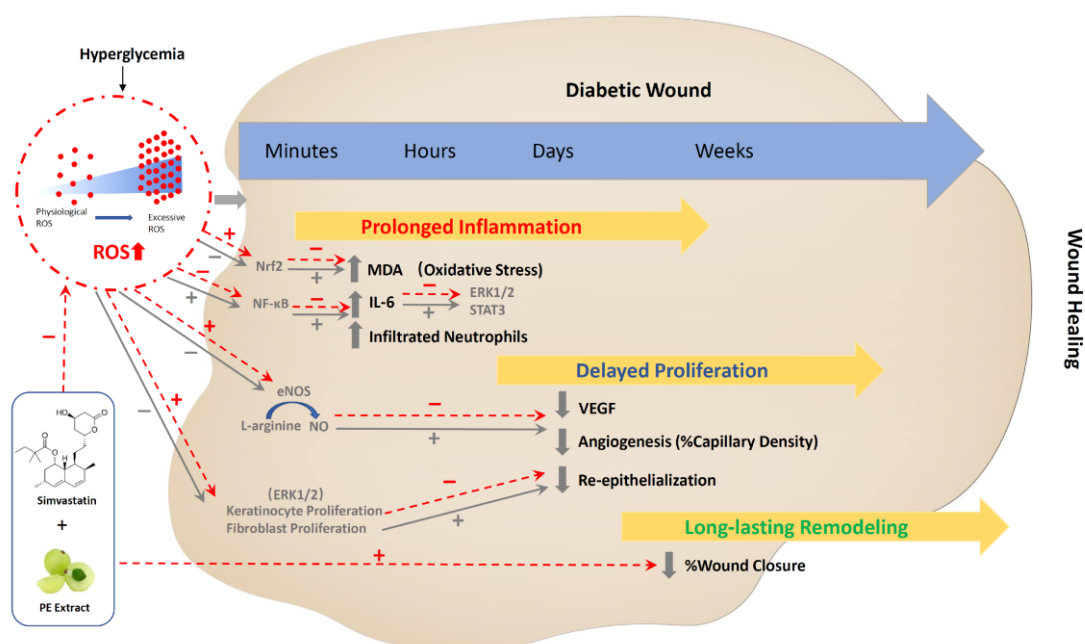


Figure 49. Proposed Mechanisms of Topical Application of PE and SIM Combined Cream in Diabetic Wound.

Based on the above discussion, the proposed mechanisms of PE and simvastatin combined cream in diabetic wound is proposed here. The mechanisms of combined effects of PE and simvastatin on wound healing in diabetic mice were indicated through oxidative stress and inflammation reduction, leading to improving angiogenesis, re-epithelialization, and wound closure. In prolonged inflammation stage, the decrease of MDA content probably reduced through Nrf2 related pathway. The inflammation status in the prolonged inflammation stage was reduced by PE and simvastatin combination, with downregulated IL-6 protein level and infiltrated neutrophils. This may relate to NF-κB regulated IL-6/ERK1/2 or IL-6/STAT3 pathways. In proliferation stage in diabetic wound, PE and simvastatin increased re-epithelialization, therefore, preventing the delay of proliferation phase probably through ERK1/2 related keratinocyte proliferation and fibroblast proliferation. PE and simvastatin increased VEGF expression and angiogenesis by enhancing eNOS induced NO upregulation.

CHAPTER VI

CONCLUSIONS

This study aims to find out the combined effect of topical application of PE and simvastatin on diabetic wound healing and the potential pathways whether involved in anti-inflammatory, antioxidative stress or pro-angiogenesis effect or not. To get the goals achieved, we measured %WC, %CV, VEGF protein level, IL-6 protein level, neutrophil infiltration, re-epithelialization and MDA content from the wound site area. The results are summarized as below:

1. The results showed that percentage of mouse body weight change of each group was less than 20% on day 4, day 7 and day 14 post-wounding in Protocol 1 and Protocol 2.
2. Fasting blood glucose result showed that all the diabetic mouse remained the diabetic status at the experiment endpoint on day4, day7 and day14 post-wounding in Protocol 1 and Protocol 2.
3. PE and SIM combined treatment could increase wound healing on day 14 significantly, while on day 7 post-wounding, combine treatment only had a tendency on increase wound healing in diabetic wound.
4. PE and SIM combined treatment could increase angiogenesis and VEGF in diabetic wound both on day 7 and day 14 post-wounding. Further, on day 7 post-wounding, there was a strong correlation (Pearson correlation $r > 0.7$) between VEGF protein level and %WC.
5. PE and SIM combined treatment could decrease neutrophil infiltration both on day 4 and day 7 in diabetic wound. However, PE and SIM combined treatment only showed tendency ($p=0.248$, and $p=0.127$, respectively) in downregulating IL-6 protein level on both day 4 and day 7. Moreover, there was a strong correlation (Pearson correlation coefficient $r > 0.7$) between percentage of wound closure (%WC) and IL-6 protein level on day 7 post-wounding, which indicated that reduction of proinflammatory cytokine IL-6 contributed to diabetic wound healing.

6. PE and SIM combined treatment could ameliorate oxidative stress in diabetic wound on day 4 and day 14, with only tendency in reducing oxidative stress on day 7 post-wounding.

7. In Protocol 1, on day 14 post-wounding, the result suggested that there were moderate linear correlations (Pearson correlation coefficient $r > 0.6$, respectively) of %WC and %CV increase as simvastatin dose increased within range of 0 to 10%SIM, w/v. In PE treatment groups, there was a strong linear correlation (Pearson correlation coefficient $r > 0.7$) of wound %CV increase as PE dose increased within range of 0 to 200%PE, w/v.

8. In Protocol 2, there was a strong correlation (Pearson correlation coefficient $r > 0.7$) between %CV and %WC on day 7 post-wounding, which suggest that the increase of angiogenesis mainly contributed to diabetic wound healing.

The conclusion was that topical application of PE and simvastatin combination has a combined effect on diabetic wound healing by the pathways of inhibition of anti-inflammation, anti-oxidative stress and enhancement of angiogenesis.

Limitation of This Study:

In this study, we used the diabetic wound model in mice, however, there are still gaps between mice and human skin wound healing in preclinical and clinical studies. However, till now, rodent model is the widely used mode in medicinal research. Further drug reactions and drug dose adjustment are still needed in clinical trials. New technological approaches are expected to surpass the gaps in transitional research in the future.

REFERENCES

จุฬาลงกรณ์มหาวิทยาลัย
CHULALONGKORN UNIVERSITY

APPENDIX

Appendix 1: Percentage of Bodyweight Change (%BW) of Each Mouse in Groups on Day 4
in Protocol 2

Groups	n	Wounding Day (g)	Endpoint Day (g)	Bodyweight Increase (g)	%BW	Mean	SE	SD
4-Day DM+Vehicle	1	26.31	27.68	1.37	5.21%	-0.91%	1.98%	4.43%
	2	29.37	28.59	-0.78	-2.66%			
	3	31.68	29.60	-2.08	-6.57%			
	4	24.16	24.48	0.32	1.32%			
	5	23.45	23.02	-0.43	-1.83%			
4-Day DM+100%PE	1	26.37	26.06	-0.31	-1.18%	-0.24%	1.19%	2.66%
	2	25.08	25.74	0.66	2.63%			
	3	26.53	25.97	-0.56	-2.11%			
	4	23.74	23.01	-0.73	-3.07%			
	5	20.12	20.63	0.51	2.53%			
4-Day DM+5%SIM	1	25.35	23.33	-2.02	-7.97%	-3.22%	2.03%	4.54%
	2	22.76	21.10	-1.66	-7.29%			
	3	24.99	25.58	0.59	2.36%			
	4	22.98	23.04	0.06	0.26%			
	5	24.65	23.8	-0.85	-3.45%			
4-Day DM+Combine	1	25.89	25.05	-0.84	-3.24%	-1.65%	0.98%	2.18%
	2	21.65	20.84	-0.81	-3.74%			
	3	24.48	24.33	-0.15	-0.61%			
	4	24.3	23.75	-0.55	-2.26%			
	5	22.22	22.58	0.36	1.62%			

Appendix 2: Percentage of Body Weight (%BW) Increase of Each Mouse in Groups on
Day 7 in Protocol 2

Groups	n	Wounding Day (g)	Endpoint Day (g)	Bodyweight Increase (g)	%BW	Mean	SE	SD
7-Day DM+Vehicle	1	27.13	25.69	-1.44	-5.31%	-1.39%	2.17%	4.86%
	2	23.63	25.29	1.66	7.02%			
	3	26.70	25.66	-1.04	-3.90%			
	4	23.24	22.60	-0.64	-2.75%			
	5	20.65	20.24	-0.41	-1.99%			
7-Day DM+100%PE	1	25.67	23.24	-2.43	-9.47%	-4.43%	2.54%	5.68%
	2	26.82	25.76	-1.06	-3.95%			
	3	26.57	24.89	-1.68	-6.32%			
	4	27.01	24.99	-2.02	-7.48%			
	5	27.33	28.72	1.39	5.09%			
7-Day DM+5%SIM	1	30.91	31.46	0.55	1.78%	-8.16%	2.55%	5.71%
	2	30.26	26.74	-3.52	-11.63%			
	3	24.40	22.27	-2.13	-8.73%			
	4	27.80	24.46	-3.34	-12.01%			
	5	35.01	31.43	-3.58	-10.23%			
7-Day DM+Combine	1	31.26	27.99	-3.27	-10.46%	-8.71%	1.63%	3.64%
	2	28.58	26.37	-2.21	-7.73%			
	3	28.42	25.84	-2.58	-9.08%			
	4	32.93	28.63	-4.30	-13.06%			
	5	24.79	23.99	-0.80	-3.23%			

Appendix 3: Percentage of Bodyweight Increase (%BW) of Each Mouse in Groups on Day 14 in Protocol 2

Groups	n	Wounding Day (g)	Endpoint Day (g)	Bodyweight Increase (g)	%BW	Mean	SE	SD
14-Day CON+Vehicle	1	25.23	25.92	0.69	2.73%	4.20%	1.13%	2.26%
	2	25.63	26.89	1.26	4.92%			
	3	26.50	28.37	1.87	7.06%			
	4	27.54	28.11	0.57	2.07%			
14-Day DM+Vehicle	1	31.65	29.58	-2.07	-6.54%	-2.20%	2.93%	6.55%
	2	29.01	31.61	2.60	8.96%			
	3	30.11	29.51	-0.60	-1.99%			
	4	28.77	26.74	-2.03	-7.06%			
	5	26.79	25.62	-1.17	-4.37%			
14-Day DM+100%PE	1	27.92	25.42	-2.50	-8.95%	-8.67%	1.48%	3.30%
	2	28.87	26.71	-2.16	-7.48%			
	3	27.38	25.47	-1.91	-6.98%			
	4	27.18	23.32	-3.86	-14.20%			
	5	28.80	27.15	-1.65	-5.73%			
14-Day DM+5%SIM	1	24.79	27.48	2.69	10.85%	0.74%	3.41%	6.82%
	2	27.05	26.23	-0.82	-3.03%			
	3	27.01	26.68	-0.33	-1.22%			
	4	30.25	29.15	-1.10	-3.64%			
14-Day DM+Combine	1	29.15	25.66	-3.49	-11.97%	-5.13%	2.27%	5.09%
	2	27.07	25.96	-1.11	-4.10%			
	3	22.92	21.52	-1.40	-6.11%			
	4	26.80	27.40	0.60	2.24%			
	5	28.08	26.47	-1.61	-5.73%			

Appendix 4: Fasting Blood Glucose (mg/dL) on Day 4 in Protocol 2

Mice #	4-Day DM+Vehicle	4-Day DM+100%PE	4-Day DM+5%SIM	4-Day DM+Combine
1	503	245	230	314
2	438	293	318	297
3	351	455	321	307
4	503	364	277	403
5	383	312	263	288

Appendix 5: Fasting Blood Glucose (mg/dL) on Day 7 in Protocol 2

Mice #	7-Day DM+Vehicle	7-Day DM+100%PE	7-Day DM+5%SIM	7-Day DM+Combine
1	425	508	211	586
2	370	294	330	450
3	417	426	407	448
4	340	313	390	350
5	610	438	210	459

Appendix 6: Fasting Blood Glucose (mg/dL) on Day 14 in Protocol 2

Mice #	14-Day Con + Vehicle	14-Day DM + Vehicle	14-Day DM + 100%PE	14-Day DM + 5%SIM	14-Day DM + Combine
1	57	256	209	313	576
2	52	306	391	555	275
3	132	403	486	232	546
4	62	204	527	472	246
5	-	327	708	-	610

Appendix 7: %WC Data of Each Mouse of PE on Day 14 in Protocol 1

Mice #	14-Day DM+Vehicle	14-Day DM+10%PE	14-Day DM+100%PE	14-Day DM+200%PE
1	94.57%	96.50%	99.07%	94.19%
2	98.53%	99.09%	98.16%	97.31%
3	91.89%	96.12%	99.27%	97.93%
4	94.32%	98.37%	99.85%	97.90%

Appendix 8: %CV Data of Each Mouse of PE on Day 14 in Protocol 1

Mice #	14-Day DM+Vehicle	14-Day DM+10% PE	14-Day DM+100% PE	14-Day DM+200% PE
1	34.56%	40.68%	40.00%	40.94%
2	37.50%	37.78%	37.39%	41.66%
3	37.41%	37.31%	40.75%	41.21%
4	35.75%	38.22%	39.45%	39.19%

Appendix 9: %WC Data of Each Mouse of SIM on Day 14 in Protocol 1

Mice #	14-Day DM+Vehicle	14-Day DM+0.5% SIM	14 Day DM+5% SIM	14-Day DM+10% SIM
1	94.57%	97.30%	98.17%	99.37%
2	98.53%	94.91%	99.86%	98.12%
3	91.89%	96.87%	98.99%	99.99%
4	94.32%	98.96%	99.27%	99.94%

Appendix 10: %CV Data of Each Mouse of SIM on Day 14 in Protocol 1

Mice #	14-Day DM+Vehicle	14-Day DM+0.5% SIM	14-Day DM+5% SIM	14-Day DM+10% SIM
1	34.56%	38.54%	37.51%	43.33%
2	37.50%	39.17%	40.62%	41.77%
3	37.41%	38.09%	36.63%	38.97%
4	35.75%	38.17%	42.48%	41.02%

Appendix 11: %WC Data of Each Mouse of Groups on Day 7 in Protocol 2

Mice #	7-Day DM+Vehicle	7-Day DM+100% PE	7-Day DM+5% SIM	7-Day DM+Combine
1	29.87%	45.30%	69.58%	77.60%
2	65.08%	54.78%	73.06%	70.97%
3	70.39%	47.22%	64.58%	48.19%
4	53.86%	67.58%	56.57%	64.86%
5	-	70.15%	50.42%	79.86%
6	-	-	39.96%	77.81%

Appendix 12: %CV Data of Each Mouse of Groups on Day 7 in Protocol 2

Mice #	7-Day DM+Vehicle	7-Day DM+100% PE	7-Day DM+5% SIM	7-Day DM+Combine
1	34.08%	38.57%	44.04%	40.24%
2	39.59%	41.75%	42.08%	44.92%
3	34.98%	39.60%	39.84%	38.10%
4	34.43%	39.54%	40.53%	39.45%
5	-	42.76%	37.68%	44.61%
6	-	-	39.33%	43.74%

Appendix 13: Data Set of Each Mouse of Correlation of %WC and %CV
on Day 7 in Protocol 2

Mice #	7-Day DM+Vehicle		7-Day DM+100%PE		7-Day DM+5%SIM		7-Day DM+Combine	
	%CV	%WC	%CV	%WC	%CV	%WC	%CV	%WC
1	39.59%	65.08%	38.57%	45.30%	44.04%	69.58%	44.92%	70.97%
2	34.98%	70.39%	39.60%	47.22%	42.08%	73.06%	38.10%	48.19%
3	34.43%	53.86%	39.54%	67.58%	39.84%	64.58%	44.61%	79.86%
4	34.08%	29.87%	42.76%	70.15%	37.68%	50.42%	43.74%	77.81%

Appendix 14: %WC Data of Each Mouse of Groups on Day 14 in Protocol 2

Mice #	14-Day CON+Vehicle	14-Day DM+Vehicle	14-Day DM+100%PE	14 Day DM+5%SIM	14-Day DM+Combine
1	99.42%	94.57%	98.93%	99.27%	99.21%
2	99.38%	98.53%	99.27%	98.79%	99.30%
3	99.01%	91.89%	98.71%	99.86%	99.60%
4	-	94.32%	98.04%	98.99%	99.10%
5	-	-	98.81%	98.16%	99.46%

Appendix 15: %CV Data of Each Mouse of Groups on Day 14 in Protocol 2

Mice #	14-Day CON+Vehicle	14-Day DM+Vehicle	14-Day DM+100%PE	14-Day DM+5%SIM	14-Day DM+Combine
1	39.33%	34.56%	41.93%	37.51%	41.45%
2	43.05%	37.50%	40.75%	40.62%	37.17%
3	39.66%	37.41%	40.89%	36.63%	40.90%
4	-	35.75%	33.87%	35.34%	42.05%
5	-	-	39.45%	42.48%	40.89%

Appendix 16: Data Set of Each Mouse of Correlation of %WC and %CV on Day 14 in Protocol 2

Mice #	14-Day CON+Vehicle		14-Day DM+Vehicle		14-Day DM+100%PE		14-Day DM+5%SIM		14-Day DM+Combine	
	%CV	%WC	%CV	%WC	%CV	%WC	%CV	%WC	%CV	%WC
1	39.33%	99.42%	34.56%	94.57%	41.93%	98.93%	37.51%	99.27%	41.45%	99.21%
2	43.05%	99.38%	37.50%	98.53%	40.75%	99.27%	40.62%	98.79%	37.71%	99.30%
3	39.66%	99.01%	37.41%	91.89%	40.89%	98.71%	36.63%	99.86%	40.90%	99.60%
4	-	-	35.75%	94.32%	33.87%	98.04%	35.34%	98.99%	42.05%	99.10%
5	-	-	-	-	39.45%	98.81%	42.48%	98.16%	40.89%	99.46%

Appendix 17: VEGF Protein Level (pg/mg total protein) of Wound Site
on Day 7 in Protocol 2

Mice #	7-Day DM+Vehicle	7-Day DM+100%PE	7-Day DM+5%SIM	7-Day DM+Combine
1	154.9	153.3	258.9	235.4
2	203.4	75.3	175.1	252.6
3	206.3	78.8	196.8	240.2
4	167.8	245.0	222.5	315.2

Appendix 18: VEGF Protein Level (pg/mg total protein) of Wound Site
on Day 14 in Protocol 2

Mice #	14-Day DM+Vehicle	14-Day DM+100%PE	14-Day DM+5%SIM	14-Day DM+Combine
1	50.1	92.3	95.6	155.5
2	102.8	98.4	90.9	113.0
3	63.4	79.6	129.3	84.3
4	89.6	112.7	96.8	100.3

Appendix 19: Data Set of Each Mouse of Correlation of %WC and VEGF
on Day7 in Protocol 2

Mice #	7-Day DM+Vehicle		7-Day DM+100%PE		7-Day DM+5%SIM		7-Day DM+Combine	
	VEGF (pg/mg)	%WC	VEGF (pg/mg)	%WC	VEGF (pg/mg)	%WC	VEGF (pg/mg)	%WC
1	216.9	65.08%	69.5	45.30%	258.9	69.58%	235.4	77.60%
2	206.3	70.39%	153.3	54.78%	175.1	73.06%	252.6	70.97%
3	167.8	53.86%	75.3	47.22%	130.4	64.58%	168.3	64.86%
4	-	-	78.8	67.58%	196.8	50.42%	240.2	79.86%
5	-	-	245.0	70.15%	-	-	315.2	77.81%

Appendix 20: Data Set of Each Mouse of Correlation of %CV and VEGF
on Day 7 in Protocol 2

Mice #	7-Day DM+Vehicle		7-Day DM+100%PE		7-Day DM+5%SIM		7-Day DM+Combine	
	VEGF (pg/mg)	%CV	VEGF (pg/mg)	%CV	VEGF (pg/mg)	%CV	VEGF (pg/mg)	%CV
1	154.9	34.08%	69.5	38.57%	258.9	44.04%	252.6	44.92%
2	216.9	39.59%	75.3	39.60%	175.1	42.08%	168.3	39.45%
3	167.8	34.43%	78.8	39.54%	130.4	39.84%	240.2	44.61%
4	-	-	245.0	42.76%	222.5	39.33%	315.2	43.74%

Appendix 21: Percentage of Re-epithelialization of Groups on Day 7 in Protocol 2

Mice #	7-Day DM+Vehicle	7-Day DM+100%PE	7-Day DM+5%SIM	7-Day DM+Combine
1	98.87%	51.02%	89.31%	100.00%
2	73.84%	46.58%	61.27%	100.00%
3	95.72%	46.39%	92.05%	82.93%
4	76.92%	100.00%	97.68%	91.36%
5	-	-	79.38%	81.68%

Appendix 22: Percentage of Re-epithelialization of Groups on Day 14 in Protocol 2

Mice #	14-Day DM+Vehicle	14-Day DM+100%PE	14-Day DM+5%SIM	14-Day DM+Combine
1	100.00%	100.00%	100.00%	100.00%
2	95.58%	100.00%	100.00%	100.00%
3	100.00%	100.00%	100.00%	100.00%
4	100.00%	100.00%	100.00%	100.00%
5	100.00%	100.00%	100.00%	100.00%

Appendix 23: Number of Infiltrated Neutrophils on Day 4 in Protocol 2

Mice #	4-Day DM+Vehicle	4-Day DM+100%PE	4-Day DM+5%SIM	4-Day DM+Combine
1	100	74	82	50
2	86	85	71	41
3	117	86	62	53
4	83	76	65	45
5	-	-	58	-

Appendix 24: Number of Infiltrated Neutrophils on Day 7 in Protocol 2

Mice #	7-Day DM+Vehicle	7-Day DM+100%PE	7-Day DM+5%SIM	7-Day DM+Combine
1	72	38	40	19
2	36	38	36	22
3	47	36	36	20
4	-	45	22	30
5	-	32	-	-

Appendix 25: IL-6 Protein Level (pg/mg total protein) of Wound Site
on Day 4 in Protocol 2

Mice #	4-Day DM+Vehicle	4-Day DM+100%PE	4-Day DM+5%SIM	4-Day DM+Combine
1	576.3	372.4	545.2	570.3
2	386.9	403.5	415.9	301.0
3	575.6	473.6	367.2	310.3
4	342.9	571.3	326.9	329.9
5	-	384.7	-	420.8

Appendix 26: IL-6 Protein Level (pg/mg total protein) of Wound Site
on Day 7 in Protocol 2

Mice #	7-Day DM+Vehicle	7-Day DM+100%PE	7-Day DM+5%SIM	7-Day DM+Combine
1	100.8	190.6	74.8	118.0
2	139.7	130.9	157.1	102.5
3	115.3	151.4	154.6	120.2
4	225.3	68.3	119.4	68.6
5	-	123.7	157.3	99.8

Appendix 27: Correlation of % WC and IL-6 Protein Level on Day 7 in Protocol 2

Mice #	7-Day DM+Vehicle		7-Day DM+100%PE		7-Day DM+5%SIM		7-Day DM+Combine	
	IL-6 (pg/mg)	%WC	IL-6 (pg/mg)	%WC	IL-6 (pg/mg)	%WC	IL-6 (pg/mg)	%WC
1	100.8	65.08%	190.6	45.30%	74.8	73.06%	102.5	70.97%
2	115.3	79.30%	123.7	54.78%	157.1	64.58%	154.2	64.86%
3	61.1	70.39%	130.9	47.22%	154.6	56.57%	68.6	79.86%
4	-	-	68.3	70.15%	157.3	39.96%	99.8	77.81%

Appendix 28: MDA Content (nmol/mg total protein) in Groups
on Day 4 in Protocol 2

Mice #	4-Day DM+Vehicle	4-Day DM+100%PE	4-Day DM+5%SIM	4-Day DM+Combine
1	1.12	0.95	1.10	1.55
2	2.75	0.98	0.63	1.05
3	1.80	0.44	1.77	0.81
4	1.70	0.84	1.01	0.63
5	-	0.42	1.62	-

Appendix 29: MDA Content (nmol/mg total protein) in Groups
on Day 7 in Protocol 2

Mice #	7-Day DM+Vehicle	7-Day DM+100% PE	7-Day DM+5% SIM	7-Day DM+Combine
1	1.60	2.12	1.38	0.69
2	1.29	3.68	1.90	1.63
3	0.83	0.85	2.54	1.64
4	1.28	2.41	2.76	0.71
5	9.09	1.49	2.63	0.59

Appendix 30: MDA Content (nmol/mg total protein) in Groups
on Day 14 in Protocol 2

Mice #	14-Day DM+Vehicle	14-Day DM+100% PE	14-Day DM+5% SIM	14-Day DM+Combine
1	6.30	7.62	6.18	1.76
2	7.23	6.75	4.20	1.40
3	9.53	0.63	6.10	0.98
4	5.87	8.89	1.69	

Appendix 31: Correlation of VEGF Protein Level and Percentage of Re-epithelialization on Day7 in Protocol 2

Mice #	7-Day DM+Vehicle		7-Day DM+100% PE		7-Day DM+5% SIM		7-Day DM+Combine	
	VEGF (pg/mg)	Re-epithelialization	VEGF (pg/mg)	Re-Epithelialization	VEGF (pg/mg)	Re-Epithelialization	VEGF (pg/mg)	Re-Epithelialization
1	154.9	98.87%	69.5	51.02%	258.9	89.31%	235.4	100.00%
2	216.9	73.84%	153.3	46.58%	175.1	61.27%	252.6	100.00%
3	167.8	95.72%	78.8	46.39%	130.4	92.05%	168.3	82.93%
4	206.3	76.92%	245.0	100.00%	196.2	97.68%	240.3	91.36%
5	-	-	-	-	222.5	79.38%	315.2	81.68%



VITA

NAME	Tingting Liao
DATE OF BIRTH	07 July 1983
PLACE OF BIRTH	CHONGQING, P.R.China
INSTITUTIONS ATTENDED	China Pharmaceutical University
HOME ADDRESS	Bld.13, Apartment DaHua, Street JiangDong, Fuling District, Chongqing, P.R.China, 408003
PUBLICATION	<ol style="list-style-type: none"> 1. Liao T.T., Luo X.Q., Huang C.G., Huang S.X., Liu J.Y., Xu J.H.. Research on the Function of Baji Oral Solution in Improving Kidney Health and Sexual Function. Chongqing Journal of Research on Chinese Drugs and Herbs, Vol. 60, 23-26, 2009. 2. Liao T.T., Zhang L.. Modulation of Buspirone on Rats Behavior with High and Low Level of Anxiety. Chongqing Journal of Research on Chinese Drugs and Herbs, Vol.58, 48-56,2008.(Translated from Arzneimittelforschung Drug Research) 3. Zhou L., Wang Y., etc., Research progress of Sustained or Controlled Release Preparations. Chongqing Journal of Research on Chinese Drugs and Herbs, Vol. 57, 38-41, 2008. 4. Lee H.H., Liao T.T.. Research, Development and Application Focus of Atratyloides macrocephala Loidz. Chongqing Journal of Research on Chinese Drugs and Herbs, Vol. 56, 55-61, 2007. 5. Liao T-T, Sukpat S, Chansriniyom C, Patumraj S. Dose-dependent effect of local treatment of Phyllanthus emblica L. cream on diabetic wound. Chula Med J. 2021;65.